2018-09-19

Histone Deacetylase 3 (HDAC3) Regulates Lymphatic Vascular Development

Harish P. Palleti Janardhan
University of Massachusetts Medical School

HISTONE DEACETYLASE 3 (HDAC3) REGULATES LYMPHATIC VASCULAR DEVELOPMENT

A Dissertation Presented

By

HARISH PALLETI JANARDHAN

Submitted to the Faculty of the
University of Massachusetts Graduate School of Biomedical Sciences, Worcester
In partial fulfillment of the requirements for the Degree of

DOCTOR OF PHILOSOPHY

SEPTEMBER 19, 2018

TRANSLATIONAL SCIENCE PROGRAM

HISTONE DEACETYLASE 3 (HDAC3) REGULATES LYMPHATIC VASCULAR DEVELOPMENT

A Dissertation Presented

By

HARISH PALLETI JANARDHAN

Thesis Advisor

CHINMAY TRIVEDI MD PhD
Associate Professor, Cardiovascular Medicine

Dissertation Defense Committee GSBS Members

GREGORY PAZOUR PhD
Professor, Molecular Medicine Program

JOHN KEANEY MD
Professor & Chief, Cardiovascular Medicine

ROGER DAVIS PhD
Investigator, Howard Hughes Medical Institute
Professor, Molecular Medicine Program

Chair of the Dissertation Committee

SCOT WOLFE PhD
Professor, Molecular, Cell & Cancer Biology

External Dissertation Committee Member

JOYCE BISCHOFF PhD
Professor, Harvard Medical School

Student Program

Translational Science Program

September 19, 2018

Acknowledgements

I am immensely grateful to all the people who I have crossed paths with during the course of my graduate studies here at UMassMed. I would like to specially thank the members of the Trivedi Lab, past and present, including all summer students, for their invaluable contributions to help me grow as a scientist. I would like to thank all members of Cardiovascular Medicine for providing a communal work atmosphere. I would like to acknowledge my thesis research advisory committee members including Dr. Greg Pazour, Dr. Scot Wolfe and Dr. John Keaney for granting me their time and for their guidance in shaping my thesis research and importantly, helping me to think as an independent scientist. I'm also grateful to Dr. Roger Davis and Dr. Joyce Bischoff for graciously accepting to be a part of my Dissertation defense committee. I would like to thank my Thesis advisor, Dr. Chinmay Trivedi for his constant support and guidance through my graduate career and for his invaluable contributions to my thesis research. I would like to thank Dr. Masahiro Shin and Dr. Nathan Lawson for their help with my thesis research. Finally, I would like to thank my friends and family for their constant source of support, encouragement and sacrifice, without whom this work would not be possible.

Abstract

Cardiovascular disease continues to be the leading cause of morbidity and mortality worldwide with an estimated 17 million annual deaths. A majority of cases are attributed to disease affecting the vascular system including arterial, venous and lymphatic vessels. Despite progress in understanding the molecular bases of vascular development and disease, the role of chromatin modifying enzymes in vascular processes remains ill defined. Here we show that the histone-modifying enzyme Hdac3 is a critical regulator of lymphatic vascular development. Endothelial specific loss of Hdac3 in mice affects the development of lymphovenous and lymphatic valves resulting in aberrant blood lymph separation, lymphedema and complete lethality. We demonstrate that Hdac3 functions in a flow responsive manner to regulate the expression of Gata2, a transcription factor essential for lymphatic valve development. In response to flow, transcription factors Tal1, Ets1/2 and Gata2 recruit Hdac3 to an evolutionarily conserved intragenic enhancer of Gata2 gene. In turn, Hdac3 recruits p300, a histone acetyl transferase, to render activation of the Gata2 enhancer, and thus promotes Gata2 transcription. Together, our findings demonstrate the molecular basis by which cell extrinsic and intrinsic cues cooperate to regulate lymphatic development.

TABLE OF CONTENTS

List of tables

List of Figures

List of copyrighted Materials Produced by the Author

Chapter II is adapted from a published manuscript to include supplemental data and is included with permission not required. The term ‘enhanceosome’ has been removed or replaced by ‘protein complexes’.

Janardhan HP, Milstone ZJ, Shin M, Lawson ND, Keaney JF Jr, Trivedi CM. Hdac3 regulates lymphovenous and lymphatic valve formation.

J Clin Invest. 2017 Nov 1;127(11):4193-4206

CHAPTER I: Introduction

The cardiovascular system, composed of a central pump (the heart) and a network of conduits (the blood vessels), is the first functional organ system to develop during mammalian embryogenesis. The heart and blood vessels collaborate to send oxygen- and nutrient-rich blood throughout the embryo to support and sustain growth and development. Initial assembly of the vascular system occurs through vasculogenesis (Risau and Flamme, 1995), a complex process whereby endothelial cells, which will eventually line all vessels in the body, differentiate from the mesoderm to form a primitive plexus of blood vessels. Subsequently, angiogenesis, remodeling, expansion, and maturation of this primitive plexus forms a hierarchical network of vessels of varying calibers and composition for efficient nutrient delivery and waste removal throughout the body (Potente et al., 2011; Risau, 1997). The blood vascular system is further differentiated molecularly and functionally into two serial systems - a pre-capillary high-pressure arterial system and a post-capillary low-pressure venous system. In parallel, a low-pressure system of channels, the lymphatic vasculature develops through a process of lymph-angiogenesis to complement the function of the blood vessels (Alitalo et al., 2005; Tammela and Alitalo, 2010). Defective development of the blood and/or lymphatic vascular system can result in diseases ranging from embryonic death to congenital vascular anomalies manifesting at various stages of postnatal life (Uebelhoer et al., 2012; Wassef et al., 2015). Although substantial progress has been made in defining the molecular regulators of arterial and venous vessel development, the lymphatic system is relatively understudied.

Lymphatic vascular development and disease

The lymphatic system encompasses a tiered network of channels culminating in blind-ending capillaries and constitutes an essential part of a functioning mammalian circulatory system. In addition, lymph nodes, which are tissue structures composed of T and B immune cells embedded in a stromal network, are inter-positioned within larger lymphatic vessels (Blum and Pabst, 2006). The lymphatic system performs multiple tasks including draining excess protein-rich interstitial fluid back into the systemic circulation, trafficking immune cells from tissues to lymph nodes, for antigen presentation and immune surveillance, and transferring lipid-rich chyle from the intestine to the blood (Swartz, 2001).

Primary lymphedema encompasses disorders arising due to failure in the development of the lymphatic system (Mortimer and Rockson, 2014). Global prevalence is estimated at 1:6000 in the general population, including syndromic and non-syndromic cases of primary lymphedema. Mutations in several regulators of lymphatic endothelial cell structure and function including growth factors, cell surface proteins, cell signaling molecules and transcription factors have been implicated in human patients, suggesting genetic heterogeneity (Brouillard et al., 2014; Michelini et al., 2018). In addition, genes identified so far have been shown to regulate multiples aspects of lymphatic development. Despite recent progress in identifying disease-causing genes, the precise mechanism by which their expression and/or function during lymphatic development are regulated is not clear.

Historically, descriptions of the lymphatic system can be traced back to the ancient Greeks; however, it was not until the 17th century that a more systematic study of the lymphatics took place (Loukas et al., 2011). Gasparo Aselli, an Italian anatomist, through the dissection of abdomens of dogs in unfed and fed state, described the presence of 'veiue albae aut lacteae' in the intestine or 'vein like vessels that lack pulsation and transport a milky fluid' within them. He also described the presence of valves within these vessels and inferred that they might help prevent fluid backflow (Loukas et al., 2011). Subsequently, scholars of the 18th-19th centuries described the detailed anatomy of the lymphatic system and examined the primary significance of the lymphatics in health and in disease.

During the early 20th century, two groups put forth theories addressing the developmental origin of the lymphatic system. Using ink injection into embryos, Florence Sabin deciphered that the lymphatic system originated by budding from the centrally located cardinal vein and grew peripherally to all other tissues (Sabin, 1909). In contrast, Huntington and McClure postulated that lymphatics develop from peripheral tissues and then make connections with the central venous system based on wax reconstruction of cat embryos at different stages of development (Huntington and McClure, 1910). Almost a century later, the use of modern molecular and genetic tools, largely support Sabin's theory (Srinivasan et al., 2007). However, more recent evidence suggests that several organ specific lymphatic vessels draw some lymphatic endothelial cells from local sources including those of the heart, the intestine and the skin (Klotz et al., 2015; Martinez-Corral et al., 2015; Stanczuk et al.,

2015). Integrating these more-recent theories, the current model suggests that central cardinal vein derived lymphatics cooperate with local sources to form mature lymphatic vessel endothelium (Ulvmar and Makinen, 2016). A critical function of the lymphatic system is the anterograde movement of excess interstitial fluid from tissues back into the blood vascular system (Swartz, 2001). The lymphatic endothelium lining the lymphatic vessels is in continuity with the central venous system, yet the lymphatic vessels remain clear of blood, thus mechanisms preventing the back flow of blood, from high-pressure blood vessels into the lower pressure lymphatic vessels, are operational. These findings raise a critical question: how is the separation of blood - lymphatic system established and maintained?

Blood Lymph Separation

The lymphatics are an open vascular system that carry excess extravasated interstitial fluid unidirectionally from peripheral tissues and return it to the blood vascular system at the bilateral lymphovenous junction (LVJ). The right LVJ interfaces with the right lymphatic duct at the right subclavian and jugular vein junction (Smith et al., 2013). The left LVJ interfaces with the thoracic duct at the junction created by the left subclavian and left jugular veins (Ratnayake et al., 2018). As it serves as the connection between lymphatic and blood vascular spaces, a critical physiological function of the LVJ is to prevent reflux of blood from the high-pressure blood vascular system into the low-pressure lymphatic vasculature.

Lymphovenous Junction in health and disease

Florence Sabin, through detailed studies on human embryos in the early 20th century, revealed the structural and developmental anatomy of the human lymphovenous junction including the identification of a valve guarding the junction (Sabin, 1909). Subsequent studies in cadavers and surgical patients identified the common features and variations in terminal branches of thoracic duct and its interface with the central venous system (Davis, 1915; Kinnaert, 1973; Langford et al., 1999; Yalakurthi et al., 2013). The thoracic duct drains lymph fluid from the lower limbs, abdomen, pelvis, left thorax, head, and neck back into venous circulation. The right lymphatic duct drains lymph from the right thorax and right cervical regions (Smith et al., 2013). Approximately 87.5% humans have the thoracic duct with a single opening into the venous system, while the rest have 2 or more openings. In almost half of humans, the thoracic duct opens either into the left internal jugular vein or the venous angle at the of the left internal jugular vein and left subclavian veins. The thoracic duct drains lymph exclusively into the left lymphovenous junction in nearly 95% of humans (Ratnayake et al., 2018). Recent advances in imaging technologies, such as high-resolution ultrasonography, make it possible to image the terminal thoracic duct and motion of the lymphovenous valves (Seeger et al., 2009).

The lymphovenous valve is composed of bicuspid leaflets that open obliquely into the central venous system such that one of the cusps is anatomically superior to the other (Shimada and Sato, 1997). At the lymphovenous junction, the thoracic duct is narrow with a thin endothelial

layer and a sub-endothelial layer composed of smooth muscle fibers, elastic and collagenous fibers. The internal elastic lamina has a thin, network like structure accompanied by two or three layers of longitudinally arranged smooth muscle. The medial layer is composed of very few connective tissue or elastic fibers. Scanning electron microscopy showed thinner smooth muscle layer and fine connective tissue fibers near the lymphovenous junction. Immunostaining identified strong expression of extracellular matrix proteins, such as Collagen I, Collagen III, and Laminin within human lymphovenous valves (Shimada and Sato, 1997).

Several factors control the anterograde movement of lymph from peripheral tissues to the LVJ including propulsive forces generated by contractions of smooth muscle surrounding collecting lymphatic vessels, passive body movements, pulsatile forces of adjacent blood vessel flow and respiratory cycle dynamics (Swartz, 2001). Measurement of thoracic duct pressure provides a functional assessment of the lymphovenous valves in humans. During inspiration, central venous pressure drops and venous wall relaxes, which in turn opens the lymphovenous valves allowing anterograde drainage of lymph from the thoracic duct into the venous system. In contrast, expiration increases central venous pressure, thus closing the lymphovenous valves (Calnan et al., 1970; Pelug and Calnan, 1968). However, pathologic increases in central venous pressure in conditions such as chronic renal failure and congestive heart failure, leads to failure of lymphovenous valve-mediated blood/lymph segregation (Kochilas et al., 2014; Ratnayake et al., 2018; Witte et al., 1969). Accordingly, patients with chronic renal failure show

blood in the thoracic duct (Kinnaert, 1973). Of note, physiological venous reflux into the thoracic duct has been observed in approximately 20% patients by CT scans (Kammerer et al., 2016; Liu et al., 2006; Seeger et al., 2009). Not withstanding the observations in the clinic, until recently, little progress was seen in understanding the molecular and cellular development of the LVJ.

Lymphovenous valve development and function

Human embryological studies by Sabin in the beginning of the 20th century described the embryonic LVJ (Sabin, 1909). Anterior jugular lymph sacs connect to jugular veins via an immature valve, thus enforcing blood/lymph segregation. Nearly a century later, with the discovery of molecular markers specific to the lymphatic system such as Prox1, more detailed anatomical studies of the lymphovenous junction were possible using the murine model system (Srinivasan et al., 2011). Immuno-staining for Prox1, a transcription factor critical for lymphatic system development, in serial sections of the murine embryos established that the lympho-venous segregation is maintained by the presence of pairs of symmetric Lympho-Venous Valves (LVVs) located bilaterally. On each side, one valve is situated dorso-medially relative to the other and is formed by the confluence between the jugular lymph sac, internal jugular veins, and external jugular veins. Its partner is formed by the junction between lymph sac, the superior vena cava, external jugular vein, and the subclavian vein (Srinivasan et al., 2011). The valve leaflets are made of two layers of endothelial cells: an outer layer of Lympho-

Venous Valve Endothelial Cells (LVV-ECs) oriented towards the lumen of the superior vena cava, in continuity with the endothelial lining of the jugular or subclavian veins and an inner layer of Lymphatic Endothelial Cells (LECs) oriented towards the lumen of the lymph sac (Geng et al., 2016; Srinivasan et al., 2011). LVV-ECs are characterized by high expression of Prox1, Gata2, Foxc2, integrin-α9 and integrin-α5 and low expression of Vegfr3 and do not express Podoplanin or Lyve1 (Geng et al., 2016). In contrast, LECs express a comparatively reduced level of Prox1, Gata2 and Foxc2 but express lymphatic markers such as Vegfr3, Lyve1 and Podoplanin (Geng et al., 2016).

Murine LVV development is orchestrated in a step-wise manner beginning with specification of LVV-ECs from venous endothelial cells at embryonic day 12 after fertilization. In the next 12-hours following specification, invagination of LECs and LVV-ECs into the venous lumen forms an immature valve-like structure. Finally, from embryonic day 14.5 till birth, the immature valve develops, characterized by endothelial cell elongation, extracellular matrix deposition and recruitment of mural cells including pericytes and smooth muscle cells to the valve leaflets (Geng et al., 2016).

Murine genetic models continue to be a valuable resource for elucidating the molecular basis of lymphatic development. Several mouse models with targeted deficiencies for specific proteins including Prox1, Foxc2, Cx37, Gata2, CYP26B1, EphB4, beta catenin, integrin-α5 (ITGA5), display defective LVV formation at various stages of development (Bowles et al., 2014; Cha et al., 2016; Turner et al., 2014; Geng et al., 2016; Kazenwadel et al., 2015; Martin-Almedina et al., 2016; Srinivasan et al., 2011). For instance,

mice with reduced expression of Prox1 ($Prox1^{+/-}$) do not properly specify LLV-ECs and consequently do not form LVVs (Srinivasan et al., 2011). Instead, the jugular lymph sacs in $Prox1^{+/-}$ mice were shown to make abnormal connections with the central veins as a consequence of increase fluid pressure within the lymph sac. Furthermore, a small fraction of the embryos displayed peripheral blood filled lymphatic vessels possibly due to back flow of blood from the high-pressure venous vessels to low-pressure lymphatic vessels. This body of work suggests that Prox1 not only marks the presence of lymphovenous valves but also is required for their formation and maintenance (Srinivasan et al., 2011).

GATA2 is a zinc-finger transcription factor mutated in patients presenting with primary lymphedema (Kazenwadel et al., 2012; Ostergaard et al., 2011). Analysis of mice genetically deficient for endothelial Gata2 show multilayered, poorly organized LVV leaflets and consequent defective blood lymph separation. Interestingly, Prox1 expression is significantly reduced in the Gata2-null LVV-ECs possibly resulting in loss of LVV-EC identity in the developing LVV leaflets (Geng et al., 2016; Kazenwadel et al., 2015).

FOXC2 is a transcription factor that is frequently mutated in patients with lymphedema-distichiasis (Fang et al., 2000). Mice with deletion for Foxc2 have immature collecting vessels lacking lymphatic valves, recapitulating human disease (Petrova et al., 2004). Foxc2- heterozygous and homozygous knockout mice revealed reduced number or complete absence of LVVs, respectively (Geng et al., 2016). Interestingly, the number of LVVs negatively correlates with the presence of embryonic edema. Mechanistically, loss of

Foxc2 leads to defective specification of LVV-ECs (Geng et al., 2016). Foxc2 transcriptionally regulates Cx37, a gap junction protein required for LECs to function in a coordinated manner (Sabine et al., 2012). Although specification of LVV-ECs is not perturbed in mice lacking Cx37, the cells fail to form functional valve leaflets due to a failure of normal invagination (Geng et al., 2016).

CYP26B1, a cytochrome P450 enzyme, catalyzes the breakdown of Retinoic Acid (RA). Global loss of Cyp26b1 in mice results in excess activation of RA signaling within the developing lymphatic system leading to loss of polarized Prox1 expression within the cardinal vein and excessive specification/proliferation of LEC progenitor cells. Mice lacking Cyp26b1 display enlarged blood filled lymph sacs with abnormal LVV leaflets composed of increased number of $Prox1^{+}$ cells (Bowles et al., 2014).

Hydrops fetalis is a disorder characterized by fluid accumulation in the fetus. As a major regulator of tissue fluid balance, lymphatic system dysfunction is implicated in nearly 15% of non-immune-related cases of hydrops fetalis (Bellini et al., 2015). A recent study of two families with a history of non-immune hydrops found mutations in the endothelial tyrosine kinase EphB4 (Martin-Almedina et al., 2016). Mice with targeted deletion of EphB4 within lymphatic endothelial cells showed defective LVV development characterized by shortened valve leaflets and abnormal clustering of Prox1 positive cells at the LV Junction (Martin-Almedina et al., 2016). Kinase inactive EphB4 mutant mice show defective collecting vessel lymphatic valve development but whether the kinase activity of EphB4 is required for normal

LVV development remains to be defined (Zhang et al., 2015). Other mutations identified in cases of non-immune related hydrops fetalis include CCBE1, FAT4 and PEIZO1, however their requirement for LVV development is not known (Alders et al., 2014; 2009; Fotiou et al., 2015; Shah et al., 2013).

Finally, another developmentally active pathway demonstrated to be required for LVV development is the Wnt-beta catenin signaling pathway. Mice with targeted deletion of Ctnnb1, encoding beta-catenin, within LECs, have no LVV valves and a complete absence of LVV-EC differentiation (Cha et al., 2016).

Platelet mediated Inter-vascular Hemostasis

In addition to the presence of LVVs, platelet mediated physiological hemostasis at the LV junction prevents backflow of venous blood into the lymphatic circulation, thus establishing and maintaining lifelong blood lymph separation (Hess et al., 2013). In contrast to platelet mediated hemostasis that occurs after endothelial cell injury in blood vessels, LVJ hemostasis involves interaction of platelets with uninjured lymphatic endothelial cells at the LV junction. This interaction activates platelets resulting in a platelet plug and thrombus formation (Welsh et al., 2016). This phenomenon was first detected in mice deficient in immune receptor activated platelet signaling proteins Slp-76 and Syk (Abtahian et al., 2003). Slp-76 deficient mice presented with partial perinatal lethality; surviving mice showed chylous peritoneal hemorrhage suggesting involvement of lymphatic system. Irradiated wild-type mice transplanted with Slp-76 deficient hematopoietic

cells recapitulated the phenotype of Slp-76 knockout mice suggesting that Slp-76 and Syk were required within hematopoietic cells and not in endothelial cells for blood lymph separation (Abtahian et al., 2003).

Analyses of how hematopoietic cells regulate the separation of the two vascular systems revealed Clec2, a platelet cell surface receptor, functions upstream of Slp-76 and Syk (Suzuki-Inoue, 2006). A subsequent study identified Podoplanin, an O-glycosylated protein expressed on the surface of LECs, as a ligand for Clec2 (Suzuki-Inoue et al., 2007). Mechanistically, the interaction between Podoplanin and Clec2 robustly induced platelet aggregation in a Syk, Slp-76 and Plcγ dependent manner (Suzuki-Inoue et al., 2007). Accordingly, interfering with platelet aggregation through injecting pregnant mice with anti-podoplanin antibody, treatment of mice with acetyl salicylic acid, or mice deficient in Kindlin3 (a platelet integrin) resulted in defective blood lymph separation (Uhrin et al., 2010).

Consistent with these observations, Podoplanin knockout mice exhibit aberrant presence of blood within intestinal lymphatics (Bertozzi et al., 2010; Uhrin et al., 2010). In addition, conditional deficiency of O-glycan synthase, the enzyme required for o-glycosylation of Podoplanin in hematopoietic and endothelial cells, resulted in intestinal blood lymph mixing and reduced expression of Podoplanin (Fu et al., 2008). In contrast to the hematopoietic requirement for Syk and Slp-76, bone marrow transplant experiments with reconstitution of O-glycan synthase deficient hematopoietic cells, did not display the blood lymph separation phenotype indicating that Podoplanin is required in a non-hematopoietic cell type (Fu et al., 2008). Interestingly,

Podoplanin-null mice exhibit variable survival and surviving mice show complete blood-lymph separation at postnatal stages suggesting additional ligands of Clec2 in LECs (Suzuki-Inoue et al., 2010; Uhrin et al., 2010). However, a more recent study determined that Podoplanin is essential throughout postnatal life to maintain blood lymph separation (Bianchi et al., 2017).

Animal studies established the in vivo requirement of hematopoietic Clec2 in blood lymph separation and normal lymphatic development. Irradiated wildtype mice reconstituted with hematopoietic cells lacking Clec2 exhibit defective blood-lymph separation. Consistent with this observation, Bertozzi et al demonstrated that megakaryocyte or platelet Clec2 is critical for maintenance of blood lymph separation (Bertozzi et al., 2010). However, Clec2 function in other hematopoietic lineages, including neutrophils and macrophages, is dispensable (Finney et al., 2012).

The exact location of platelet Clec2-LEC-Podoplanin interaction, after careful analysis of histology and staining for platelet aggregates and thrombus, was found by Uhrin et al to be at the developing LVJ. They found that Clec2-Podoplanin interaction at the developing LVJ resulted in platelet aggregation in wildtype embryos but that this aggregation was lost in Podoplanin-null embryos (Uhrin et al., 2010). In addition, Hess et al determined that even through late gestation, the LV junction continues to remain the only site where platelets aggregate. In this model, treatment with an anti-Clec2 antibody in wildtype mice rapidly causes a failure of blood/lymph segregation, resulting in blood filled intestinal lymphatics (Hess et al., 2013). A

careful analysis of phenotype development revealed that blood flowed into the lymphatics in a retrograde fashion from the thoracic duct, through the mesenteric lymph nodes into the mesenteric collecting lymphatic vessels and finally into the intestinal lymphatics. This suggested that the point of interaction between platelets and endothelial cells was away from the intestine. Importantly, blood filled lymphatics also developed in $LTA^{-/-}$ and $RORC^{-/-}$ mice (characterized by a lack of lymph nodes) suggesting that the site of platelet-LEC interaction is not in the lymph node (Hess et al., 2013). Syk inhibitor treated mice exhibit complete blood lymph separation, suggesting that even minor amounts of preserved platelet signaling can maintain blood-lymph separation (Hess et al., 2013).

Finally, as platelet mediated thrombus formation is the key endpoint of Podoplanin-Clec2 signaling, the studies provide further evidence for a hemostatic mechanism of blood-lymphatic separation. Together these findings highlight the critical in vivo role of Podoplanin–Clec2 interaction and the importance of platelet aggregation in effecting blood lymph separation.

These results raise an interesting question: How does establishment of a thrombus at the LVJ prevent back flow of venous blood yet allows the simultaneous unimpeded anterograde lymph flow? Recent work from the Griffin laboratory demonstrates that Chd4, a component of the NuRD chromatin repressive complex, is required for establishment of blood lymph separation in mice (Crosswhite et al., 2016). LEC-specific ablation of Chd4 in mice causes robust expression of Plasminogen activator uPA, activating plasmin, an anticoagulant enzyme; and leading to dissolution of the thrombus

at the jugular lymph sac. Genetic deletion of uPA rescued both thrombus formation and blood-lymph separation defect in Chd4-null mice, however the genetically rescued pups were not recovered at birth suggesting uPA independent increase of plasmin activity (Crosswhite et al., 2016). Currently three models have been proposed to explain how the LVJ could both maintain forward lymph drainage and prevent blood reflux (Welsh et al., 2016). First, in a dynamic lymphovenous clot model, thrombi at the LVJ block retrograde blood flow while sustaining increasing pressure within the jugular lymph sac/thoracic duct. Increase in lymphatic pressure beyond a threshold dislodges the thrombus allowing transient anterograde lymph flow (Welsh et al., 2016). Because of the existence of multiple LVJ's, in the second 'pressure mediated dormant valve model', some junctions allow anterograde lymph flow while others prevent retrograde venous blood flow (Welsh et al., 2016). Finally, in the lymph fluid lysis model, forward lymph flow occurs when lymph fluid, normally enriched for clot lysis factors, is in proximity to the LVJ allowing the dissolution of the clot. In contrast when venous blood comes in contact with the LVJ, a clot is formed preventing retrograde flow of blood into the lymphatic system (Welsh et al., 2016).

Finally, Clec2 deficient mice exhibit a normally sized and structured LVV in absence of platelet-LEC interaction and thrombus formation (Hess et al., 2013). Whether a defective LVV or defective lymphatic valves affect LV hemostasis was addressed by examining the lymphatics in embryos with absent LVVs (Prox1+/-) and those with absent lymphatic valves (Itga9-/-). Both Prox1+/- mice and Itga9-/- embryos had more extensive thrombus

formation in the thoracic duct and only some Prox1+/- embryos had blood-filled dermal lymphatic vessels suggesting compensation by platelets. The fact that some Prox1+/- embryos presented with blood-filled dermal lymphatics, we can infer that the LVV is required for segregation of blood and lymphatic systems (Hess et al., 2013). In conclusion, both platelet-mediated lymphovenous hemostasis together with LVVs effect complete blood lymph separation.

Lymphatic Valve Development

In addition to the lymphovenous valves that guard the lymphovenous junction, the lymphatic vascular system also contain bicuspid valves within peripheral collecting vessels which mediate the unidirectional anterograde flow of lymph from capillary beds to the thoracic duct. Insights into the molecular regulation of lymphatic valve development were first derived from studies modeling the human syndrome Lymphedema Distichiasis in mice (Petrova et al., 2004). Loss of Foxc2 in these mice resulted in complete agenesis of lymphatic valves. Analysis of Foxc2 chromatin binding sites in LECs identified enrichment for Nfatc1 binding sites, suggesting cooperation between Foxc2 and Nfatc1 in regulating lymphatic development (Norrmén et al., 2009). Indeed, genetic studies using heterozygous Foxc2 treated with the calcineurin signaling inhibitor CsA exhibit loss of nuclear Nfatc1 and valve agenesis (Sabine et al., 2012). The cell autonomous requirement for Nfatc1 in lymphatic valve formation and maintenance was further confirmed by

inactivating the regulatory subunit of calcineurin (Cnb1) in LECs in mice (Sabine et al., 2012).

Based on morphological and molecular analysis, mesenteric collecting vessel lymphatic valve formation occurs in four distinct developmental stages: initiation, condensation, elongation, and maturation. In murine embryos, initiation of valve formation starts around embryonic day 16 and is marked by the presence of LECs with increased expression of Prox1 ($Prox1^{high}$) and Foxc2. The cells then condense into a ring like state accompanied by polarized but contrasting expression of Prox1 and Foxc2 upstream and downstream of the future valve. In stage 3, the cell reorientation and invagination into the vessel lumen is accompanied by deposition of extracellular matrix proteins such as laminin alpha 5. Finally, the valve matures with the deposition of a thickened matrix core (Sabine et al., 2012).

The highly regulated orientation of the valve forming LECs during lymphatic valve development suggests coordination between these LECs, likely via gap junction proteins. Indeed, mice lacking gap junction proteins, Cx37 and Cx43 display immature lymphatic valves (Kanady et al., 2011). Furthermore, mice heterozygous for Foxc2 and Cx37 have decreased numbers of mature valves, suggesting a genetic interaction between transcription factors and gap junction proteins (Kanady et al., 2015).

Further insights into the process of valve development were derived from the observations that flow within the mesenteric lymphatic system is initiated about 12 hours prior to the onset of valve forming regions, in between lymphangions, and valves are more frequently found near areas of disturbed

flow such as vessel bifurcations. Remarkably, mimicking in vivo flow conditions by subjecting cultured LECs to oscillatory shear stress (OSS) resulted in similar morphological and molecular changes in LECs including increased Foxc2, Gata2, and Cx37 expression (Kazenwadel et al., 2015). Experiments from Kahn lab further supported the role of lymph flow in initiating valve formation (Sweet et al., 2015). Sweet et al demonstrated that Clec2 deficient embryos exhibit blood filled lymphatics resulting in blockade of anterograde lymphatic flow. These mice displayed reduced number of lymphatic valves and decreased expression of Foxc2 and Cx37.

Patients presenting with hereditary lymphedema, associated with Emberger and MonoMac syndromes, revealed another key zinc finger transcription factor, Gata2, in lymphatic valve development (Hsu et al., 2013; Kazenwadel et al., 2012; Ostergaard et al., 2011). Gata2 is expressed in all lymphatic vessels with higher expression in lymphatic valves (Kazenwadel et al., 2012; 2015). Knockdown of Gata2 in cultured LECs resulted in reduced expression of Foxc2, Cx37, Itga9, and Prox1 suggesting Gata2 is an upstream regulator of key genes in valve development. Furthermore, Gata2 has been shown to directly bind enhancers regulating Foxc2 and Prox1 (Kazenwadel et al., 2015). Indeed, mice lacking Gata2 within lymphatic endothelial cells exhibit significantly reduced number of lymphatic valves, suggesting that Gata2 is a critical regulator of lymphatic valve development (Kazenwadel et al., 2015). Despite this evidence, the exact molecular pathways that translate shear stress signals to downstream transcriptional changes in genes critical for lymphatic valve formation are not well understood.

Recently, the Wnt/β-catenin signaling pathway has been shown to be active in developing lymphatic valves with deletion of β-catenin in lymphatic endothelial cells in mice arresting valve initiation (Cha et al., 2016). Follow up in vitro experiments suggested that β-catenin directly binds to upstream regulatory elements of Foxc2 and Prox1 to regulate their expression. Despite the interaction, genetic expression of Foxc2 in β-catenin-null mice failed to rescue lymphatic valve formation suggesting the involvement of other targets (Cha et al., 2016).

The identification of a blood endothelial cell shear stress mechanosensory complex composed of endothelial membrane proteins Vegfr2, Vegfr3, Pecam1, and Cdh5; and another endothelial transmembrane proteoglycan, Syndecan-4 in regulating endothelial alignment to flow suggests the possibility of similar complexes or proteins playing a role in lymphatic endothelial cells (Baeyens et al., 2014; Coon et al., 2015; Tzima et al., 2005). A recent study evaluated whether Pecam1 and Syndecan-4 could mediate shear stress responsiveness of LECs (Wang et al., 2016). Analysis of mesenteric lymphatic collecting vessels revealed that Pecam1 deficient mice and Syndecan-4 deficient mice failed to form mature valves. Instead the valve forming regions were occupied by disoriented $Prox1^{high}$ valve forming LECs, suggesting a functional relationship between the lymphatic mechanosensory complex and planar cell polarity (Wang et al., 2016). Indeed, knockdown of Syndecan-4 causes increased expression of Vangl2, a component of planar cell polarity signaling, and misalignment of cultured LECs in response to laminar flow. Simultaneous knockdown of Syndecan-4 and Vangl2 restored

flow-mediated LEC orientation (Wang et al., 2016). Consistent with this, mice lacking planar cell polarity signaling components, Vangl2 or Celsr1, show disoriented Prox1^{high} valve forming LECs, indicating defective lymphatic valve development (Tatin et al., 2013). Patients with mutations in genes regulating planer cell polarity, such as FAT4 and CESLR show lymphedema (Alders et al., 2014; M L Gonzalez-Garay, 2016). Loss of Fat4 in mice cause decreased percent of lymphatic valve formation, however, initiation of Prox1 expressing clusters remains unaltered (Pujol et al., 2017).

Interestingly, Syndecan-4 has been shown to play a role in regulating the activity of several signaling pathways including Calcineurin/NFAT signaling, Wnt-b catenin signaling and Wnt/Planar cell polarity pathway that have been implicated in lymphatic valve development as noted above. For examples, activation of Calcineurin/NFAT signaling in response to mechanical stretching of cardiomyocytes is dependent on Syndecan-4; and a genetic interaction between Vangl2 and Syndecan-4 has been shown to orchestrate spinal neural tube closure and orientation of stereocilia bundles in cochlea of mice (Escobedo et al., 2013; Finsen et al., 2011).

Tie1, a receptor tyrosine kinase has been implicated in shear stress dependent initiation and maintenance of atherosclerotic plaques, positioning it a LEC mechanotransducer candidate (Woo et al., 2011). Indeed, lymphatic specific Tie1 ablation in mice causes mesenteric lymphatic valvular agenesis and a dramatic reduction in the number of Prox1^{high} expressing valve clusters (Qu et al., 2015).

Several other developmentally active signaling pathways, such as Bone morphogenic protein (Bmp), Notch, Semaphorin, Plexin, and Ephrin, have been shown to regulate murine lymphatic valve development (Bouvrée et al., 2012; Jurisic et al., 2012; Levet et al., 2013; Murtomaki et al., 2014; Mäkinen et al., 2005; Zhang et al., 2015). For instance, Notch1 expression and activity are enriched in developing lymphatic valves suggested a role for the Notch pathway in lymphatic valvulogenesis. Indeed, Prox1^{high} LECs failed to cluster and reorient to form valves in mice lacking Notch1 or expressing a dominant negative regulator of MAML, a component of the Notch signaling pathway (Murtomaki et al., 2014). In addition, Notch expression in cultured LECs induced the expression of Itga9, Fibronectin EIIIA, and Cx37, proteins critical for lymphatic valve maturation (Murtomaki et al., 2014).

Analysis of the transcriptome profile of LECs isolated from mouse colonic tissue revealed an unexpected enrichment for axonal guidance proteins Sema3A and Sema3D (Jurisic et al., 2012). Nrp1, a receptor for Semaphorin ligands, is expressed by smooth muscle cells surrounding the lymphatic collecting vessel and also in lymphatic valve leaflets. Injection of Nrp1 antibodies into mice resulted in increased pericyte coverage of collecting lymphatics. Interestingly, quantification of valve number revealed no significant differences, yet the expression of Itga9 appeared mislocalized and distribution of fibronectin EIIIA appeared diffuse in these mice (Jurisic et al., 2012). In a parallel independent study, mice deficient in Sema3a or either the Sema3a-receptors Nrp1 or PlexinA1, resulted in formation of smaller lymphatic valves with excessive smooth muscle cell coverage (Bouvrée et al.,

2012). Ephrin B2-EphB4 signaling is also required for lymphatic valve development. Mice with homozygous deletion of a C-terminus valine residue in the PDZ interaction domain of Ephrin B2 or loss of EphB4 completely lack of mesenteric lymphatic valves (Mäkinen et al., 2005). An independent study revealed that tyrosine kinase activity of EphrinB2 receptor, EphB4, is required for lymphatic valve development and maintenance (Zhang et al., 2015).

Bmp9 signaling is required for lymphatic valve development. Bmp9 KO mice have reduced number of mesenteric collecting vessel valves with defective initiation and maturation (Levet et al., 2013). Addition of Bmp9 to cultured LECs increased Foxc2 and Cx37 expression in an Alk1 receptor dependent manner (Levet et al., 2013).

Finally, maturation of lymphatic valves is associated with deposition of a core matrix of extracellular matrix proteins that provides structural integrity allowing the valve to weather constant shear stress. LEC-integrin and extracellular matrix interactions are critical for lymphatic valve function in humans and mice. For instance, mutations in Itga9 have been found in fetuses presenting with bilateral chylothorax (Ma et al., 2008). Consistent with this, mice lacking Itga9 display defective lymphatic valves and die postnatally due to bilateral chylothorax (Bazigou et al., 2009). Itga9 binds multiple ECM ligands including Emilin1, Fibronectin EIIIA, Osteopontin, and Tenascin C, however; only Emilin1 and Fibronectin EIIIA have so far been shown to be important for valve maturation (Carla Danussi, 2008; Bazigou et al., 2009).

Histone acetylation/deacetylation and transcription

Embryonic development is a complex process characterized by the generation of multiple cell types which organize to form tissues, organs and organ systems. Precise coordination of gene expression in a spatiotemporal manner is critical for expression of unique cellular programs, and plays an integral role in all developmental processes. Alterations in global and local chromatin architecture work in concert to orchestrate and regulate gene expression (Perino and Veenstra, 2016). The basic structural unit of chromatin is made up of 146 base pairs of DNA wound around an octamer core of 2 subunits each of basic proteins, the histones H2A, H2B, H3 and H4 (Luger et al., 1997). Chemical modifications of histones, such as acetylation, methylation, and phosphorylation can modulate compaction of DNA or serve as docking sites for other proteins, thereby regulating transcription (Bannister and Kouzarides, 2011). For example, acetylation of H3 at lysine 56 (H3K56ac), located at a part where the DNA enters and exits the nucleosome, results in opening of surrounding DNA sequences, allowing binding of transcription factors and the progression of RNA polymerase (Marushige, 1976; Xu et al., 2005).

Histone acetyl transferases (HATs), a group of histone-modifying enzymes, catalyze the addition of acetyl group to generate ε-N-acetyl lysine residues in histones (Roth et al., 2001). These enzymes lack DNA binding domains and are recruited to the chromatin as part of multi-protein complexes (Lee and Workman, 2007). For example, the HAT Gcn5, part of the SAGA and SLIK complexes, acetylates histones H3 and H2B (Suka et al., 2001).

Similarly, chromodomain proteins, which bind to methylated histones, recruit HATs specifically to H3 lysine 4 methylation in promoters and H3 lysine 36 methylation sites in gene bodies (Cavalli and Paro, 1998). Bromodomain containing HATs not only acetylate histone lysines, but also directly bind to already acetylated lysine residues, and maintain their presence at the loci (Fujisawa and Filippakopoulos, 2017). Overall, HATs facilitate transcription of genes through a series of coordinated steps starting with recruitment to specific loci by transcription factors, subsequent acetylation of lysine residues, opening of local chromatin, and further recruitment of factors and other chromatin remodeling complexes (Shahbazian and Grunstein, 2007).

Opposing HATs, Histone deacetylases (HDACs) are an evolutionarily conserved group of histone modifying enzymes that catalyze the removal of acetyl groups from ε-N acetyl lysine residues in histone and non-histone proteins. Broadly, mammalian HDACs are divided into four classes including the Classes I, II, III (NAD+ dependent deacetylases, Sirtuins) and IV (Haberland et al., 2009b). The majority of nuclear histone deacetylation is mediated by class I deacetylases, Hdac1, 2, 3 and 8, defined by their homology to yeast deacetylase Rpd3. Class II Hdacs, defined by homology to yeast deacetylase Hda1 are subdivided into 2 groups, IIa (Hdacs 4, 5, 7, 9) and IIb (Hdacs 6, 10). Class II Hdacs are signal responsive and shuttle between the cytoplasm and nucleus. In addition, Class II Hdacs possess weak intrinsic deacetylase activity and depend on Class I Hdacs for their nuclear deacetylase function (Fischle et al., 2002). Hdac11 is the sole deacetylase within Class IV and contains a conserved core catalytic domain

similar to Class I and II Hdacs (Gao et al., 2002). Studies in yeast have determined that Rpd3 acts on all 4 histones while Hda1 acts only on H3 and H2B. Like HATs, HDACs function as a part of multi-protein complexes and are thus recruited to site-specific loci by transcription factors or cofactors (Jepsen and Rosenfeld, 2002). For example, Hdac1 and Hdac2 are a part of the NuRD, CoREST and Sin3a complexes while Hdac3 associated with NCoR and SMRT.

In addition to deacetylation and chromatin compaction, HDACs permit recruitment of factors to unacetylated histones. For instance, the SANT domain containing repressor complexes, such as NCoR, SMRT, and CoREST, bind deacetylated H4 lysine 5. SMRT has 2 SANT domains, one binds to Hdac3 and the other binds to H4 lysine 5. Hdac3 in turn deacetylates H4 lysine 5 resulting in a self-propogating loop of Hdac3 recruitment (Yu, 2003). In addition to recruiting histone-modifying enzymes, SANT domain containing proteins can also recruit chromatin-remodeling complexes both for repression and activation (Boyer et al., 2004).

Although HDACs have been traditionally associated with transcriptional repression; recent chromatin-binding profiles for HDACs exhibit a robust presence at actively transcribed regions of the genome (Wang et al., 2009). There is also evidence for recruitment of both HATs and HDACs by common interacting factors to active genes. For example EAF3, a chromodomain containing protein that binds to methylated H3 lysine 56, is part of both the NuA4 HAT complex and also a complex with Rpd3c (HDAC homologue) (Sun et al., 2008). While there is no conclusive model, HDAC recruitment at active

genes could function to prepare for rapid repression following stimuli induced activation. For example, in response to growth factor stimuli transcription factor Elk3 recruits Hdac1 to the c-Fos gene. This recruitment is required for rapid abatement of c-Fos transcriptional activation (Yang et al., 2001). Simultaneous recruitment of HDACs along with HATs could also serve to limit the amount of transcriptional activation in response to stimuli. Presence of HDACs at active genes could also promote transcription. Supporting this, rate of histone acetylation turnover appears to be correlated with transcription. For instance, Hos2 deacetylase is required for induction of Gal1 gene. Loss of Hos2 results in hyper-acetylation of H3 and H4, which in turn, leads to failed induction of Gal1 (Wang, 2002). Using fluorescence resonance energy transfer analysis, HDACs and HATs have been observed to exist in close proximity within cells such that they physically interact (Yamagoe et al., 2003). Such an association has been proposed to facilitate rapid turnover of acetylation and increased transcription (Yamagoe et al., 2003). More recently, Hdac3 has been shown to interact and recruit p300, a histone acetyltransferase; to target genes for activation in a deacetylase-independent fashion, suggesting broader mechanisms by which HDACs control gene transcription (Zhang et al., 2016).

HDACs in vascular development and disease

Recent evidences from our laboratory and others suggest tissue-specific and spatiotemporal functions of HDACs during development (Goldfarb et al., 2016; Lewandowski et al., 2014; 2015). Although substantial

progress has been made in understanding the role of class I HDACs in cardiac development and beyond, their functions in vascular development remain unknown. Initial interest in endothelial function of HDACs developed because of the potential utility of HDAC inhibitors in cancer therapy. Studies suggest that Trichostatin A (TSA), a pan-HDAC inhibitor, inhibits hypoxia induced VEGF expression in cultured tumor cells (Williams, 2005). Subsequent studies have shown that HDACs may regulate the proliferation, migration, apoptosis and differentiation of cultured endothelial cells (Zhou et al., 2011). For instance, loss of Hdac3 in ex vivo cultured aortic segments leads to endothelial cell apoptosis. In cultured endothelial cells Hdac3 forms a complex with AKT and increases its kinase activity leading to an endothelial pro-survival function in response to shear stress (Zampetaki et al., 2010). Among Class II HDACs, Hdac5 modulates migration and sprouting of endothelial cells through its regulation of Fgf2 expression in a deacetylase-independent manner (Urbich et al., 2009). Similarly, Hdac6 deacetylates cortactin, a cytoplasmic protein, to control endothelial cell migration and sprout formation (Kaluza et al., 2011). Consistent with this finding Tubacin, a Hdac6 inhibitor, decreased tube formation and sprouting in cultured endothelial cells.

Hdac7, a class II HDAC, is specifically expressed in endothelial cells during early murine development. Using tissue-specific mouse model, Hdac7 has been shown to maintain vascular integrity by repressing the expression of matrix metalloproteinase, an enzyme that degrades the extracellular matrix (Chang et al., 2006). Hdac7 function can be regulated by phosphorylation

mediated by PLCγ/PKC/PKD pathway in response to VEGF leading to decreased tube formation ability of endothelial progenitor cells (Margariti et al., 2010). Despite this progress, there is a relative lack of understanding of the vivo function of class I HDACs during embryonic and postnatal vascular development.

Conditional inactivation of genes in vascular endothelium

Deciphering the molecular regulation of embryonic vascular development and postnatal vessel homeostasis requires inactivation of genes in a temporal and cell type specific manner within the endothelium. Over the last two decades murine studies have increasingly utilized the Cre/LoxP system to conditionally inactivate genes in various tissues. Cre/LoxP system involves the catalytic action of bacteriophage P1 - derived recombinase (Cre) on an identical pair of LoxP sites, similarly oriented 34bp DNA sequences. The LoxP sites flank an intervening DNA sequence within the gene targeted for inactivation. In vivo expression of Cre, under the control of a cell type specific promoter, results in recombination of the LoxP sites and permanent removal of the intervening DNA sequence from the host cell and its lineage. Breeding of transgenic mice lines that express Cre under the control of specific promoters with those that contain the floxed gene results in conditional gene inactivation in a tissue specific and spatiotemporal manner. Constitutively active Cre transgenic mice used in the study of gene function in blood endothelial cells or lymphatic endothelial cells include Tek-Cre, Cdh5-Cre, and Lyve1-Cre (Kisanuki et al., 2001; Alva et al., 2006; Pham et al., 2010). Tek-Cre mice contain a transgene expressing Cre under the control of Tek promoter and enhancer elements

(Kisanuki et al., 2001). During embryonic development, Tek-Cre; as determined using a beta-galactosidase reporter, is expressed as early as embryonic day 8.5 (E8.5) and E9.5 in majority of vascular endothelial cells of the yolk sac and embryo respectively (Kisanuki et al., 2001). Although initial studies did not detect Tek-Cre activity in hematopoietic cells, subsequent studies by Tang et al determined that a majority of primitive hematopoietic cells in the yolk sac, primitive erythroid cells and adult hematopoietic cells including those from the bone marrow and spleen are of Tek-Cre lineage (Tang Y et al., 2010). To limit expression of Cre to endothelial cells, Alva et al used an alternate endothelial gene promoter to drive Cre recombinase in endothelial cells, Cdh5-Cre. Approximately 2.5Kb fragment of DNA sequence upstream of the translational start site of Cdh5 spliced to the gene encoding Cre was used for generating Cdh5-Cre transgenic mice (Alva et al., 2006). In contrast to Tek-Cre mice, Cdh5-Cre shows patchy activity in endothelial cells of embryonic vasculature at e8.5 and e9.5. However, by e14.5 nearly 96% of endothelial cells show Cre activity. Further, analysis of various hematopoietic organs such as the fetal liver, bone marrow, thymus and spleen together with circulating blood cells showed that nearly 50% of the cells were positive for Cre activity. In addition to blood endothelial cells, Cdh5-Cre activity is also noted in embryonic lymphatic vessels as early as e12.5 (Alva et al., 2006). To dissociate the requirement of gene function in blood endothelial cells versus lymphatic endothelial cells, transgenic mice that express Cre specifically in LECs have been developed. Lyve1-Cre mice express Cre under the control of promoter of Lyve1, a membrane protein expressed in LECs (Pham et al.,

2010). Cre activity is noted as early as e9.5 in the cardinal vein prior to the development of first embryonic lymphatic structures, the lymph sacs. In addition to Cre expression in majority of the LECs, activity of Cre is also noted in Yolk sac blood vessels, vitelline blood vessels, sinusoidal endothelial cells of the liver and patchy expression in the endocardium, dorsal aorta and inter-somitic blood vessels (Pham et al., 2010). Similar to other endothelial specific Cre transgenic mice, Lyve1-Cre activity is also noted in a fraction of CD45+ hematopoietic cells of the fetal liver including lymphocytes and myeloid cells. Further, about 35-40% of adult hematopoietic stem and progenitor cells are of Lyve1-Cre lineage (Lee et al., 2010).

Aim of this work

Class I Histone deacetylases comprising Hdacs 1, 2, 3 and 8, function primarily in the nucleus and account for the majority of cellular histone deacetylase activity. Germline loss of any Class I Histone deacetylase results in embryonic or perinatal lethality. The role of Class I Histone deacetylases in cardiac development has been investigated, however their roles in vascular development are unknown. The work presented here aims to advance the understanding of the role of Hdacs 1, 2 and 3 in vascular development. The findings presented here reveal that endothelial Histone deacetylase 3 (Hdac3), not Hdac1 or Hdac2, is critical for lymphatic vascular development. Further, the findings presented provide novel insights into the role of Hdac3 in orchestrating the coordination between cell extrinsic and intrinsic cues to regulate lymphatic valve development.

Chapter II: Hdac3 regulates lymphovenous and lymphatic valve formation

Chapter II is adapted from a published manuscript to include supplemental data and is included with permission not required. The term ‘enhanceosome’ has been removed or replaced by ‘protein complexes’.

Janardhan HP, Milstone ZJ, Shin M, Lawson ND, Keaney JF Jr, Trivedi CM. Hdac3 regulates lymphovenous and lymphatic valve formation.
J Clin Invest. 2017 Nov 1;127(11):4193-4206

Author Contributions

CMT conceived the study. HPJ and CMT designed the experiments. HPJ, ZJM, and CMT performed experiments and acquired and analyzed data. MS, NDL, and JFK contributed reagents, materials, methodology, and analysis tools. HPJ, ZJM, NDL, JFK, and CMT wrote the manuscript.

Abstract

Lymphedema, the most common lymphatic anomaly, involves defective lymphatic valve development; yet the epigenetic modifiers underlying lymphatic valve morphogenesis remain elusive. Here, we showed that during mouse development, the histone-modifying enzyme histone deacetylase 3 (Hdac3) regulates the formation of both lymphovenous valves, which maintain the separation of the blood and lymphatic vascular systems, and the lymphatic valves. Endothelium-specific ablation of Hdac3 in mice led to blood-filled lymphatic vessels, edema, defective lymphovenous valve morphogenesis, improper lymphatic drainage, defective lymphatic valve maturation, and complete lethality. Hdac3-deficient lymphovenous valves and lymphatic vessels exhibited reduced expression of the transcription factor Gata2 and its target genes. In response to oscillatory shear stress, the transcription factors Tal1, Gata2, and Ets1/2 physically interacted with and recruited Hdac3 to the evolutionarily conserved E-box–GATA–ETS composite element of a Gata2 intragenic enhancer. In turn, Hdac3 recruited histone acetyltransferase Ep300 to form a complex that promoted Gata2 expression. Together, these results identify Hdac3 as a key epigenetic modifier that maintains blood-lymph separation and integrates both extrinsic forces and intrinsic cues to regulate lymphatic valve development.

Introduction

Thin-walled lymphatic capillaries collect interstitial fluid (lymph) and transport it via collecting lymphatic vessels to the thoracic duct, which in turn drains into the subclavian vein (Yang and Oliver, 2014). Improper drainage of this extravasated protein-rich fluid from the tissues causes it to accumulate, resulting in lymphedema (Alitalo, 2011). Intraluminal lymphatic valves within the collecting lymphatic vessels and bicuspid lymphovenous valves ensure anterograde lymph drainage into the venous circulation (El Zawahry, 1983). Additionally, these valves prevent backflow of venous blood into the thoracic and right lymphatic ducts, effectively separating the blood and lymphatic systems (Hess et al., 2013; Srinivasan et al., 2011). Platelet-mediated intervascular hemostasis also functions with lymphovenous valves to maintain this separation throughout life (Hess et al., 2013). Developmental or functional defects in these valves can cause both primary and secondary lymphedema (Jurisic and Detmar, 2009; Petrova et al., 2004).

Lymphatic endothelial cells (LECs), the building blocks of the mammalian lymphatic vasculature, experience shear stress generated by the cephalad movement of lymphatic fluid (Sabine et al., 2012). Recent evidence demonstrates that this oscillatory lymph flow–mediated shear stress initiates stepwise morphological and molecular changes within LECs that lead to the formation of lymphatic valves (Kazenwadel et al., 2015; Sabine et al., 2012; Sweet et al., 2015; Tatin et al., 2013). Specifically, oscillatory shear stress (OSS) induces the expression of genes, including GATA2, FOXC2, GJA4,

and ITGA9, in LECs that are important for lymphatic valve development (Kazenwadel et al., 2015; Sabine et al., 2015; Sweet et al., 2015). GATA2, an upstream transcriptional regulator of FOXC2, PROX1, GJA4, and ITGA9, is important for blood-lymph separation and the development of lymphovenous and lymphatic valves (Brouillard et al., 2014; Kazenwadel et al., 2015; Lim et al., 2012; Sweet et al., 2015). Despite this evidence, the mechanisms driving OSS-mediated GATA2 expression during lymphatic valve development remain elusive.

GATA2 belongs to an evolutionarily conserved family of zinc finger transcription factors that play important roles in diverse developmental programs (Bresnick et al., 2010; Tsai et al., 1994). Monoallelic missense mutations and intragenic microdeletions in human GATA2 cause Emberger syndrome, characterized by primary lymphedema with a predisposition to myelodysplastic syndrome or acute myeloid leukemia (Mansour et al., 2010; Ostergaard et al., 2011). Moreover, 2 recurrent mutations that cause reduced GATA2 expression (c.1017+512del28 and c.1017+572C>T) within a highly conserved 167-bp intragenic enhancer of intron 5 of GATA2 have been found in patients with primary lymphedema (Ganapathi et al., 2015; Hsu et al., 2013; Spinner et al., 2014). Recent studies in transgenic mice demonstrate that this intragenic enhancer confers GATA2 expression specifically within endothelial cells of the lymphatic, cardiac, and vascular systems (Khandekar et al., 2007; Lim et al., 2012). Indeed, murine embryos lacking this Gata2 intragenic enhancer have reduced Gata2 expression and phenocopy the endothelial knockout of Gata2 (Johnson et al., 2012). Thus, there is strong evidence that

reduced GATA2 expression leads to lymphedema (Kazenwadel et al., 2012; 2015; Spinner et al., 2014).

Broadly, enhancers function as cis-regulatory elements controlling gene expression in a spatiotemporal and cell type–specific manner (Ong and Corces, 2011). Enhancer element activation is dependent on recruitment of specific transcription factors, coactivators, chromatin remodelers, and histone-modifying enzymes (Long et al., 2016). The latter establish histone marks that often serve to recruit a multitude of transcription factors and cofactors to gene regulatory elements (Calo and Wysocka, 2013; Ong and Corces, 2011). In addition, active enhancers show enrichment of Lys-27 acetylation on histone H3 (H3K27ac) and occupancy of the histone acetyltransferase EP300 (Creyghton et al., 2010; Rada-Iglesias et al., 2010; Zhang et al., 2013). While the complex regulation of enhancer elements is starting to be defined, the role of histone-modifying factors in regulating the transcriptional activity of the Gata2 intragenic enhancer remains unknown.

Two opposing classes of histone-modifying enzymes, histone acetyltransferases (HATs) and histone deacetylases (HDACs), regulate the acetylation state of histones within an enhancer (Yang and Seto, 2008). Acetylation by HATs is generally associated with transcriptional activation, while HDAC-mediated deacetylation usually results in transcriptional repression (Yang and Seto, 2008). On the basis of their catalytic mechanism and sequence homology, HDACs are classified into 5 subfamilies: class I (Hdac1, 2, 3, and 8), class IIa (Hdac4, 5, 7, and 9), class IIb (Hdac6 and 10), class III (Sirt1, 2, 3, 4, 5, 6, and 7), and class IV (Hdac11) (Montgomery et al.,

2008). Among HDACs, global loss of class I HDACs in mice causes embryonic or neonatal lethality, suggesting that these enzymes play pivotal roles in development (Bhaskara et al., 2008; Haberland et al., 2009a; Lagger, 2002; Montgomery et al., 2008; Trivedi et al., 2007). Recent studies from our laboratory and others have identified unique and tissue-specific functions of ubiquitously expressed class I HDACs during cardiac and craniofacial development (Haberland et al., 2009a; Lewandowski et al., 2015; Trivedi et al., 2008; 2010). Class I HDACs lack intrinsic DNA-binding domains and are instead recruited to the chromatin in a signal-dependent manner via their interactions with multiple protein nuclear complexes, transcription factors, and cofactors (Yang and Seto, 2008). Contrary to previous assumptions, emerging data from genome-wide mapping reveal that the majority of HATs and class I HDACs are recruited to promoter and enhancer regions of actively transcribed genes with acetylated histones (Wang et al., 2009). Among class I HDACs, Hdac3 mainly occupies intragenic and intergenic regions, including enhancers marked by H3K27ac and EP300 enrichment (Feng et al., 2011; You et al., 2013; Zhang et al., 2016; Mullican et al., 2008). Despite advances in understanding the developmental roles of class I HDACs, their role in vascular and lymphatic development remains undefined.

Here, we show that endothelial Hdac3, but not Hdac1 or Hdac2, is important for blood lymphatic separation. Mice lacking endothelial Hdac3 demonstrate congenital lymphedema due to defective lymphovenous and intraluminal lymphatic valve development. Our studies reveal that Hdac3-mediated epigenetic regulation of an OSS-dependent Gata2 intragenic enhancer

orchestrates lymphatic valve development and establishes blood-lymph separation.

Results

Lymphatic endothelial Hdac3 regulates blood-lymph separation

Hdac3 is ubiquitously expressed, including within LECs of developing lymphovenous valves, mesenteric lymphatic vessels and valves, heart, and peripheral lymphatic vessels (Figure 2.1, A–G (Emiliani et al., 1998; Lewandowski et al., 2014; 2015; Yang et al., 1997). Germline deletion of *Hdac3* results in embryonic lethality before E9.5 (Bhaskara et al., 2008; Montgomery et al., 2008). To determine the function of Hdac3 in the developing blood and lymphatic vasculature, we deleted *Hdac3* in endothelial cells using $Hdac3^{fl/fl}$ mice and 3 Cre lines: *Tek-Cre* ($Hdac3^{TekKO}$), *Cdh5-Cre* ($Hdac3^{Cdh5KO}$), and *Lyve1-Cre* ($Hdac3^{Lyve1KO}$) (Figure 2.1, A, D, and G) (Alva et al., 2006; Kisanuki et al., 2001; Pham et al., 2010).

Figure 2.1

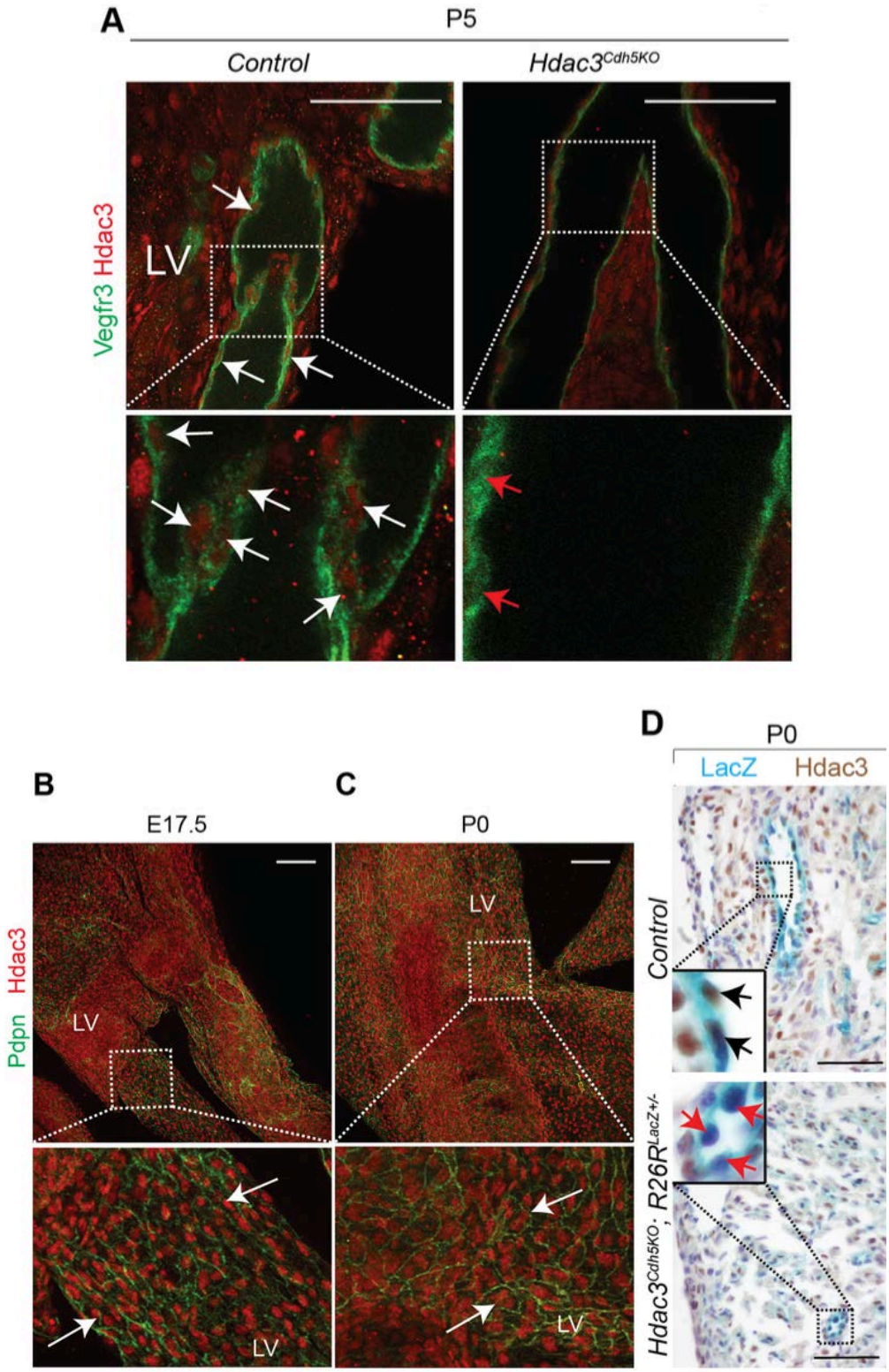
A
P5
Control
Hdac3Cdh5KO
Vegfr3 Hdac3
LV
B
E17.5
Pdpn Hdac3
LV
C
P0
LV
D
P0
LacZ Hdac3
Control
Hdac3Cdh5KO; R26RLacZ+/-

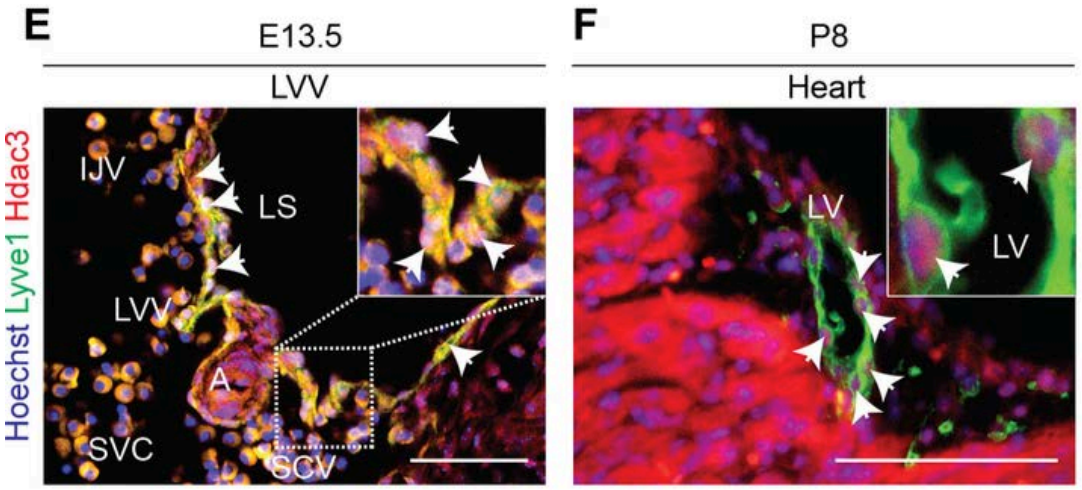
E
E13.5
LVV
Hoechst Lyve1 Hdac3
IJV
LS
LVV
A
SVC
SCV
F
P8
Heart
LV
LV

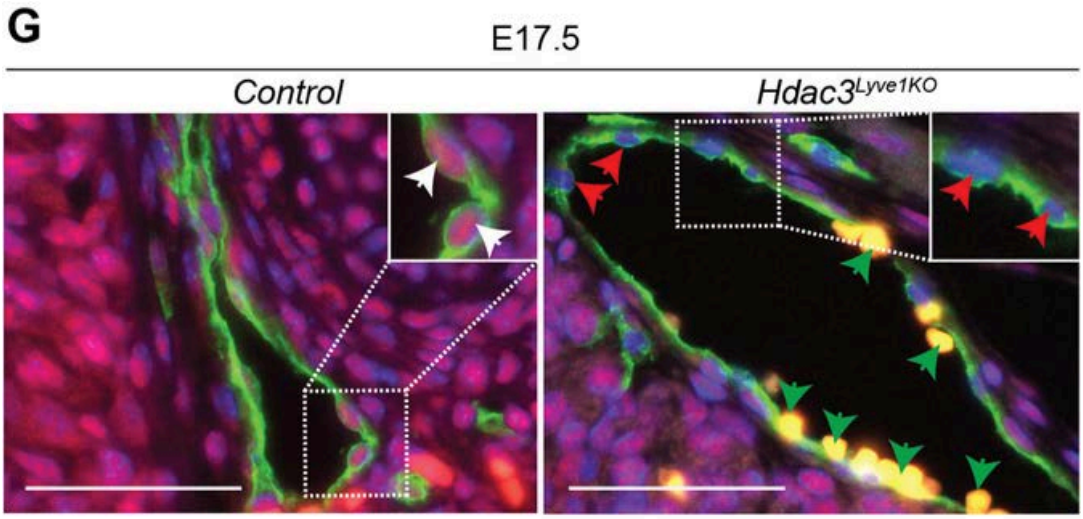
G
E17.5
Control
Hdac3Lyve1KO

Figure 2.1 Hdac3 is ubiquitously expressed in the developing lymphatic vasculature - (A) Whole-mount co-immunofluorescent staining of P5 *Hdac3*^{Cdh5KO} mesenteric lymphatic vessels reveals loss of Hdac3 expression (red) in Vegfr3+ (green) LECs (red arrow) compared to control (white arrow). Sub-stack of Z-stack images are presented. (B-C) Whole-mount co-immunofluorescent staining of E17.5 (B) or P0 (C) murine mesenteric lymphatic vessels identifies Hdac3 (red) expression in Pdpn+ lymphatic vessels (white arrows). (D) Hdac3 immunostaining of LacZ stained P0 *Hdac3*^{Cdh5KO}; *R26R*$^{LacZ+/-}$ heart section show loss of Hdac3 protein expression (red arrows) in LacZ+ cells compared to control (black arrows). (E-G) Co-immunofluorescent stain for Lyve1 (lymphatic marker – green) and Hdac3 (red) shows Hdac3 expression (white arrows) in LECs forming lymphovenous valves and lymph sac at E13.5 (E), cardiac lymphatic vessel at P8 (K), and peripheral embryonic lymphatic vessels at E17.5 (G). E17.5 *Hdac3*^{Lyve1KO} peripheral lymphatic vessel (G) reveals loss of Hdac3 expression in Lyve1+ (green) LECs (red arrow) compared to control (white arrow). Green arrows (G) show blood-filled peripheral lymphatic vessels. LV, lymphatic valve; SVC, superior vena cava; LS, lymph sac; LVV, lymphovenous valve; A, Artery; IJV, internal jugular vein; SCV, subclavian vein. Scale bar, 100µm (A-F); Scale bar, 50µm (G).

Hdac3^{TekKO} mice were identified until E14.5 but not at birth (P0), indicating complete embryonic lethality (Tables 2.1 and 2.2). *Hdac3*^{TekKO} embryos showed ectatic superficial vessels, pooling of blood in the jugular region, and severe edema at E14.5 compared with that seen in E12.5 embryos (Figure 2.2A). *Hdac3*^{Cdh5KO} and *Hdac3*^{Lyve1KO} neonates revealed similar ectatic dermal vessels at P6 and P0 and neonatal lethality at P9 and P0, respectively (Figure 2.2, B and C, and Tables 2.3 and 2.4). Endothelial cells lining blood-filled superficial vessels in *Hdac3*^{TekKO} embryos and *Hdac3*^{Cdh5KO} neonates were positive for the lymphatic marker Lyve1, but negative for the venous marker Emcn, suggesting lymphatic identity (Figure 2.2, D and E).

Additionally, *Hdac3*^{Cdh5KO} neonates exhibited blood-filled lymphatic vessels in intestine and mesentery between P5 and P6 and in heart at P0 (Figure 2.2, F–H). Similarly, *Hdac3*^{Lyve1KO} neonates had blood-filled cardiac lymphatic vessels at P0 (Figure 2.2I). We observed no apparent structural defects in *Hdac3*^{Cdh5KO} or *Hdac3*^{Lyve1KO} hearts (Figure 2.3, A and B).

Table 2.1

Hdac3$^{F/+}$; Tek-Cre mice were crossed with *Hdac3$^{F/+}$*

Genotype	P0
	Observed (Expected)
Hdac3$^{+/+}$	17 (16)
Hdac3$^{F/+}$	37 (32)
Hdac3$^{F/F}$	19 (16)
Hdac3$^{+/+}$;Tek-Cre	20 (16)
Hdac3$^{F/+}$;Tek-Cre	35 (32)
Hdac3$^{F/F}$;Tek-Cre	0*(16)
Total	128 (128)

** $p < 0.003$*

Table 2.2

Hdac3$^{F/+}$; Tek-Cre mice were crossed with *Hdac3$^{F/F}$; LacZ$^{-/-}$*

Genotype	E12.5	E13.5	E14.5
	Observed (Expected)		
Hdac3$^{F/+}$; LacZ$^{+/-}$	7 (7.25)	11 (9.5)	4 (3.5)
Hdac3$^{F/F}$; LacZ$^{+/-}$	6 (7.25)	6 (9.5)	2 (3.5)
Hdac3$^{F/+}$;Tek-Cre; LacZ$^{+/-}$	8 (7.25)	11 (9.5)	5 (3.5)
Hdac3$^{F/F}$;Tek-Cre; LacZ$^{+/-}$	8 (7.25)	10$^{\#}$ (9.5)	4* (3.5)
Total	29 (29)	38 (38)	15 (15)

*embryos were resorbing.
$^{\#}$5 out of 10 embryos were resorbing.

Figure 2.2

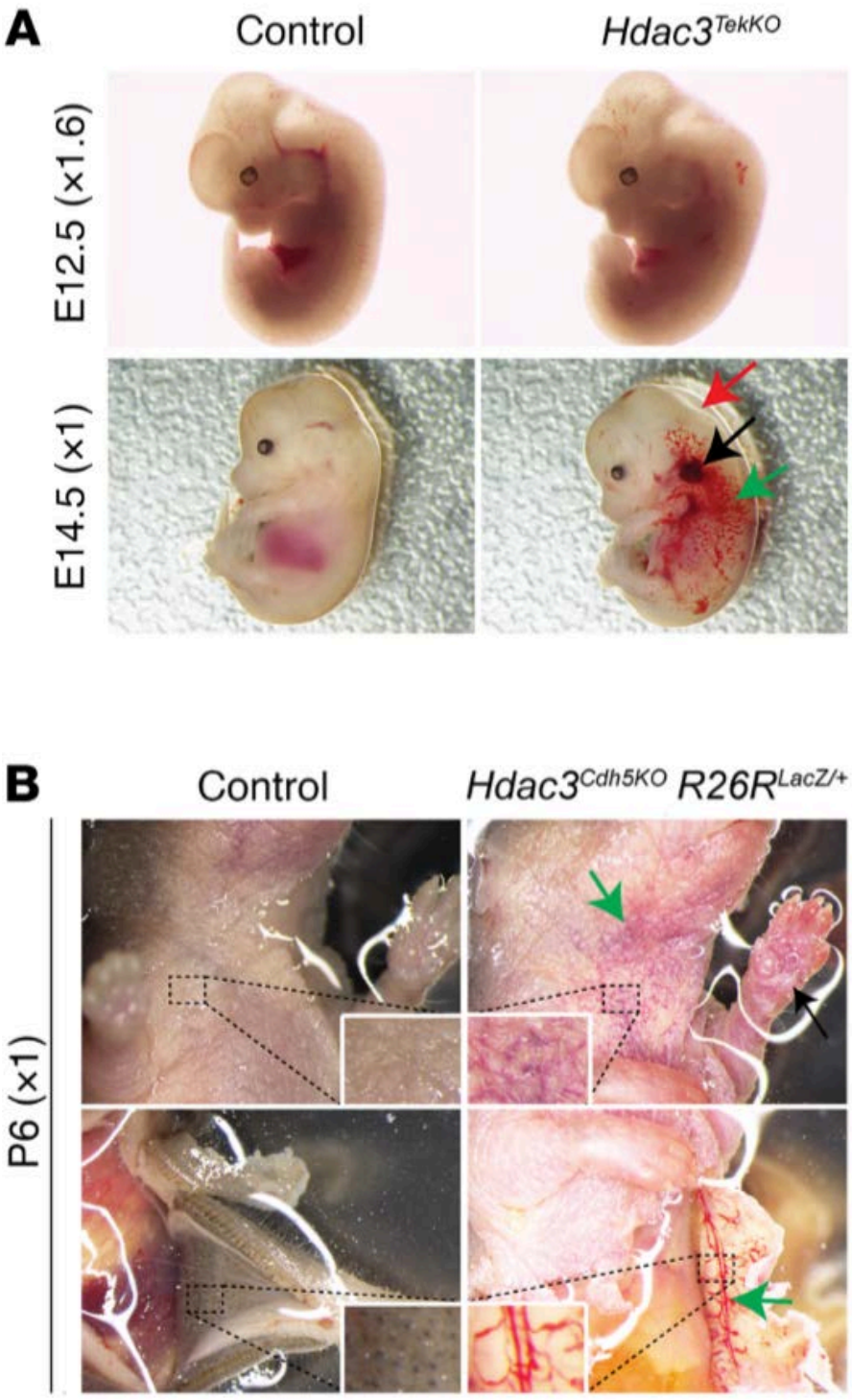
A
Control
Hdac3TekKO
E12.5 (x1.6)
E14.5 (x1)
B
Control
Hdac3Cdh5KO R26RLacZ/+
P6 (x1)

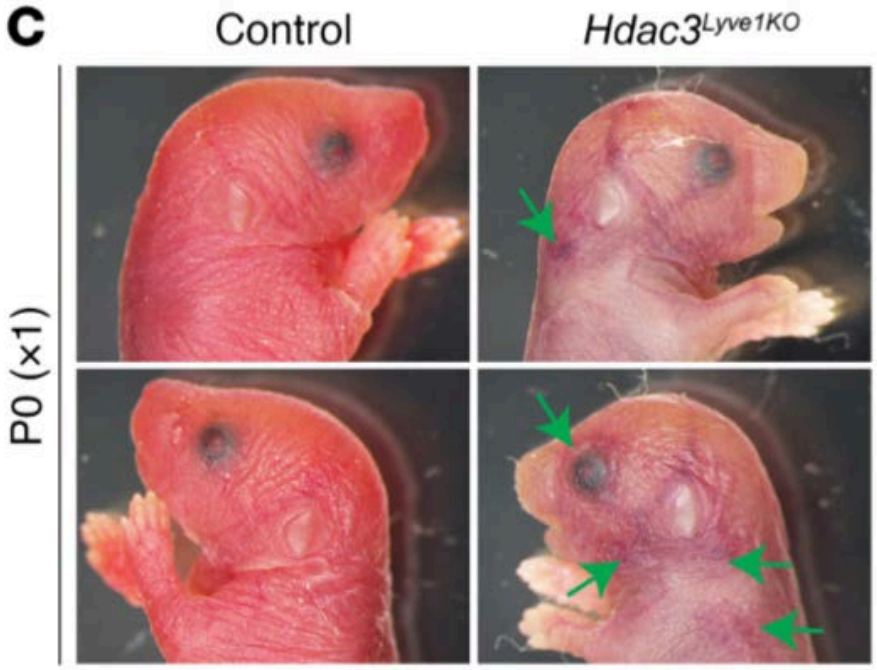
C
Control
Hdac3Lyve1KO
P0 (x1)

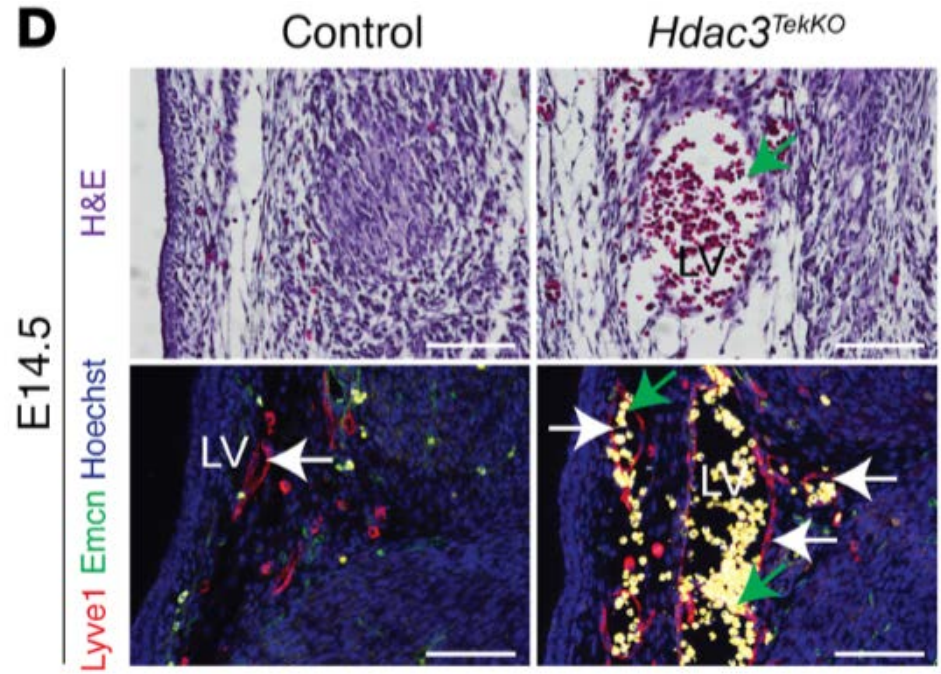
D
Control
Hdac3TekKO
E14.5
H&E
Lyve1 Emcn Hoechst
LV
LV
LV

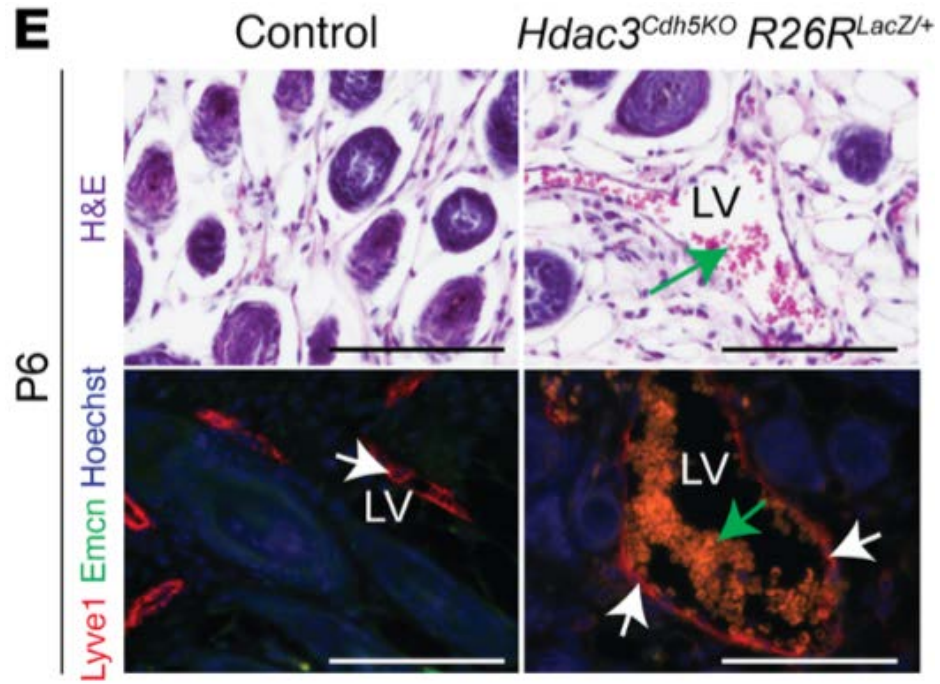
E
Control
Hdac3Cdh5KO R26RLacZ/+
P6
H&E
Lyve1 Emcn Hoechst
LV
LV
LV

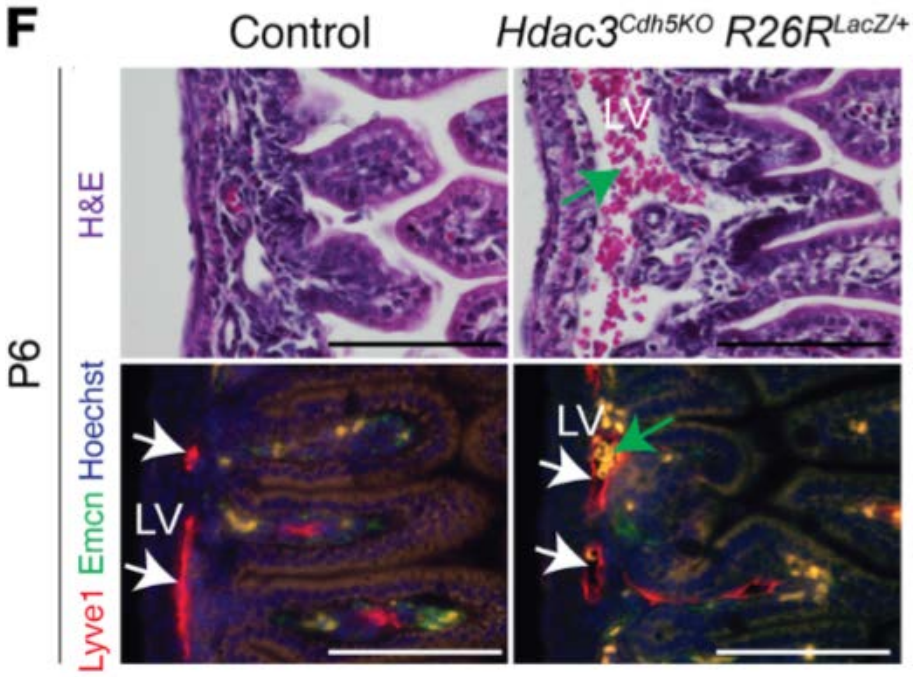
F
Control
Hdac3Cdh5KO R26RLacZ/+
P6
H&E
Lyve1 Emcn Hoechst
LV
LV
LV

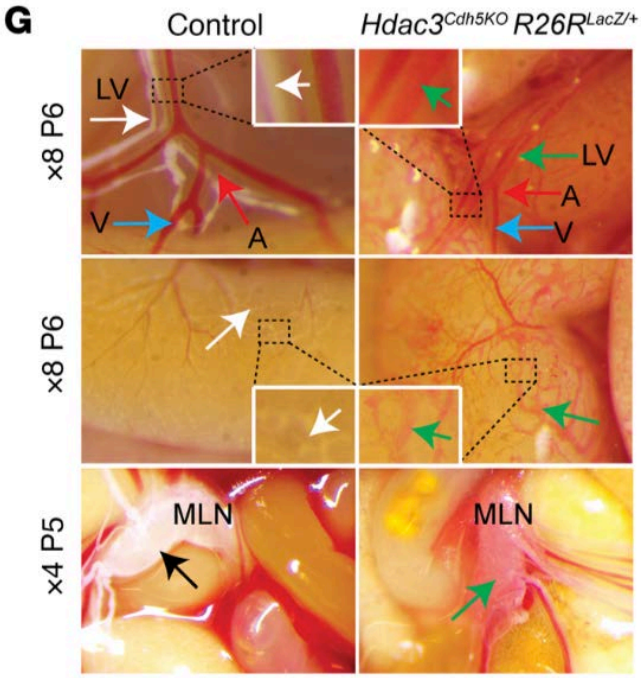
G
Control
Hdac3Cdh5KO R26RLacZ/+
x8 P6
x8 P6
x4 P5
LV
V
A
LV
A
V
MLN
MLN

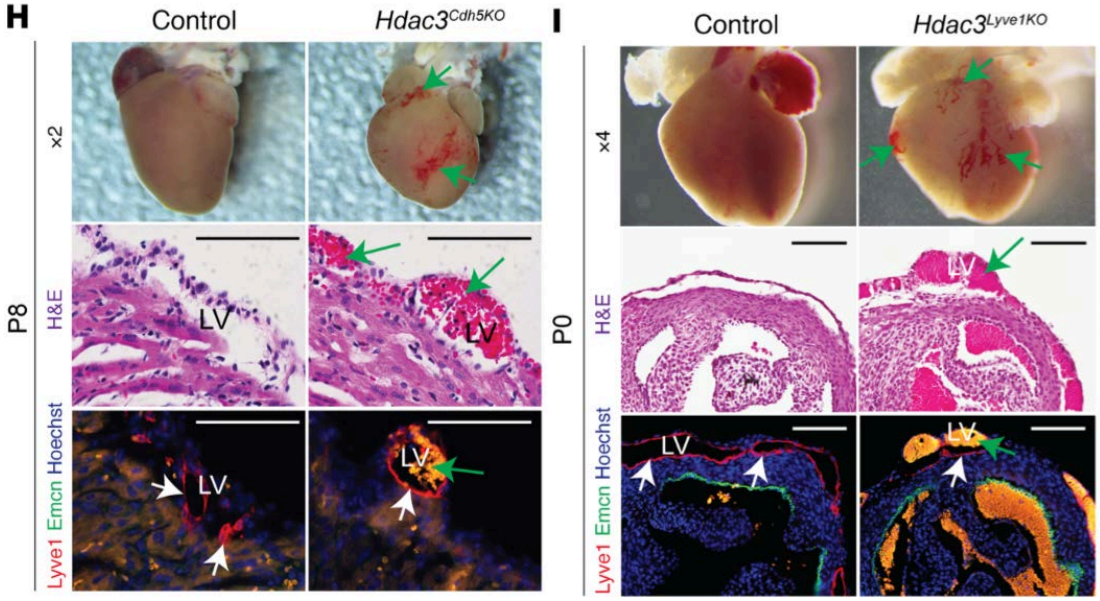
H
Control
Hdac3Cdh5KO
P8
x2
H&E
Lyve1 Emcn Hoechst
LV
LV
LV
LV
I
Control
Hdac3Lyve1KO
P0
x4
H&E
Lyve1 Emcn Hoechst
LV
LV
LV
LV

Figure 2.2 Lymphatic endothelial Hdac3 regulates blood-lymphatic separation. (A) Dissected E12.5 and E14.5 *Hdac3*^{TekKO} embryos. Green arrow shows ectatic superficial vessels; black arrow shows pooling of blood in the jugular region; red arrow shows swelling. (B and C) Neonatal (P6) *Hdac3*^{Cdh5KO} mice (B) and P0 *Hdac3*^{Lyve1KO} mice (C) had abnormal blood-filled dermal vessels (green arrows) compared with controls. (D–F) H&E and coimmunofluorescence staining for Lyve1 (lymphatic marker, red) and Emcn (venous marker, green) shows blood-filled (green arrows) dermal lymphatic vessels in E14.5 *Hdac3*^{TekKO} murine embryos (D) and blood-filled dermal (E) and intestinal lymphatic vessels (F) in P6 *Hdac3*^{Cdh5KO} neonates (E and F). White arrows show lymphatic vessels. (G) Dissected intestine of control and *Hdac3*^{Cdh5KO} P6 neonates. White, red, and blue arrows indicate lymphatic, arterial, and venous vessels, respectively; black arrow shows a mesenteric lymph node; green arrows show blood-filled lymphatic vessels and a mesenteric lymph node in *Hdac3*^{Cdh5KO} P6 neonates. (H and I) P8 *Hdac3*^{Cdh5KO} (H) and P0 *Hdac3*^{Lyve1KO} (I) hearts show ectatic and hemorrhagic superficial vessels (green arrows). H&E and coimmunofluorescence staining for Lyve1 (lymphatic marker, red) and Emcn (venous marker, green) shows blood-filled (green arrows) cardiac lymphatic vessels in P8 *Hdac3*^{Cdh5KO} (H) and P0 *Hdac3*^{Lyve1KO} (I) murine hearts. White arrows show lymphatic vessels. Scale bars: 100 μm. A, artery; LV, lymphatic vessel; MLN, mesenteric lymph node; V, vein. See also Figures 2.1, 2.3–5 and Tables 2.1–2.5.

Table 2.3

Hdac3$^{F/+}$; Cdh5-Cre mice were crossed with *Hdac3$^{F/+}$*

Genotype	P0	P8	P14
	Observed (Expected)		
Hdac3$^{+/+}$	9 (8)	17 (12)	9 (7)
Hdac3$^{F/+}$	21 (16)	18 (24)	18 (15)
Hdac3$^{F/F}$	7 (8)	14 (12)	4 (7)
Hdac3$^{+/+}$;Cdh5-Cre	9 (8)	14 (12)	14 (7)
Hdac3$^{F/+}$;Cdh5-Cre	12 (16)	30 (24)	16 (15)
Hdac3$^{F/F}$;Cdh5-Cre	6 (8)	3 (12)**	0 (7)*
Total	64 (64)	96 (96)	61 (61)

Table 2.4

Hdac3$^{F/+}$; Lyve1-Cre mice crossed with Hdac3$^{F/F}$LacZ$^{-/-}$

Genotype	P0	P5
	Observed	(Expected)
Hdac3$^{F/+}$; LacZ$^{+/-}$	3 (7.5)	7 (7)
Hdac3$^{F/F}$; LacZ$^{+/-}$	6 (7.5)	12 (7)
Hdac3$^{F/+}$; Lyve1-Cre; LacZ$^{+/-}$	13 (7.5)	9 (7)
Hdac3$^{F/F}$; Lyve1-Cre; LacZ$^{+/-}$	8 (7.5)[a]	0 (7)**
Total	30	28

a = 2 Dead ** $P < 0.02$

Figure 2.3

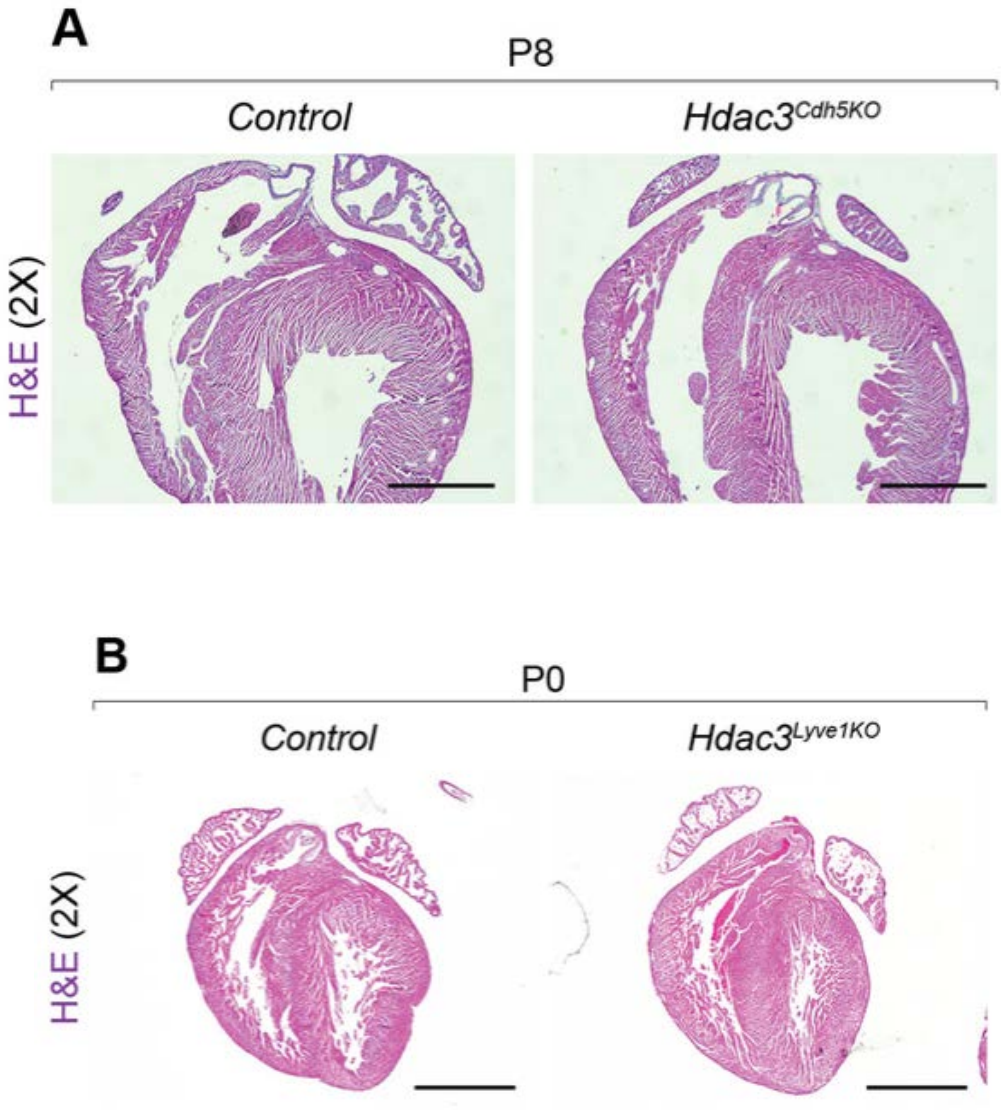

Figure 2.3 Endothelial Hdac3 is dispensible for myocardial development. (A-B) H&E-stained sections show normal myocardial development in *Hdac3*^{Cdh5KO} P8 (A) or *Hdac3*^{Lyve1KO} P0 (B) hearts. Scale bar, 1000µm.

Table 2.5

Phenotypes of mice lacking endothelial Hdac3

Genotype	Age	X^2 test	P-value
Blood-filled dermal lymphatic vessels			
Hdac3^{TekKO}	E13.5	*Hdac3*^{TekKO} (6/6): *Control* (0/4)	*P = 0.0016*
Hdac3^{Cdh5KO}	P6	*Hdac3*^{Cdh5KO} (3/3): *Control* (0/3)	*P = 0.0143*
Blood-filled cardiac lymphatic vessels			
Hdac3^{Cdh5KO}	P0	*Hdac3*^{Cdh5KO} (2/3): *Control* (0/4)	*P = 0.0533*
Hdac3^{Cdh5KO}	P8	*Hdac3*^{Cdh5KO} (3/3): *Control* (0/3)	*P = 0.0143*
Hdac3^{Lyve1KO}	P0	*Hdac3*^{Lyve1KO} (3/3): *Control* (0/3)	*P = 0.0143*
Blood-filled mesenteric lymphatic vessels			
Hdac3^{Cdh5KO}	P5	*Hdac3*^{Cdh5KO} (1/6): *Control* (0/3)	*P = 0.4533*
Hdac3^{Cdh5KO}	P6	*Hdac3*^{Cdh5KO} (3/4): *Control* (0/4)	*P = 0.0285*
Blood-filled thoracic duct			
Hdac3^{Cdh5KO}	P5	*Hdac3*^{Cdh5KO} (3/3): *Control* (0/3)	*P = 0.0143*
Defective mesenteric lymphatic valve development			
Hdac3^{Cdh5KO}	P5	*Hdac3*^{Cdh5KO} (3/3): *Control* (0/4)	*P = 0.0082*
Hdac3^{Levy1KO}	E17.5	*Hdac3*^{Cdh5KO} (3/3): *Control* (0/3)	*P = 0.0143*
Hdac3^{Lyve1KO}	P0	*Hdac3*^{Lyve1KO} (4/4): *Control* (0/4)	*P = 0.0047*
Defective lymphovenous valve development			
Hdac3^{TekKO}	E13.5	*Hdac3*^{TekKO} (3/3): *Control* (0/3)	*P = 0.0143*
Hdac3^{Cdh5KO}	E17.5	*Hdac3*^{Cdh5KO} (3/3): *Control* (0/3)	*P = 0.0143*

Among class I HDACs, murine embryos lacking Hdac1 or Hdac2 in the endothelial cells (*Hdac1*^{TekKO} or *Hdac2*^{TekKO}) appeared normal, with complete segregation of blood and lymphatic vasculature (Figure 2.4, A and B).

To determine whether ubiquitously expressed Hdac3 functions within platelets to maintain separation of the venous and lymphatic vasculature during development, we deleted Hdac3 in the platelets using *PF4-iCre* (*Hdac3*^{PF4KO}) (Tiedt et al., 2007). *Hdac3*^{PF4KO} neonatal mice were viable, appeared normal, and displayed complete blood-lymph separation (Figure 2.5, A–S). Together, these results suggest that Hdac3 functions in LECs to regulate separation of the blood and lymphatic systems during development.

Figure 2.4

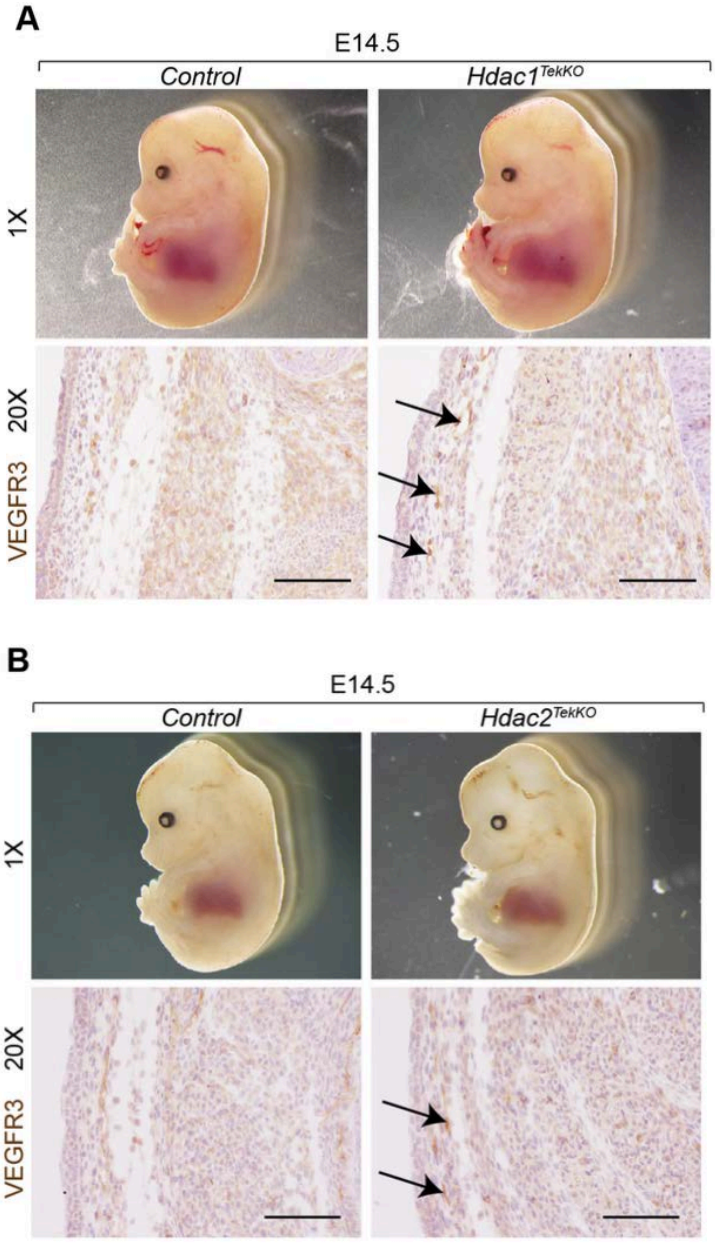

Figure 2.4 Dissected E14.5 *Hdac1*^{TekKO} (A) and *Hdac2*^{TekKO} (B) embryos appear normal. Lymphatic vessels in E14.5 *Hdac1*^{TekKO} and *Hdac2*^{TekKO} embryos do not show blood cells (black arrows). Scale bar, 100µm.

Figure 2.5

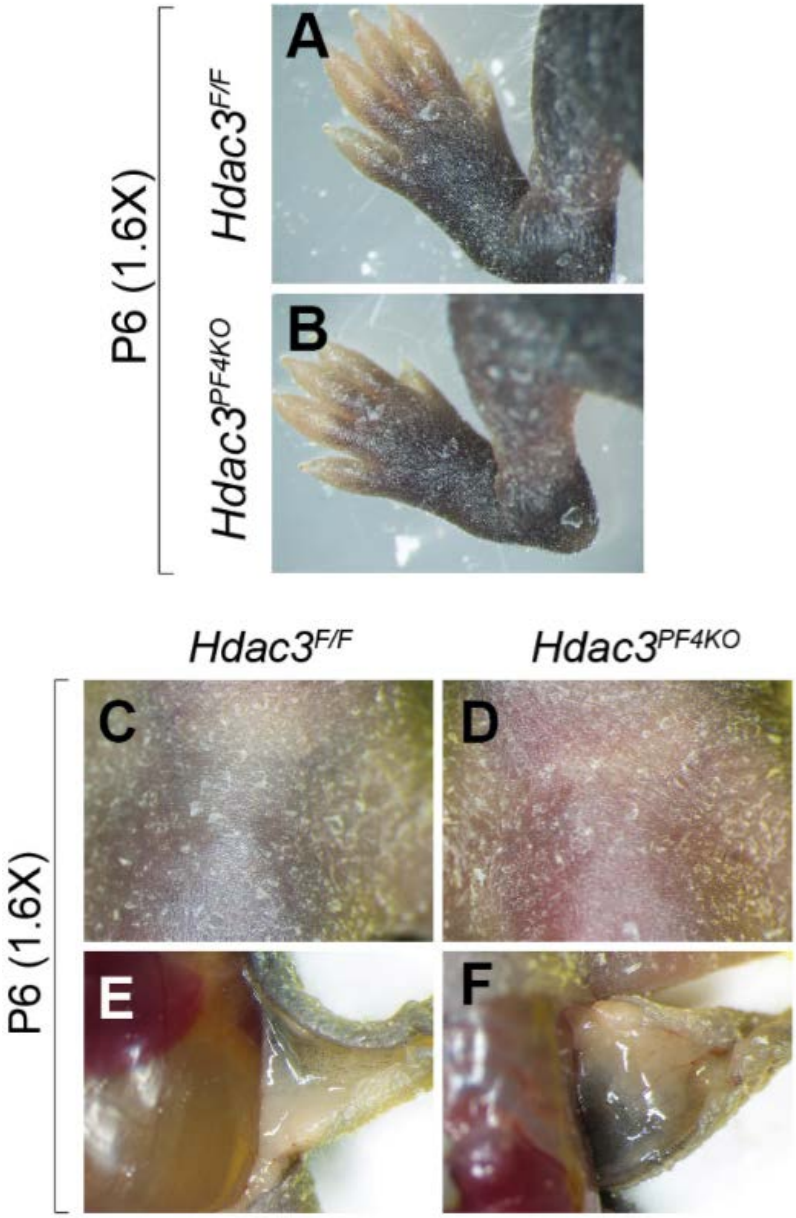
P6 (1.6X)
Hdac3F/F
Hdac3PF4KO
A
B
Hdac3F/F
Hdac3PF4KO
P6 (1.6X)
C
D
E
F

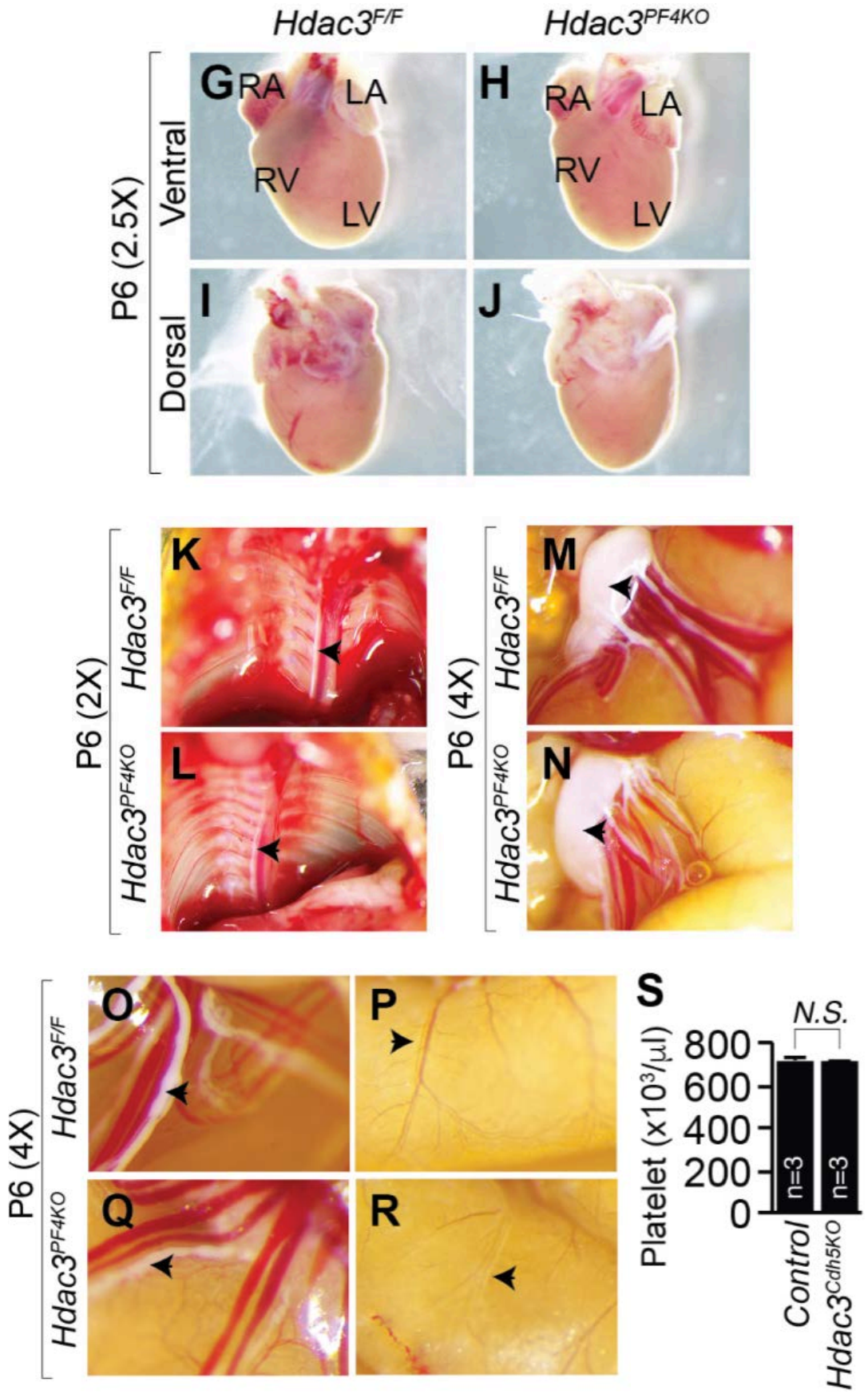
Hdac3F/F
Hdac3PF4KO
P6 (2.5X)
Ventral
Dorsal
G
H
I
J
RA
LA
RV
LV
P6 (2X)
P6 (4X)
Hdac3F/F
Hdac3PF4KO
K
L
M
N
O
P
Q
R
S
Platelet (x10³/μl)
800
600
400
200
0
N.S.
n=3
n=3
Control
Hdac3Cdh5KO

Figure 2.5 Platelet Hdac3 is dispensable for blood-lymphatic separation. (A-B) *Hdac3*^{PF4KO} mice do not show hindlimb edema (B) compared to control (A). (C-F) Perinatal (P6) *Hdac3*^{PF4KO} mice do not display abnormal blood-filled dermal vessels (D, F) compared to control (C, E). (G-J) *Hdac3*^{PF4KO} heart does not show ectatic and hemorrhagic superficial vessels at P6 (H, J) compared to control (G, I). (K-L) Dissected P6 *Hdac3*^{PF4KO} mice do not show blood-filled thoracic duct (L, arrow) compared to chyle-filled thoracic duct (K, black arrow) in control. (M-R) *Hdac3*^{PF4KO} P6 mice show normal chyle-filled white mesentery lymph node (N), intestinal lymphatic vessels (Q), and mesenteric lymphatic vessels (R) compared to control (M, O, P). (S) *Hdac3*^{Cdh5KO} P6 mice show normal platelet counts compared to control. Data represent the mean ± SEM and are representative of three independent experiments. P values are determined by Student's t test. N.S., not significant.

Hdac3 regulates lymphovenous valve development. Bicuspid lymphovenous valves, located at the thoracic duct–subclavian vein junction and right lymphatic duct–subclavian vein junction, maintain the separation between the high-pressure vascular system and the low-pressure lymphatic system (Hess et al., 2013; Srinivasan et al., 2011). To investigate blood pooling in the jugular region of the embryos lacking endothelial Hdac3 (Figure 2.2B), we examined the morphology of developing lymphovenous valves and lymph sac in transverse and coronal sections (Figure 2.6, A–C). Embryos lacking endothelial Hdac3 displayed abnormal blood-filled lymph sacs at various developmental stages (Figure 2.6, D, F, and G, and Figure 2.7). Endothelial cells lining blood-filled lymph sacs in Hdac3-null embryos revealed similar expression levels of Lyve1 or Vegfr3 (Figure 2D and Figure 2.7). Consistent with this observation, the thoracic duct in *Hdac3*^{Cdh5KO} neonates showed infiltration of blood into the normally lymph-filled duct, suggesting a functional lymphovenous valve defect (Figure 2.6, E). Indeed, *Hdac3*^{TekKO}, *Hdac3*^{Cdh5KO}, and *Hdac3*^{Lyve1KO} embryos displayed shortened lymphovenous valve leaflets with defective perpendicular alignment to the flow direction (Figure 2.6, F–H).

Figure 2.6

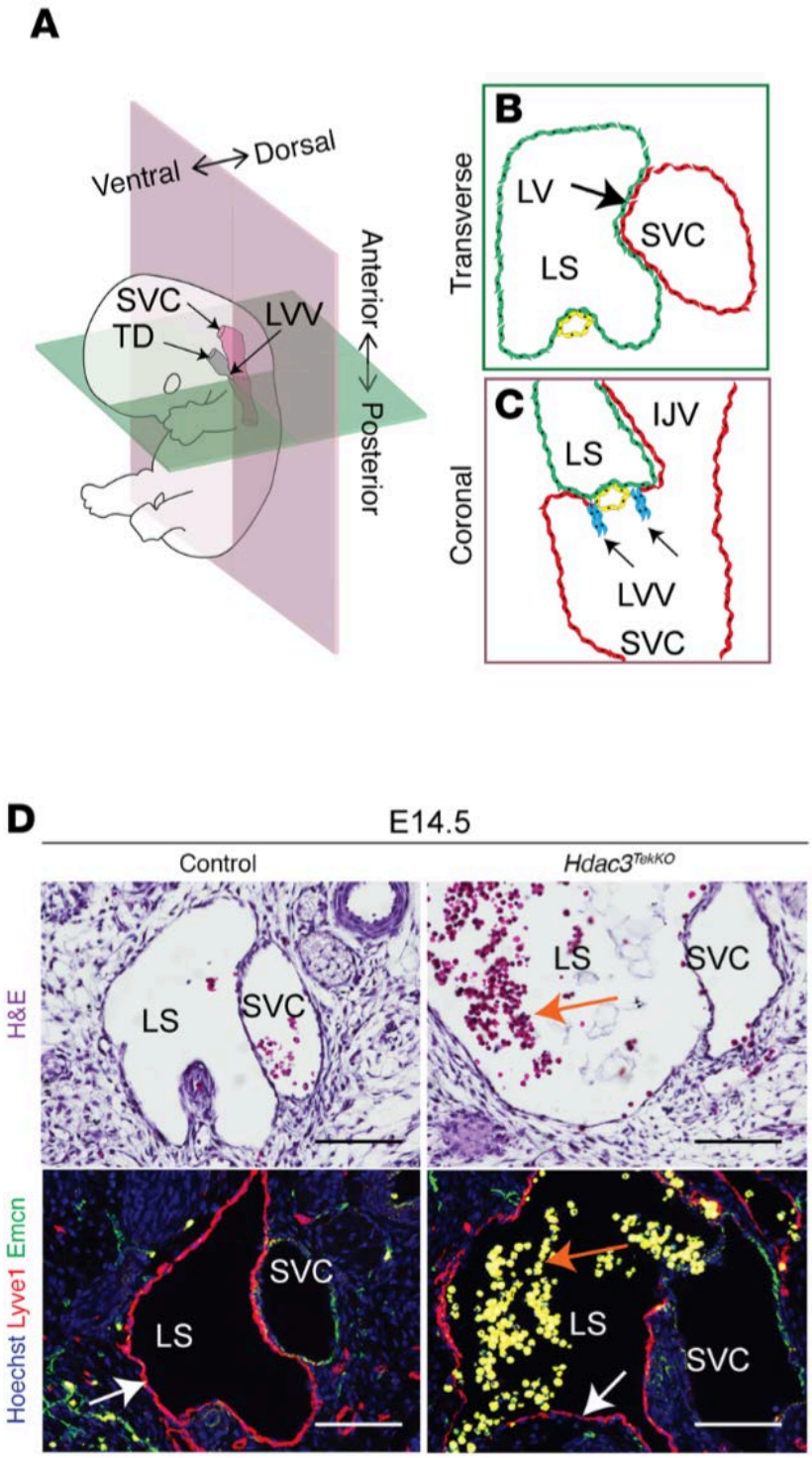
A
Ventral
Dorsal
Anterior
Posterior
SVC
TD
LVV
B
Transverse
LV
SVC
LS
C
Coronal
IJV
LS
LVV
SVC
D
E14.5
Control
Hdac3TekKO
H&E
LS
SVC
LS
SVC
Hoechst Lyve1 Emcn
SVC
LS
LS
SVC

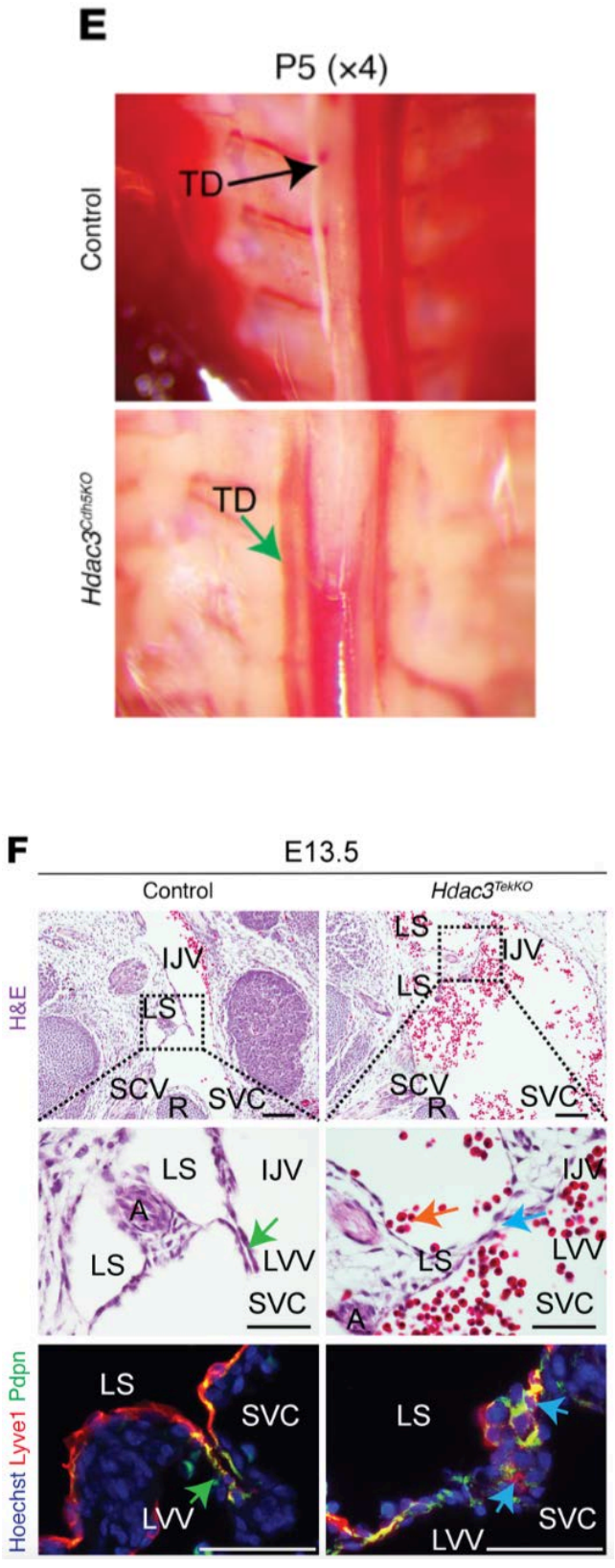
E
P5 (×4)
Control
TD
Hdac3Cdh5KO
TD
F
E13.5
Control
Hdac3TekKO
H&E
IJV
LS
SCV
R
SVC
LS
IJV
LS
SCV
R
SVC
LS
IJV
A
LS
LVV
SVC
IJV
LS
LVV
SVC
A
Hoechst Lyve1 Pdpn
LS
SVC
LVV
LS
SVC
LVV

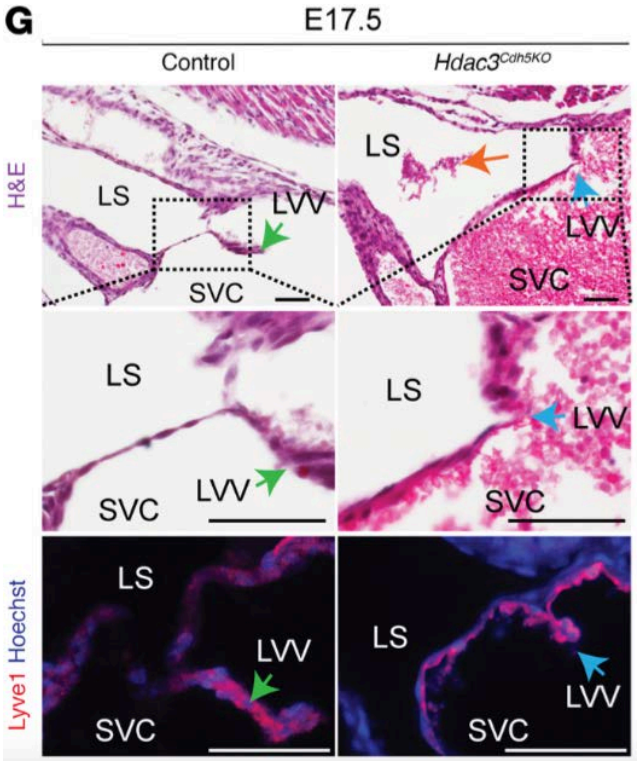
G
E17.5
Control
Hdac3Cdh5KO
H&E
LS
LVV
SVC
Lyve1 Hoechst

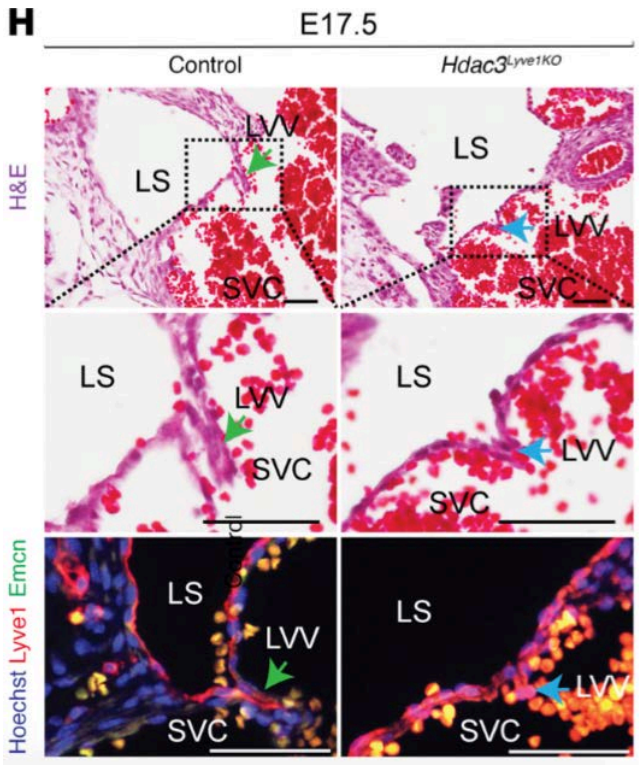
H
E17.5
Control
Hdac3Lyve1KO
H&E
LS
LVV
SVC
Hoechst Lyve1 Emcn

Figure 2.6 Hdac3 is an important regulator of lymphovenous valve development. (A–C) Schematic model depicting normal anatomy of a developing murine lymphovenous valve (A, black arrow) in transverse (B) and coronal (C) planes. (D) Transverse sections of E14.5 *Hdac3*^{TekKO} embryos revealed bloodfilled lymph sacs (orange arrows) lined by lymphatic (Lyve1 immunostaining [red], white arrows), but not venous (Emcn immunostaining, green), endothelial cells compared with that seen in controls. (E) Dissected P5 *Hdac3*^{Cdh5KO} mice had a blood-filled thoracic duct (green arrow) compared with a chyle-filled thoracic duct in control mice (black arrow). (F) H&E-stained coronal sections of an E13.5 *Hdac3*^{TekKO} embryo revealed a blood-filled lymph sac (orange arrow) and disrupted morphology of the lymphovenous valves (green arrows) compared with controls (yellow arrows). Immunofluorescence staining for podoplanin (Pdpn) (green) and Lyve1 (red) showed overlapping expression (yellow) in E13.5 LVVs. Orange arrow indicates a blood-filled lymph sac. (G and H) H&E-stained coronal sections of E17.5 *Hdac3*^{Cdh5KO} (G) and *Hdac3*^{Lyve1KO} (H) embryos revealed disrupted morphology of the lymphovenous valves (blue arrows) compared
with controls (green arrows). Orange arrow shows a blood-filled lymph sac. Lyve1 (red) was expressed in E17.5 murine lymphovenous valves (G and H). Emcn (green, venous marker) was used as a negative control for lymphovenous valves (H). IJV, internal jugular vein; LS, lymph sac; LVV, lymphovenous valve; SVC, superior vena cava; TD, thoracic duct. Scale bars: 100 µm and 50 µm (F, bottom panels, G, and H). See also Figure 2.7 and Table 2.5.

Figure 2.7

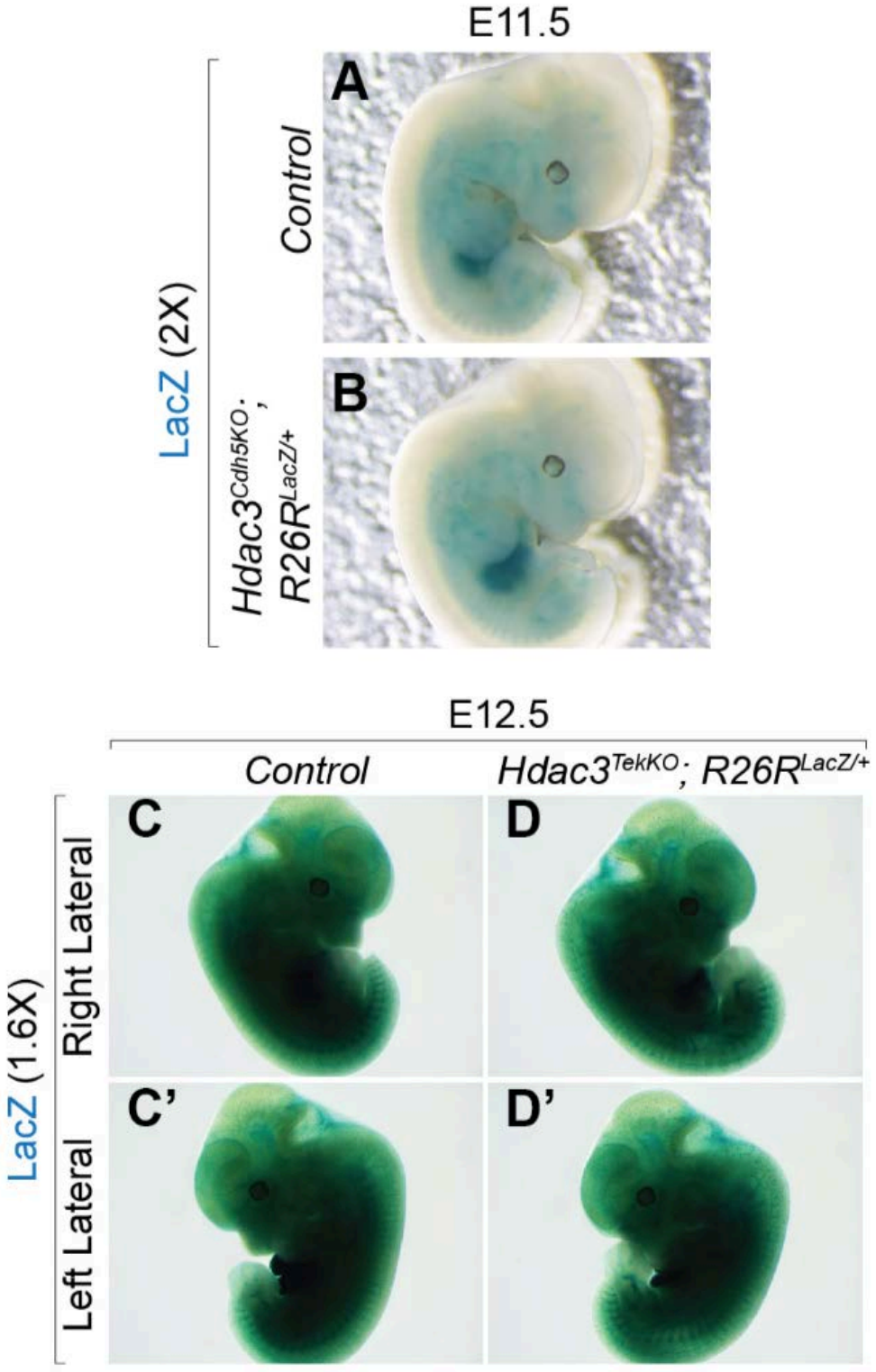
E11.5
LacZ (2X)
Control
A
Hdac3Cdh5KO; R26RLacZ/+
B
E12.5
Control
Hdac3TekKO; R26RLacZ/+
LacZ (1.6X)
Right Lateral
C
D
Left Lateral
C'
D'

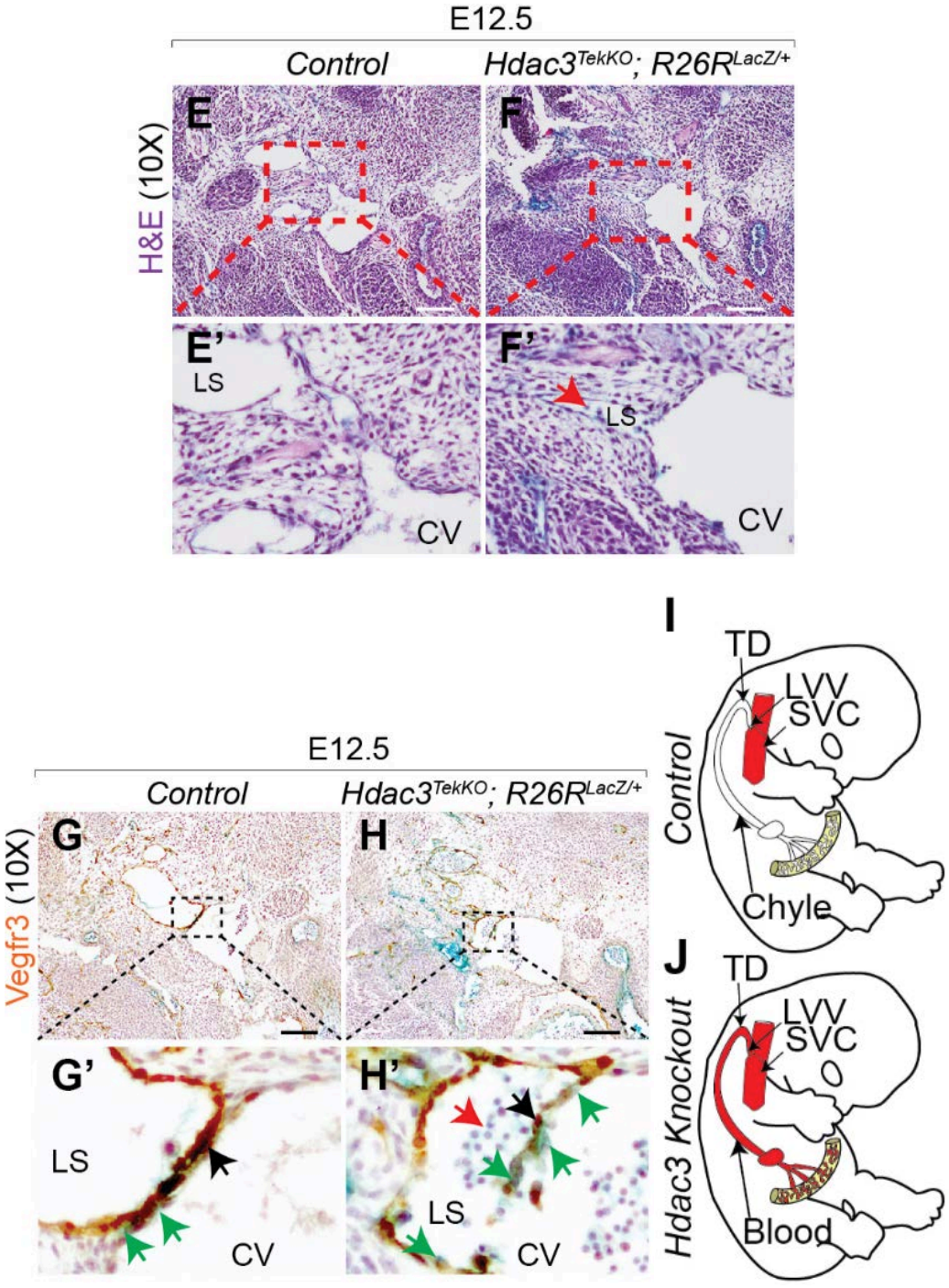
E12.5
Control
Hdac3TekKO; R26RLacZ/+
H&E (10X)
E
F
E'
LS
CV
F'
LS
CV
I
TD
LVV
SVC
Control
Chyle
E12.5
Control
Hdac3TekKO; R26RLacZ/+
Vegfr3 (10X)
G
H
G'
LS
CV
H'
LS
CV
J
TD
LVV
SVC
Hdac3 Knockout
Blood

Figure 2.7 Endothelial Hdac3 is a critical regulator of blood-lymphatic seperation at a early stage of development. (A-D) Whole-mount LacZ staining of control (A, C, C') and *Hdac3*^{Cdh5KO}; *R26R*$^{LacZ/+}$ (B) or *Hdac3*^{TekKO}; *R26R*$^{LacZ/+}$ (D, D') at E11.5 and E12.5, respectively, show similar level and pattern of LacZ expression. (E-H) H&E-stained transverse sections of LacZ-stained E12.5 *Hdac3*^{TekKO} (E, F) embryos reveal blood-filled lymph sacs (F', H' red arrows) compared to control (E', G'). Vegfr3 immunostaining (G-H) shows LECs-specific expression (G', H', black arrows) in LacZ+ (G', H', green arrows) E12.5 murine lymph sac. (I-J) Schematic model depicting loss of blood-lymphatic separation between SVC and TD due to defective lymphovenous valve development in Hdac3-null mice. H&E, Hematoxylin and Eosin; CV, cardinal vein; LS, lymph sac. Scale bar, 100mm.

Hdac3 regulates proper lymphatic transport and mesenteric lymphatic valve maturation. Dysfunctional intraluminal lymphatic valves in collecting lymphatic vessels impede the ability of the lymphatic system to effectively transport lymph, leading to lymphedema (Jurisic and Detmar, 2009; Petrova et al., 2004). To study the lymph transport in *Hdac3*^{Cdh5KO} neonates, we determined retrograde lymphatic flow reflux using Evans blue dye (Figure 2.8, A–E). *Hdac3*^{Cdh5KO} neonates had abnormal retrograde flow of Evans blue dye into the tail, right hind limb, abdomen, dermal lymphatic vessels, mesenteric lymphatic vessels, and mesenteric lymph nodes (Figure 2.8, A–D). We also observed Evans blue dye in intercostal lymphatics lateral to the thoracic duct in the thoracoepigastric region, coupled with reduced contrast drainage into the thoracic duct in *Hdac3*^{Cdh5KO} neonates compared with the control (Figure 2.8E), suggesting a severe impairment of lymph transport. Consistent with this observation, Lyve1+ dermal lymphatic capillaries revealed anomalous recruitment of smooth muscle cells in P6 *Hdac3*^{Cdh5KO} neonates (Figure 2.8F).

Figure 2.8

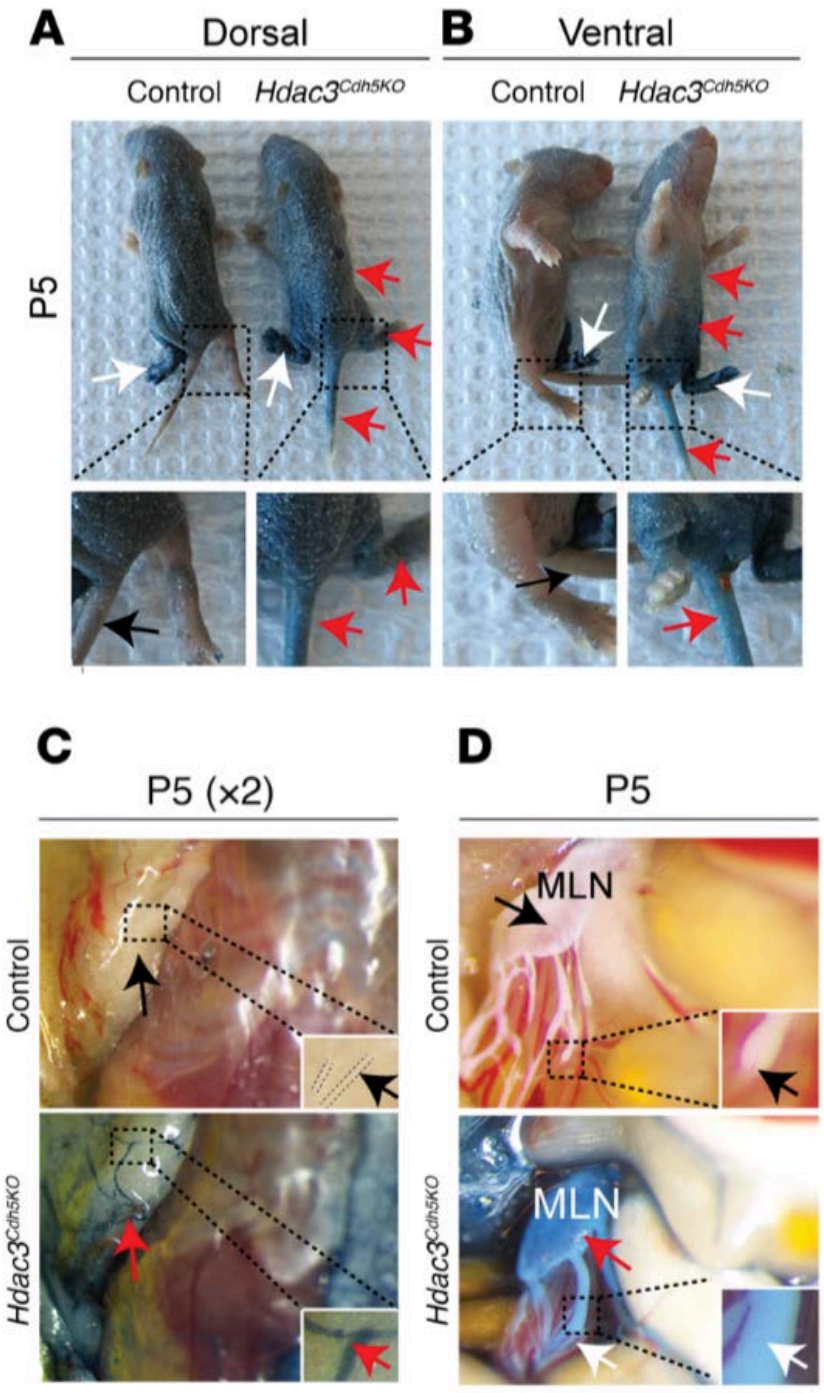
A
Dorsal
Control
Hdac3Cdh5KO
B
Ventral
Control
Hdac3Cdh5KO
P5
C
P5 (×2)
D
P5
MLN
MLN
Control
Hdac3Cdh5KO
Control
Hdac3Cdh5KO

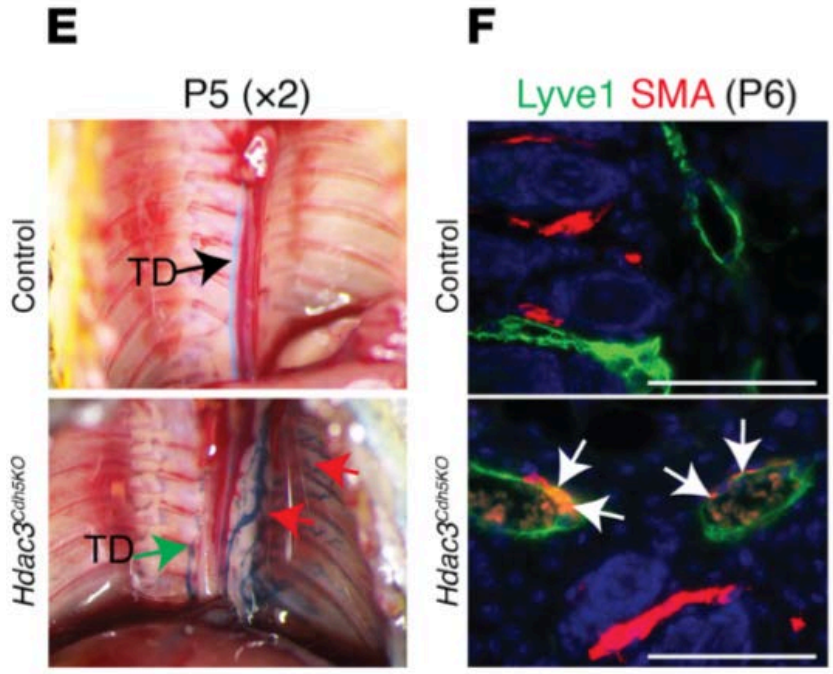
E
P5 (×2)
Control
TD
Hdac3Cdh5KO
TD
F
Lyve1 SMA (P6)
Control
Hdac3Cdh5KO

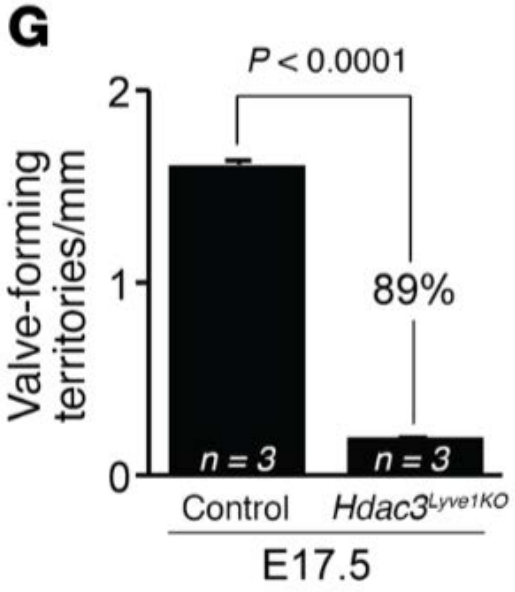
G
P < 0.0001
Valve-forming territories/mm
2
1
0
89%
n = 3
n = 3
Control
Hdac3Lyve1KO
E17.5

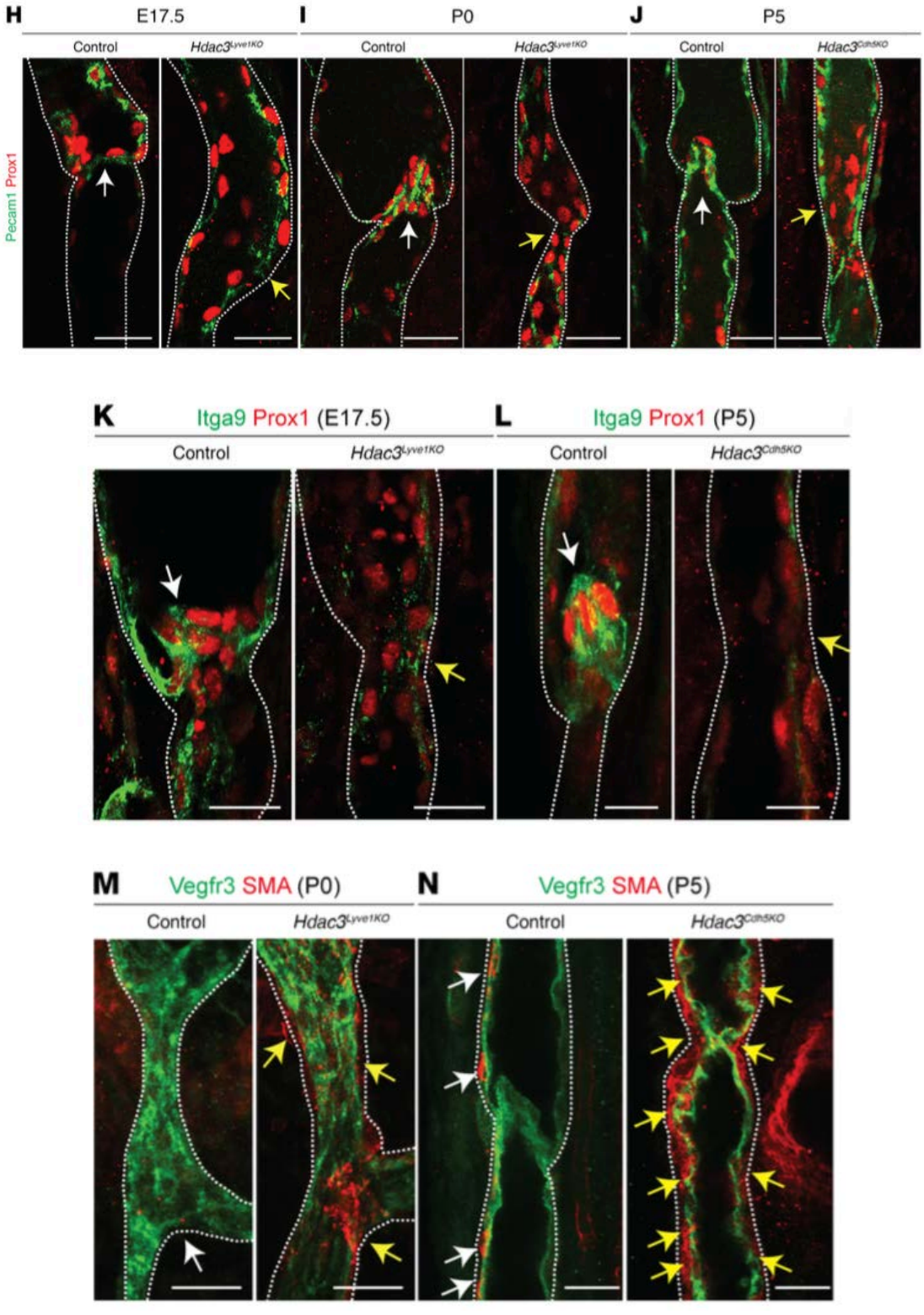
H
E17.5
I
P0
J
P5
Control
Hdac3Lyve1KO
Control
Hdac3Lyve1KO
Control
Hdac3Cdh5KO
Pecam1 Prox1
K
Itga9 Prox1 (E17.5)
L
Itga9 Prox1 (P5)
Control
Hdac3Lyve1KO
Control
Hdac3Cdh5KO
M
Vegfr3 SMA (P0)
N
Vegfr3 SMA (P5)
Control
Hdac3Lyve1KO
Control
Hdac3Cdh5KO

Figure 2.8 Hdac3 deficiency causes impaired lymphatic drainage and anomalous lymphatic valve development in mesenteric lymphatic vessels. (A and B) Evans blue dye injection into the left hind paw (A and B, white arrows) of P5 *Hdac3*^{Cdh5KO} mice showed reflux (retrograde flow) into the tail, right hind limb, and abdomen (A and B, red arrows) compared with an absence of reflux in the control mice (black arrows). Original magnification ×2.5. (C and D) P5 *Hdac3*^{Cdh5KO} mice showed Evans blue dye reflux (red arrows) into dermal lymph vessels and mesenteric lymph nodes compared with control mice (dotted line, black arrows). Original magnification ×3. (E) Control P5 mice showed normal unidirectional cephalad drainage restricted to the thoracic duct (black arrow). *Hdac3*^{Cdh5KO} mice exhibited reflux into the intercostal lymphatics lateral to the thoracic duct in the thoracoepigastric region (red arrows) and reduced drainage into the thoracic duct (green arrow). (F) Coimmunofluorescence staining for Lyve1 (green) and smooth muscle actin (SMA) (red) showed abnormal smooth muscle recruitment (white arrows) to blood-filled dermal lymphatic capillaries in P6 *Hdac3*^{Cdh5KO} mice compared with controls. (G) Quantitation of lymphatic valve territories in E17.5 *Hdac3*^{Lyve1KO} mesenteric lymphatic vessels. The P value was determined by unpaired Student's t test. (H–J) Whole-mount coimmunofluorescence staining of *Hdac3*^{Lyve1KO} (H and I) and *Hdac3*^{Cdh5KO} (J) mesenteric lymphatic vessels showed a lack of Prox1-expressing (red) lymphatic valves in Pecam1+ (green) lymphatic vessels (yellow arrows) compared with controls (white arrows). (K and L) Whole-mount coimmunofluorescence staining of *Hdac3*^{Lyve1KO} (K) and *Hdac3*^{Cdh5KO} (L) mesenteric lymphatic vessels showed a lack of Itga9-expressing (green) lymphatic valves in Prox1+ (red) lymphatic vessels (yellow arrows) compared with controls (white arrows). (M and N) Whole-mount coimmunofluorescence staining of *Hdac3*^{Lyve1KO} (M) and *Hdac3*^{Cdh5KO} (N) mesenteric lymphatic vessels showed excessive SMA (red) coverage (yellow arrows) compared with controls (white arrows). Vegfr3 (green) was used as a lymphatic vessel marker. Data represent the mean ± SEM and are representative of 3 independent experiments. Sub-stacks of Z-stack images are presented in H–N. Scale bars: 100 μm (F) and 1 μm (H–N). See also Figure 2.9.

Additionally, Hdac3-deficient mesenteric lymphatic vessels showed immature and reduced numbers of lymphatic valves at various stages of development (Figure 2.8, G–N, and Figure 2.9, A–D). Prox1 and Pecam1 whole-mount immunofluorescence costaining analyses revealed fewer and disorganized Prox1Hi LEC clusters in *Hdac3*^{Cdh5KO} and *Hdac3*^{Lyve1KO} lymphatic vessels (Figure 2.8, H–J, and Figure 2.9, A–D). *Hdac3*^{Cdh5KO} and *Hdac3*^{Lyve1KO} lymphatic vessels showed reduced integrin-α9 expression within lymphatic valve sites (Figure 2.8, K and L). In addition, Hdac3-deficient lymphatic collecting vessels exhibited excessive smooth muscle cell coverage compared with controls (Figure 2.8, M and N).

Figure 2.9

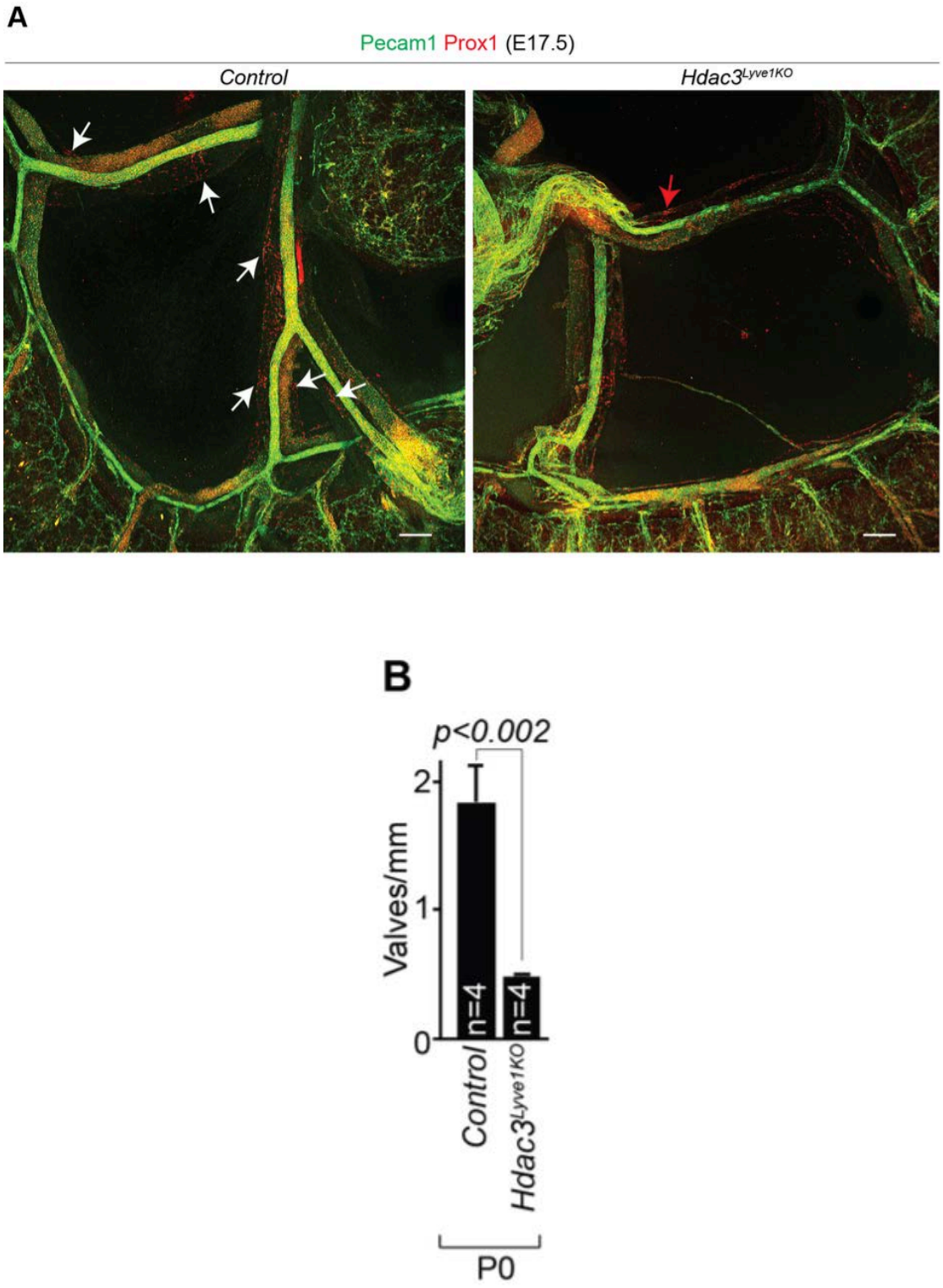
A
Pecam1 Prox1 (E17.5)
Control
Hdac3Lyve1KO
B
p<0.002
Valves/mm
2
1
0
n=4
n=4
Control
Hdac3Lyve1KO
P0

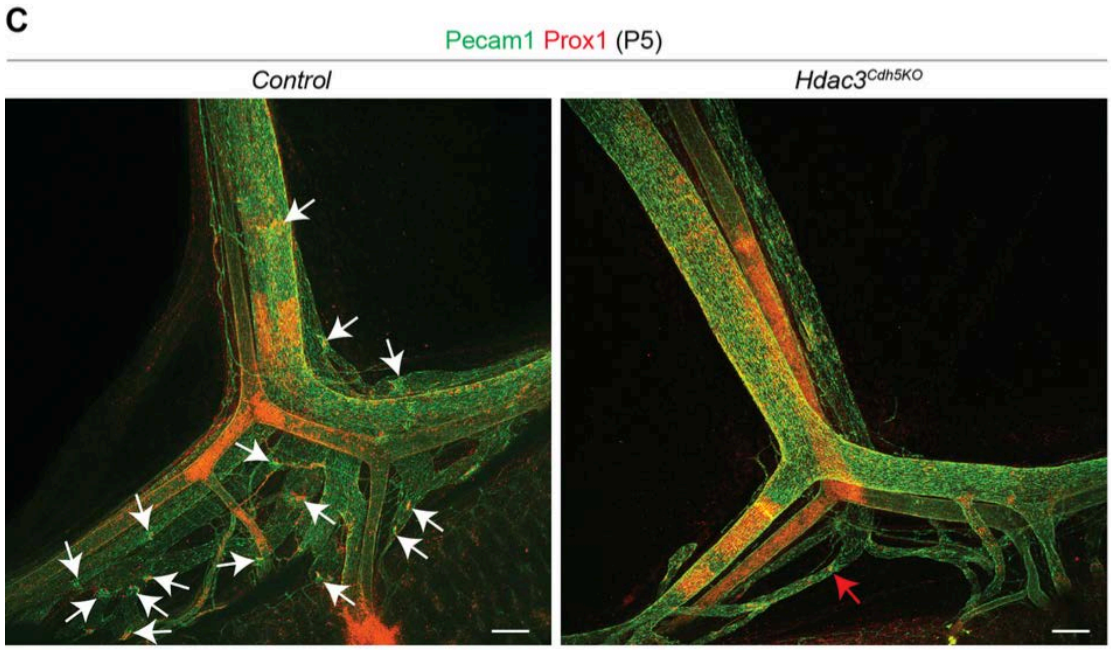
C
Pecam1 Prox1 (P5)
Control
Hdac3Cdh5KO

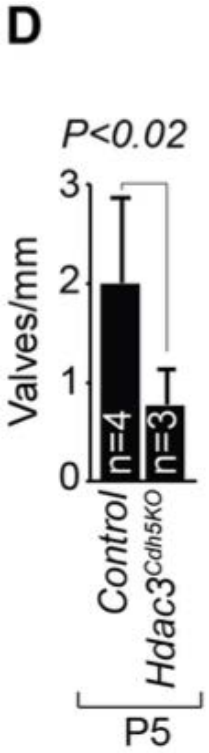
D
P<0.02
Valves/mm
3
2
1
0
n=4
n=3
Control
Hdac3Cdh5KO
P5

Figure 2.9 Whole-mount co-immunofluorescent staining of E17.5 *Hdac3*^{Lyve1KO} mesenteric lymphatic vessels show reduced number of Prox1 (red) expressing valve forming territories in Pecam1+ (green) lymphatic vessels (red arrows) compared to control (white arrows). (B) Quantitation of lymphatic valves in P0 *Hdac3*^{Lyve1KO} mesenteric lymphatic vessels. (C) Whole-mount co-immunofluorescent staining of P5 *Hdac3*^{Cdh5KO} mesenteric lymphatic vessels lake mature Prox1 (red) expressing valves in Pecam1+ (green) lymphatic vessels (red arrows) compared to control (white arrows). (D) Quantitation of lymphatic valves in P5 *Hdac3*^{Cdh5KO} mesenteric lymphatic vessels. Data represent the mean ± SEM and are representative of three independent experiments. P values are determined by Student's t test. Scale bar, 100µm.

Hdac3 regulates Gata2 expression in developing lymphovenous and lymphatic valves. Transcriptional analysis of mesenteric lymphatic vessels dissected from *Hdac3*^{Cdh5KO} neonates revealed downregulation of genes required for lymphatic valve development (Kazenwadel et al., 2015; Sabine et al., 2015; Sweet et al., 2015), such as Gata2, Foxc2, Gja4, and Itga9 (Figure 2.10A). *Hdac3*^{Cdh5KO} lymphatic vessels had endothelial marker gene transcript expression levels similar to those observed in controls (Figure 2.11A). Loss of Hdac3 in mesenteric lymphatic endothelium also resulted in reduced Prox1 expression (Figure 2.10B).

Consistent with this observation, we found that *Hdac3*^{Lyve1KO} lymphatic vessels had downregulated expression of Gata2 and Foxc2 (Figure 2.10C). Using laser-capture microdissection (LCMD), we collected lymphovenous valves from serial coronal sections of E13.5 murine embryos (Figure 2.11, B–D). *Hdac3*^{TekKO} lymphovenous valves revealed similar expression levels of endothelial marker gene transcripts (Figure 2.11D), but downregulation of Gata2, Foxc2, Gja4, and Itga9 transcripts, compared with expression levels in controls (Figure 2.10D). Consistent with this observation, IHC revealed reduced expression of Gata2, Foxc2, and Prox1 in the developing *Hdac3*^{TekKO} lymphovenous valves (Figure 2.10, E–G).

Figure 2.10

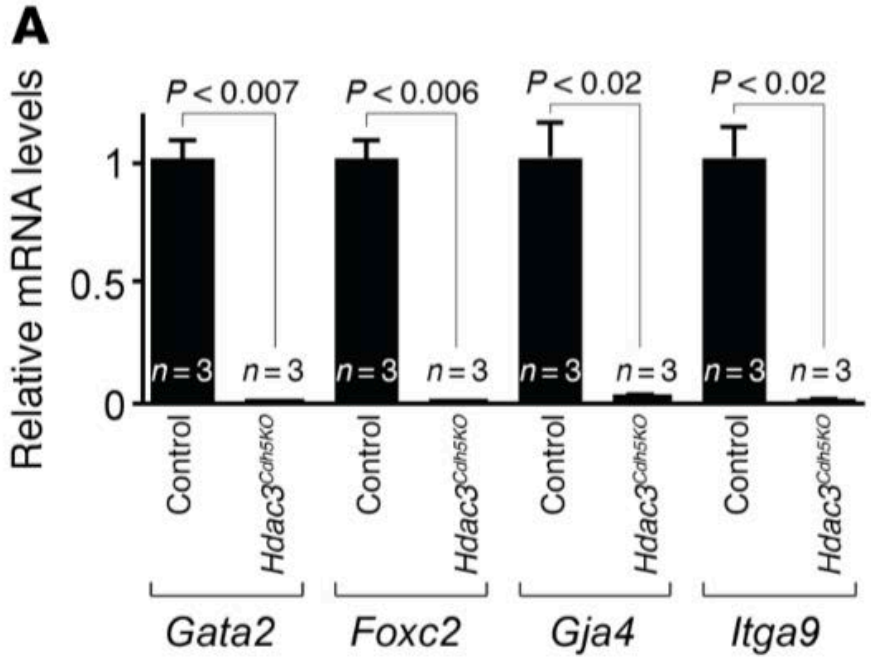
A
Relative mRNA levels
P < 0.007
P < 0.006
P < 0.02
P < 0.02
1
0.5
0
n = 3
Control
Hdac3Cdh5KO
Gata2
Foxc2
Gja4
Itga9

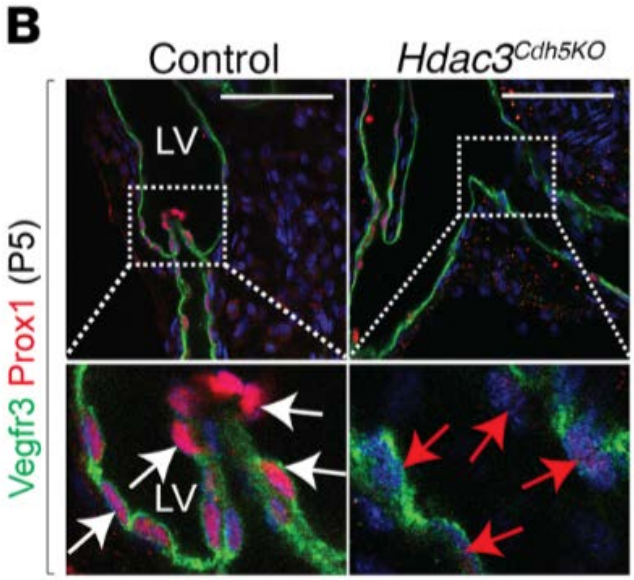
B
Control
Hdac3Cdh5KO
LV
Vegfr3 Prox1 (P5)

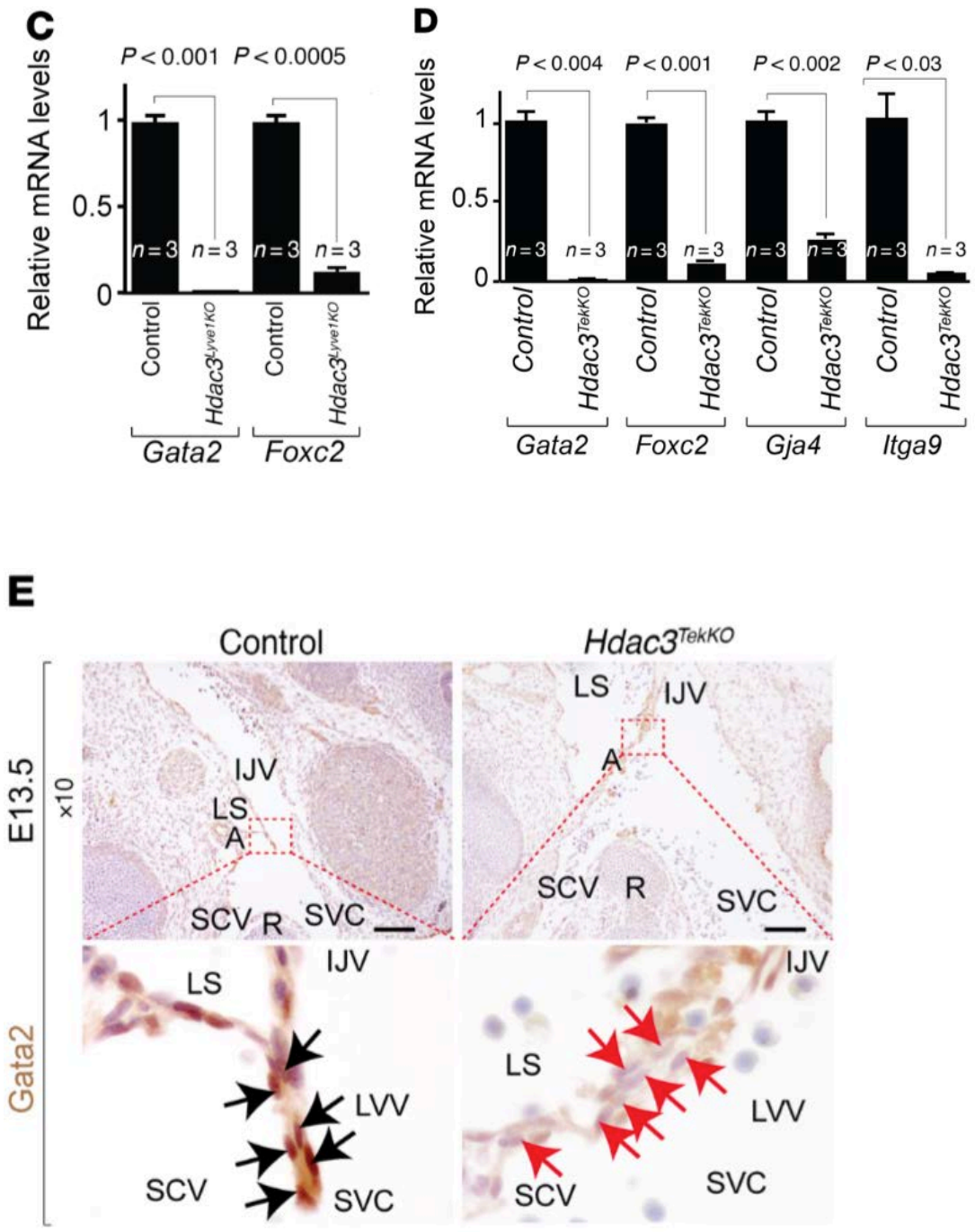
C
Relative mRNA levels
P < 0.001
P < 0.0005
1
0.5
0
n = 3
Control
Hdac3Lyve1KO
Gata2
Foxc2
D
P < 0.004
P < 0.001
P < 0.002
P < 0.03
Hdac3TekKO
Gja4
Itga9
E
Control
Hdac3TekKO
E13.5
×10
Gata2
IJV
LS
A
SCV
R
SVC
LVV

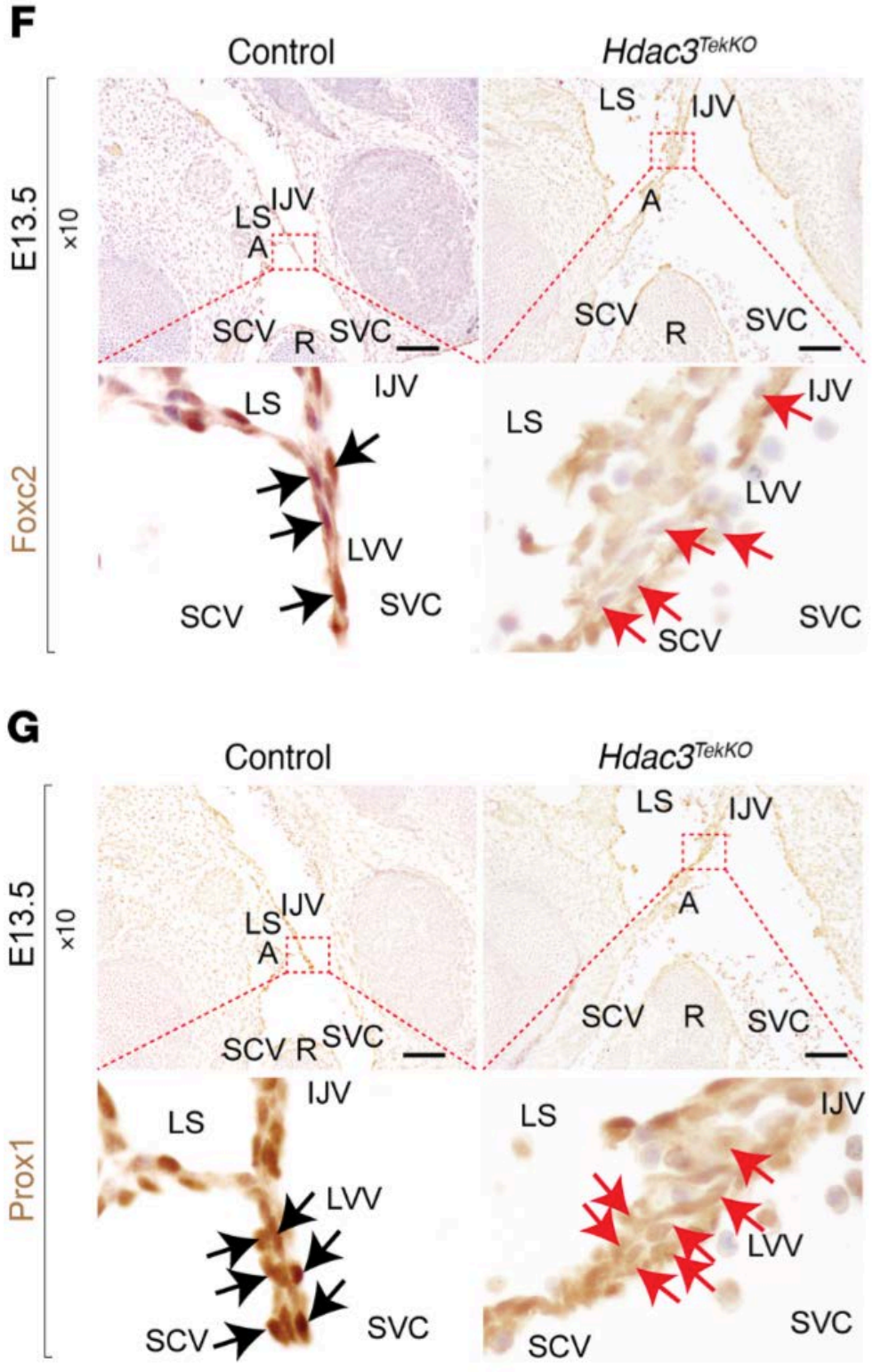
F
Control
Hdac3TekKO
E13.5
×10
Foxc2
LS
IJV
A
SCV
R
SVC
LVV
G
Control
Hdac3TekKO
E13.5
×10
Prox1
LS
IJV
A
SCV
R
SVC
LVV

Figure 2.10 Hdac3 regulates Gata2 and its target gene expression in developing lymphatic valves and lymphovenous valves. (A) Transcripts for Gata2, Foxc2, Gja4, and Itga9 were detected by ChIP-qPCR in control and *Hdac3*^{Cdh5KO} mesenteric lymphatic vessels dissected from P5 mice. (B) Whole-mount immunofluorescence staining of *Hdac3*^{Cdh5KO} mesenteric lymphatic vessels identified reduced Prox1 (red) expression in Vegfr3+ (red) LECs (red arrows) compared with controls (white arrows). (C) Transcripts for Gata2 and Foxc2 were detected by ChIP-qPCR in control and *Hdac3*^{Lyve1KO} mesenteric lymphatic vessels dissected from P0 mice. (D) Transcripts for Gata2, Foxc2, Gja4, and Itga9 were detected by ChIP-qPCR in laser-captured control and *Hdac3*^{TekKO} lymphovenous valves from E13.5 embryos. (E–G) Immunostaining of E13.5 *Hdac3*^{TekKO} lymphovenous valves revealed reduced Gata2 (E, red arrows), Foxc2 (F, red arrows), and Prox1 (G, red arrows) expression compared with controls (black arrows). LV, lymphatic valve; R, rib. Data represent the mean ± SEM and are representative of 3 independent experiments. P values were determined by Student's t test. Scale bars: 500 μm. See also Figure 2.11.

Figure 2.11

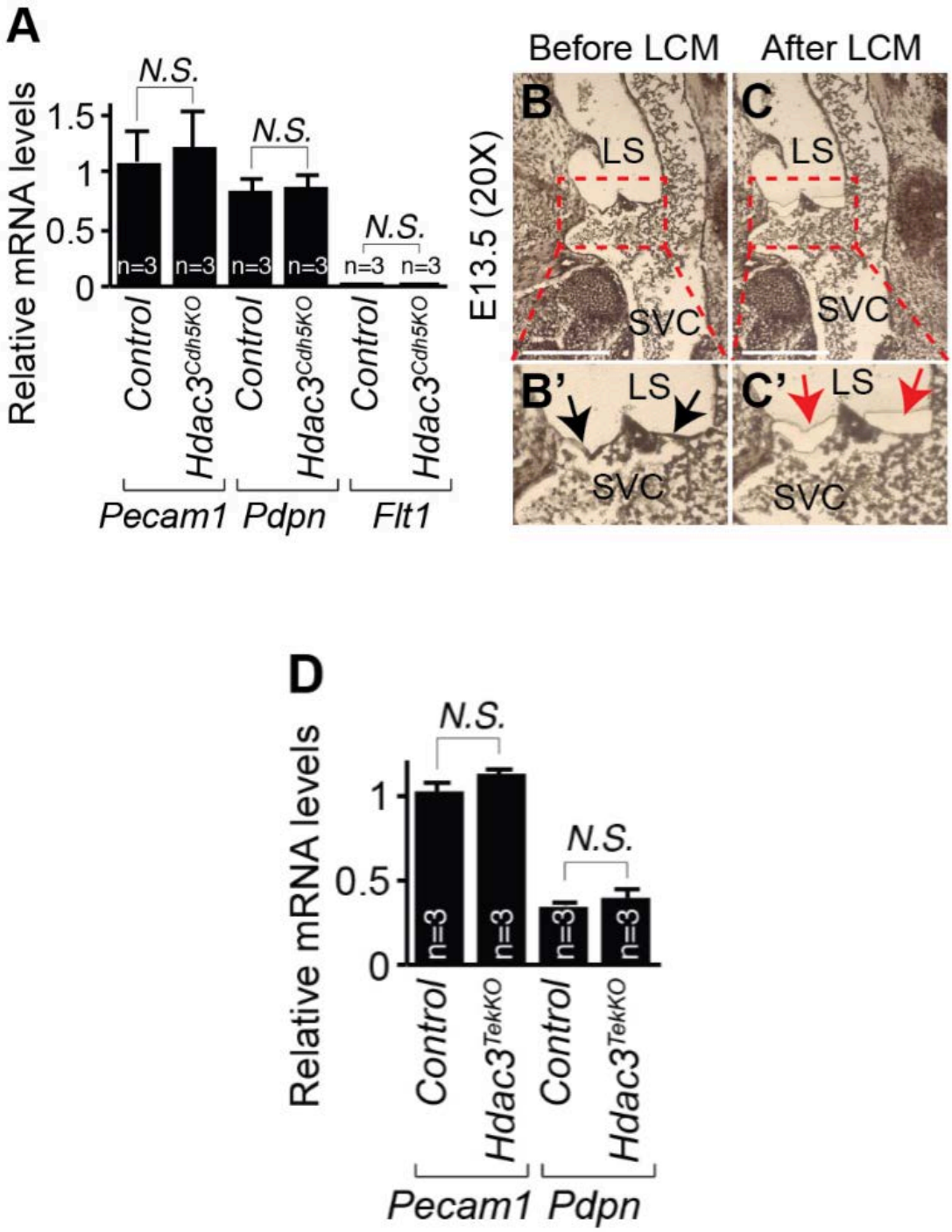
A
Relative mRNA levels
1.5
1
0.5
0
N.S.
N.S.
N.S.
n=3
Control
Hdac3Cdh5KO
Pecam1
Pdpn
Flt1
Before LCM
After LCM
E13.5 (20X)
B
C
B'
C'
LS
SVC
D
Relative mRNA levels
1
0.5
0
Control
Hdac3TekKO
Pecam1
Pdpn

Figure 2.11 (A) Transcripts for Pecam1, Pdpn, and Flt1 were detected by real-time qPCR in control and *Hdac3*^{Cdh5KO} mesenteric lymphatic vessels dissected from P5 mice. (B-C) Lymphovenous valves (B, B', black arrows) were microdissected (C, C', red arrows) from coronal sections of E13.5 murine embryos using laser capture. (D) Transcripts for Pecam1 and Pdpn were detected by real-time qPCR in control and *Hdac3*^{TekKO} lymphovenous valves laser captured from E13.5 embryos. Data represent the mean ± SEM and are representative of three independent experiments. P values are determined by Student's t test. SVC, superior vena cava; LS, lymph sac; LCM, laser capture microdissection. Scale bar, 100μm.

Hdac3 regulates OSS-mediated activation of the Gata2 intragenic enhancer. Lymph flow and OSS upregulate genes required for lymphatic valve development including Gata2 (Sabine et al., 2012; Sweet et al., 2015). Gata2, an important transcription factor for blood-lymph separation and development of lymphovenous and lymphatic valves, is an upstream transcriptional regulator of Foxc2, Prox1, Gja4, and Itga9 (Brouillard et al., 2014; Kazenwadel et al., 2015; Lim et al., 2012; Sweet et al., 2015). In addition, the Gata2 intragenic enhancer is both sufficient and necessary to drive Gata2 expression within LECs (Khandekar et al., 2007; Lim et al., 2012). Ablation of this Gata2 intragenic enhancer in mice is sufficient to reduce Gata2 expression and phenocopy the endothelial knockout of Gata2 (Johnson et al., 2012). Hence, we examined the mechanism by which Hdac3 regulates Gata2 expression. To investigate whether Hdac3 regulates Gata2 expression in response to shear stress, we analyzed LECs cultured under static or OSS conditions (Figure 2.12A). LECs showed upregulation of Gata2, Foxc2, and Gja4 in response to OSS, and Hdac3 knockdown abolished this effect (Figure 2.12B and Figure 2.13A). Catalytically inactive enzymes are frequently present in most enzyme families including HDACs (Adrain and Freeman, 2012). The biological functions of these pseudoenzymes remain largely unknown. To determine whether deacetylase activity or chromatin recruitment of Hdac3 is required to regulate Gata2 expression in response to OSS, we overexpressed 2 different mutant forms of human HDAC3 in Hdac3-deficient LECs. The first mutant, HDAC3^{HEBI}, exhibits no enzymatic activity or chromatin recruitment, while

Figure 2.12

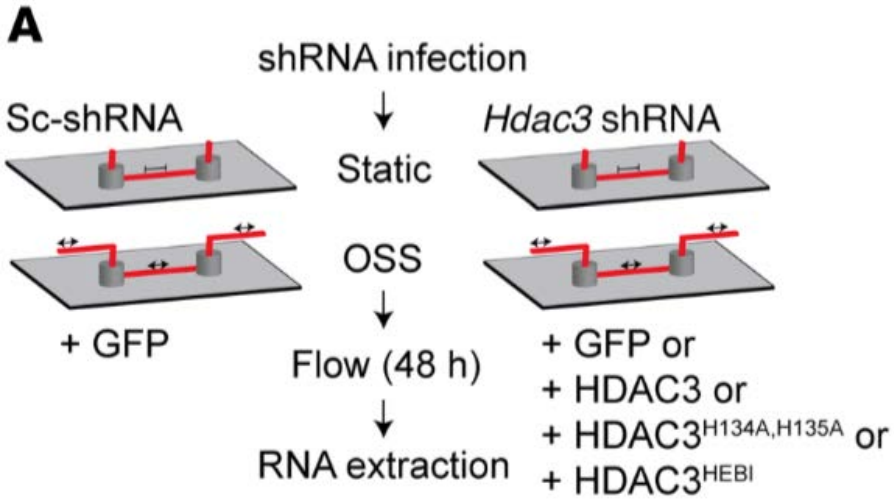
A
shRNA infection
Sc-shRNA
Hdac3 shRNA
Static
OSS
+ GFP
Flow (48 h)
RNA extraction
+ GFP or
+ HDAC3 or
+ HDAC3H134A,H135A or
+ HDAC3HEBI

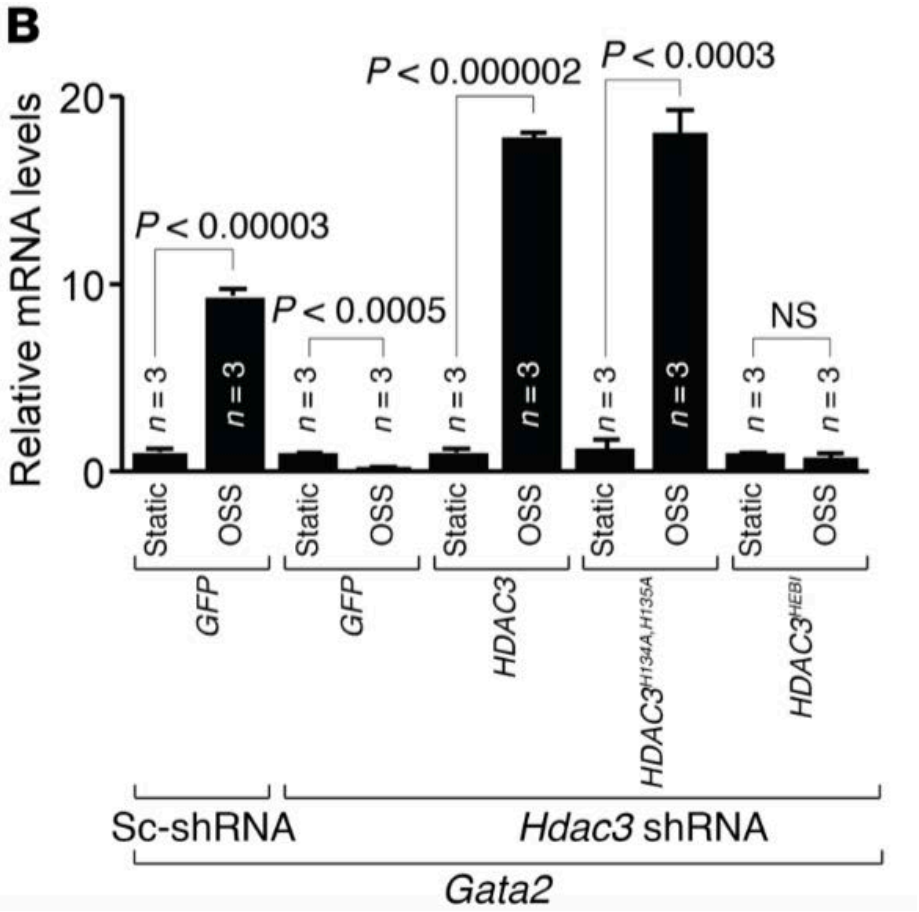
B
Relative mRNA levels
20
10
0
P < 0.00003
P < 0.0005
P < 0.000002
P < 0.0003
NS
n = 3
Static
OSS
GFP
GFP
HDAC3
HDAC3H134A,H135A
HDAC3HEBI
Sc-shRNA
Hdac3 shRNA
Gata2

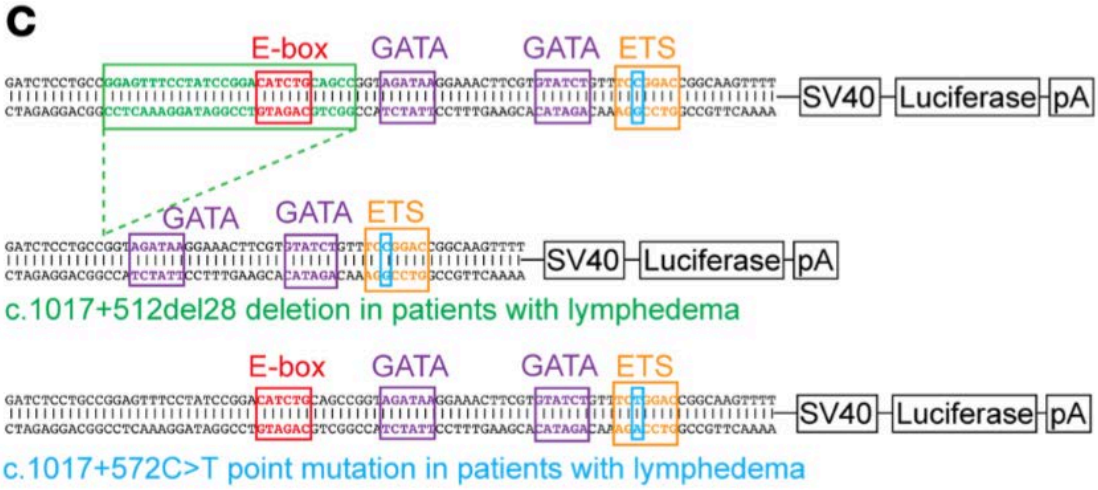
C
E-box
GATA
GATA
ETS
SV40
Luciferase
pA
c.1017+512del28 deletion in patients with lymphedema
c.1017+572C>T point mutation in patients with lymphedema

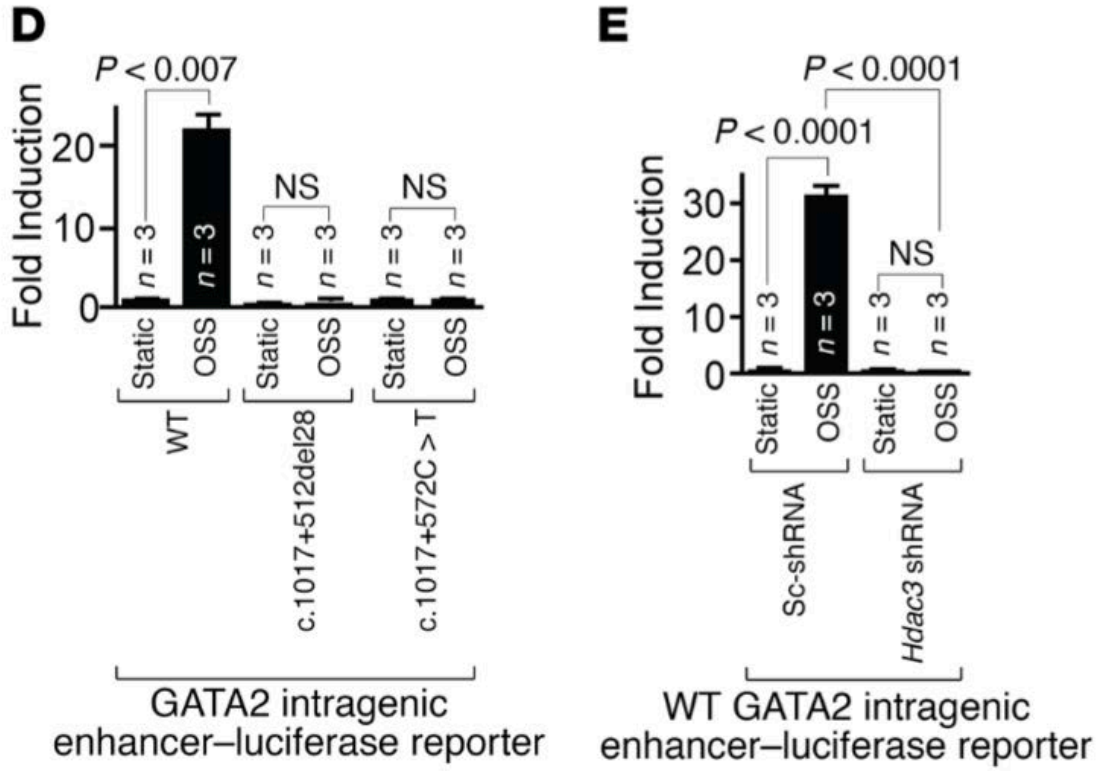

Figure 2.12 Hdac3 regulates oscillatory shear stress–mediated activation of the Gata2 intragenic enhancer. (A) Schematic of in vitro OSS assay. (B) Transcripts for Gata2 were detected by ChIP-qPCR in scrambled shRNA–(Sc-shRNA) or Hdac3 shRNA–infected LECs subjected to static or OSS conditions and coinfected with *GFP, HDAC3, HDAC3*^{H134A,H135A}, or *HDAC3*^{HEBI} lentiviruses. (C) Schematics of luciferase reporter vectors composed of WT (168 bp), c.1017+512del28 (28-bp deletion, green box, 140 bp), and the c.1017+572C>T point mutation (blue box) GATA2 intragenic enhancer. (D) A dual luciferase assay was performed in LECs transfected with WT, c.1017+512del28, or the c.1017+572C>T point mutation GATA2 intragenic enhancer luciferase reporter and subjected to static or OSS conditions. Induction is represented as a ratio of firefly to Renilla luciferase activity. (E) Scramble shRNA– or Hdac3 shRNA–infected LECs, cotransfected with the WT GATA2 intragenic enhancer luciferase reporter, were subjected to static or OSS conditions. Induction is represented as a ratio of firefly to Renilla luciferase activity. Data represent the mean ± SEM and are representative of 3 independent experiments. P values were determined by Student's t test (B and D) or by 1-way ANOVA with Sidak's multiple comparisons test (E). See also Figures 2.13 and 2.14

Figure 2.13

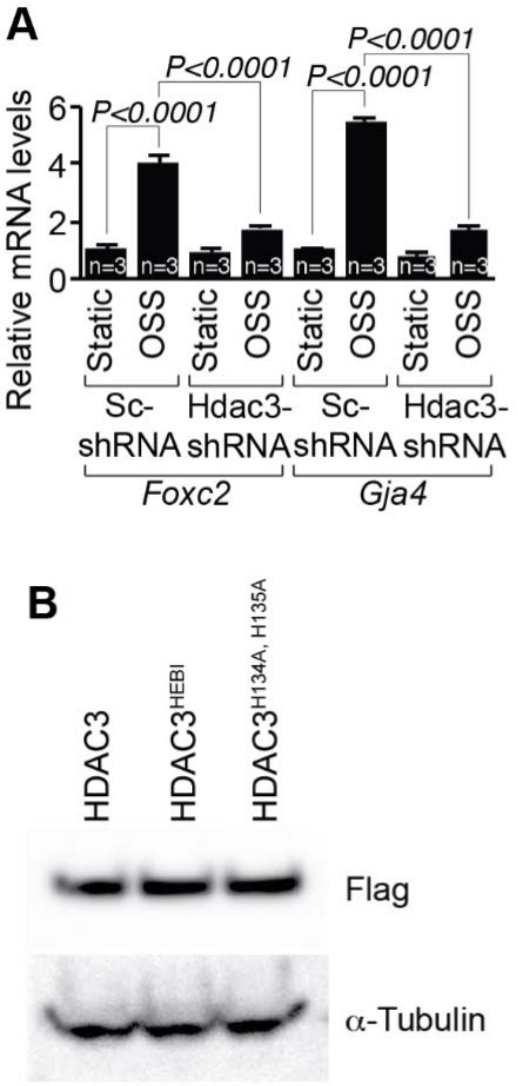

Figure 2.13 (A) Transcripts for Foxc2 and Gja4 were detected by real-time qPCR in Sc- or Hdac3-shRNA-infected LECs subjected to static or OSS and co-infected with GFP lentiviruses. (B) Total lysates from LECs expressing flag-tagged *HDAC3*, *HDAC3*^{HEBI}, or *HDAC3*$^{H134A, H135A}$ plasmids were analyzed by Western blot using anti-Flag antibody. a-Tubulin is shown as a loading control. Data represent the mean ± SEM and are representative of three independent experiments. P values are determined by one-way ANOVA using Sidak's multiple comparisons test. OSS, oscillatory shear stress; Sc, scramble.

the second mutant, HDAC3$^{H134A,\ H135A}$, lacks enzymatic activity but has preserved chromatin recruitment (Lewandowski et al., 2015; Sun et al., 2013). Flag-tagged WT and mutant HDAC3 plasmids showed similar levels of expression within LECs (Figure 2.13B). Expression of either WT Hdac3 or HDAC3$^{H134A,\ H135A}$ rescued Gata2 expression, whereas HDAC3^{HEBI} expression failed to do so (Figure 2.12B). These data indicate that Hdac3 functions in a chromatin-dependent, but deacetylase-independent, manner to regulate Gata2 expression within LECs in response to OSS. The intron 5 168-bp GATA2 intragenic enhancer region is highly conserved (Figure 2.14).

Figure 2.14

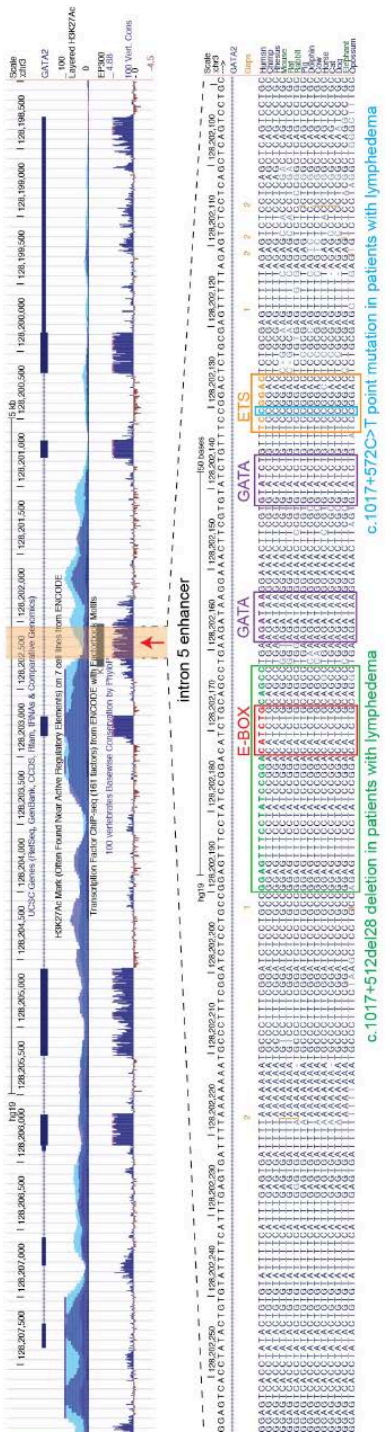
intron 5 enhancer
E-BOX
GATA
GATA
ETS
GATA2
c.1017+512del28 deletion in patients with lymphedema
c.1017+572C>T point mutation in patients with lymphedema

Figure 2.14 UCSC genome browser view of human GATA2 locus. Based on ChIP-seq data curated by the ENCODE project consortium, GATA2 intragenic enhancer region (orange highlight) is enriched for H3K27ac and EP300. 168 bp GATA2 intragenic enhancer region shows high degree of evolutionary conservation in multiple alignments of 100 vertebrate species (red arrow). Specifically, the sequence encompassing c.1017+512del28 mutation region (green box) and c.1017+572C>T point mutation (blue box), observed in patients with lymphedema, is highly conserved among mammals. The E-box sequence (red box) is located within the c.1017+512del28 deletion region (green box) while the c.1017+572C>T point mutation is within the ETS binding site (orange box). Consensus GATA binding site (purple box) is located between E-box and ETS binding sites.

Tal1, Gata2, and Ets1/2 recruit Hdac3 to the Gata2 intragenic enhancer in a shear stress–dependent manner. To investigate the mechanisms by which Hdac3 regulates the Gata2 intragenic enhancer, we determined enrichment of Hdac3 at the Gata2 intragenic enhancer region in LECs cultured under static or OSS conditions. Hdac3 occupancy at the Gata2 intragenic enhancer was increased under OSS compared with that observed under static conditions, suggesting that lymphatic flow regulates the recruitment of Hdac3 to chromatin (Figure 2.15A). TRANSFAC (TRANScription FACtor database; http://genexplain.com/transfac/) analysis of ENCODE (Encyclopedia of DNA Elements; https://www.encodeproject.org/) ChIP-sequencing (ChIP-seq) data sets suggested a composite occupancy of the transcription factors Tal1, Gata2, and Ets1/2 at the E-box–GATA–ETS element of the Gata2 intragenic enhancer (Figure 2.15B). ChIP–quantitative PCR (ChIP-qPCR) analysis confirmed enrichment of Tal1, Gata2, and Ets1/2 at the Gata2 intragenic enhancer region in LECs under static conditions (Figure 2.15C). To test the physical interaction of Hdac3 with Tal1, Gata2, or Ets1/2, we performed immunoprecipitation of endogenous Hdac3 protein from LECs cultured under static or OSS conditions, followed by immunoblotting for Tal1, Gata2, or Ets1/2. We found that OSS induced a physical interaction between Hdac3 and Tal1, Gata2, or Ets1/2 in LECs (Figure 2.15, D and E). Notably, total expression of Hdac3 protein and Tal1 and Ets1 transcripts remained unchanged in LECs in response to OSS (Figure 2.15D and Figure 2.16A).

Figure 2.15

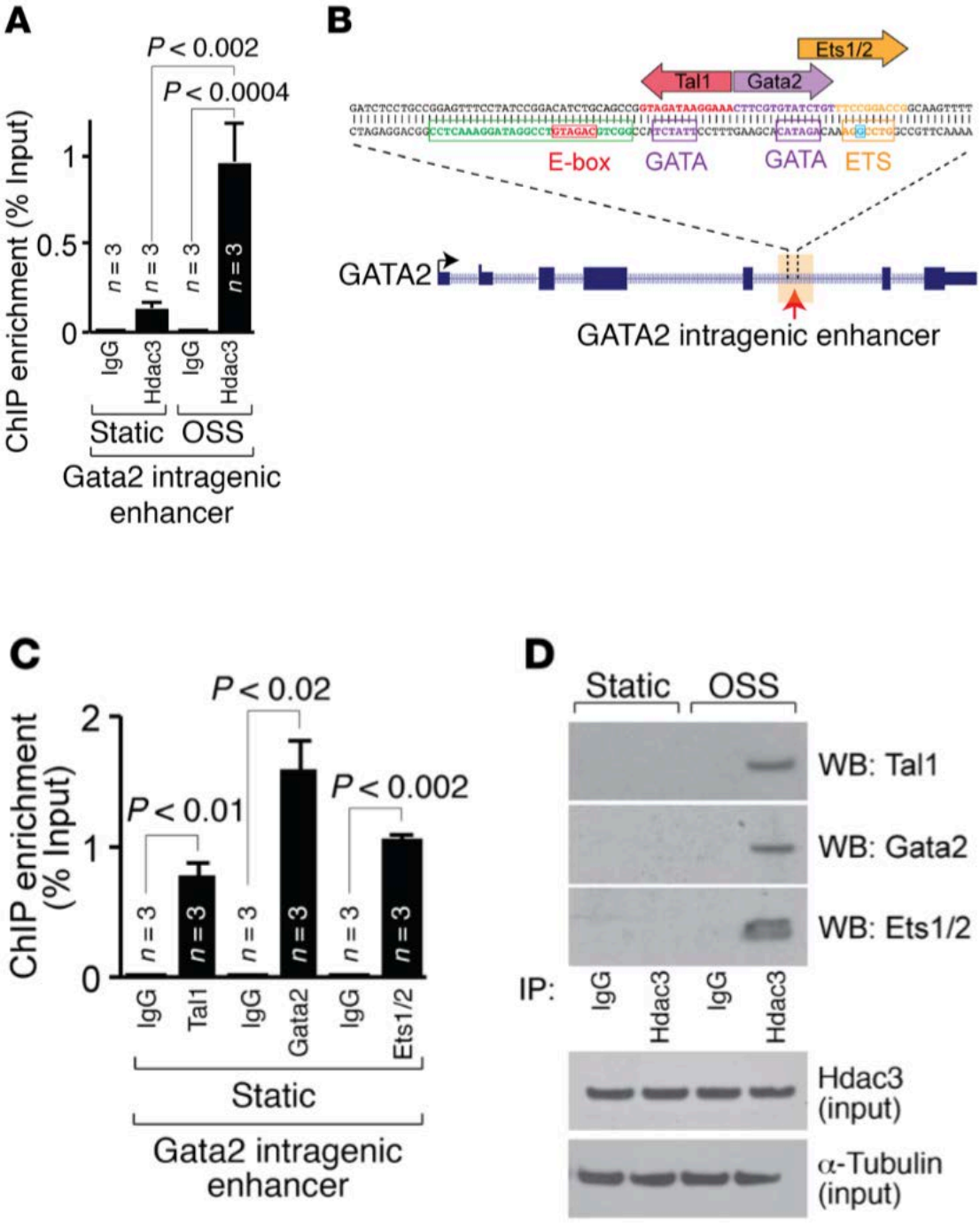
A
P < 0.002
P < 0.0004
ChIP enrichment (% Input)
1
0.5
0
n = 3
n = 3
n = 3
n = 3
IgG
Hdac3
IgG
Hdac3
Static
OSS
Gata2 intragenic enhancer
B
Ets1/2
Tal1
Gata2
E-box
GATA
GATA
ETS
GATA2
GATA2 intragenic enhancer
C
P < 0.02
P < 0.01
P < 0.002
ChIP enrichment (% Input)
2
1
0
n = 3
n = 3
n = 3
n = 3
n = 3
n = 3
IgG
Tal1
IgG
Gata2
IgG
Ets1/2
Static
Gata2 intragenic enhancer
D
Static
OSS
WB: Tal1
WB: Gata2
WB: Ets1/2
IP:
IgG
Hdac3
IgG
Hdac3
Hdac3 (input)
α-Tubulin (input)

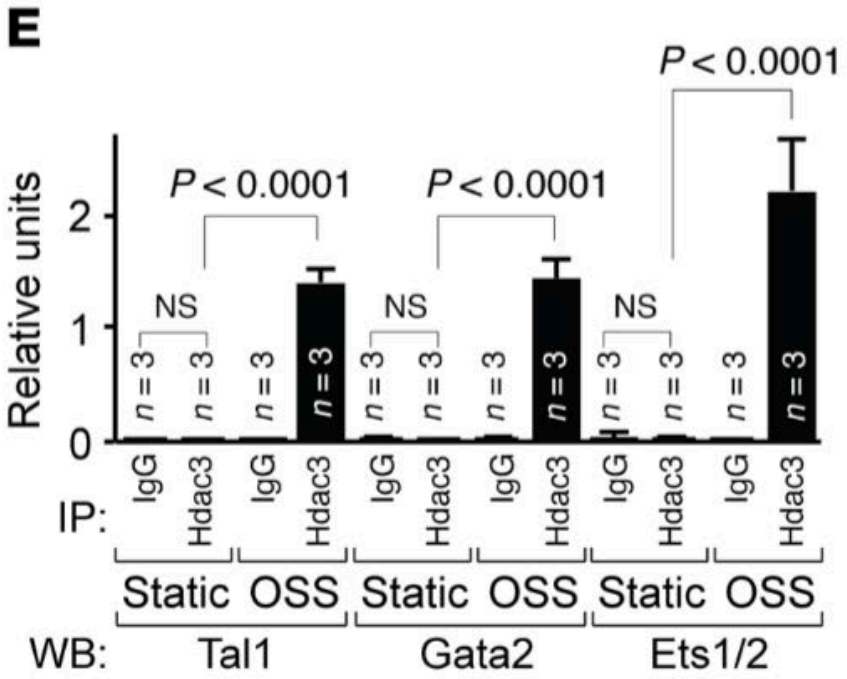
E
P < 0.0001
P < 0.0001
P < 0.0001
Relative units
2
1
0
NS
NS
NS
n = 3
IgG
Hdac3
IP:
Static
OSS
WB:
Tal1
Gata2
Ets1/2

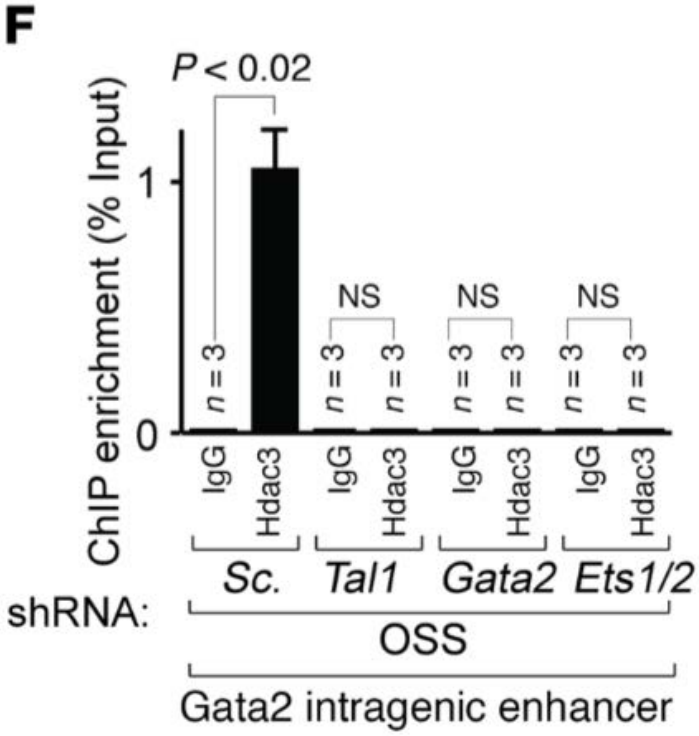
F
P < 0.02
ChIP enrichment (% Input)
1
0
NS
NS
NS
n = 3
IgG
Hdac3
Sc.
Tal1
Gata2
Ets1/2
shRNA:
OSS
Gata2 intragenic enhancer

Figure 2.15 Tal1, Gata2, and Ets1/2 recruit Hdac3 to the Gata2 intragenic enhancer in response to lymphatic shear stress. (A) ChIP-qPCR analysis of Hdac3 recruitment to the Gata2 intragenic enhancer was performed in LECs subjected to static conditions or OSS. (B) Schematic model depicting TRANSFAC analysis of ENCODE ChIP-seq data sets at the E-box–GATA–ETS element of the Gata2 intragenic enhancer. (C) ChIP–qPCR analysis of Tal1, Gata2, and Ets1/2 recruitment to the Gata2 intragenic enhancer was performed in LECs. (D and E) Total lysates from pooled LECs subjected to static or OSS conditions were immunoprecipitated by IgG or Hdac3 antibody, and Western blot analysis was performed using Tal1, Gata2, or Ets1/2 antibody (D). Total Hdac3 and α-tubulin levels are shown as an input control (D). Tal1, Gata2, and Ets1/2 expression was quantified and normalized to total input using ImageJ software (E). (F) ChIP–qPCR analysis of Hdac3 recruitment to the Gata2 intragenic enhancer in scrambled shRNA–, Tal1 shRNA–, Gata2 shRNA–, or Ets1/2 shRNA–infected LECs subjected to OSS (n = 3). Data represent the mean ± SEM and are representative of 3 independent experiments. P values were determined by Student's t test (C and F) or by 1-way ANOVA using Sidak's multiple comparisons test (A and E). WB, Western blotting. See also Figure 2.16.

Figure 2.16

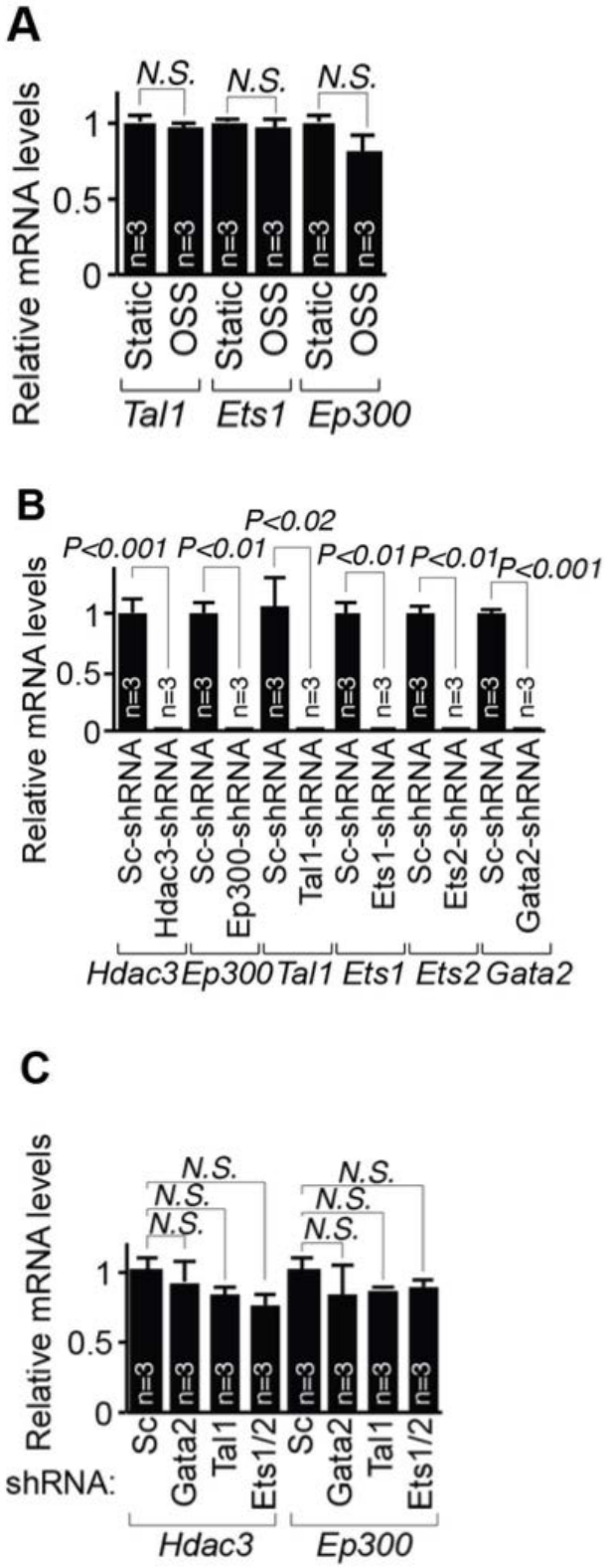
A
N.S.
N.S.
N.S.
Relative mRNA levels
1
0.5
0
n=3
Static
OSS
Tal1
Ets1
Ep300
B
P<0.02
P<0.001
P<0.01
P<0.01
P<0.01
P<0.001
Sc-shRNA
Hdac3-shRNA
Ep300-shRNA
Tal1-shRNA
Ets1-shRNA
Ets2-shRNA
Gata2-shRNA
Hdac3
Ep300
Tal1
Ets1
Ets2
Gata2
C
N.S.
shRNA:
Sc
Gata2
Tal1
Ets1/2
Hdac3
Ep300

Figure 2.16 Transcripts for Tal1, Ets1, and Ep300 were detected by real-time qPCR in LECs subjected to static or OSS. (B) Transcripts for Hdac3, Ep300, Tal1, Ets1, Ets2, and Gata2 were detected by real-time qPCR in Sc- or Hdac3/Ep300/Tal1/Ets1/Ets2/Gata2-shRNA-infected LECs respectively. (C) Transcripts for Hdac3 and Ep300 were detected by real-time qPCR in Sc-, Gata2-, Tal1-, or Ets1/2-shRNA-infected LECs. Data represent the mean ± SEM and are representative of three independent experiments. P values are determined by Student's t test (A, B) or by one-way ANOVA using Sidak's multiple comparisons test (C). OSS, oscillatory shear stress; Sc, scramble; N.S., not significant.

Loss of Tal1, Gata2, or Ets1/2 abolished OSS-dependent recruitment of Hdac3 to the Gata2 intragenic enhancer in LECs (Figure 6F and Figure 2.16B). LECs expressing Tal1, Gata2, or Ets1/2 shRNAs showed similar expression levels of Hdac3 transcripts (Figure 2.16C).

Hdac3 recruits EP300 to the Gata2 intragenic enhancer to promote Gata2 transcription in response to OSS. To investigate how Hdac3 regulates the activation of the Gata2 intragenic enhancer in response to shear stress, we determined the enrichment of H3K27ac and EP300 at the Gata2 intragenic enhancer in WT and Hdac3-deficient LECs cultured under static or OSS conditions. LECs showed enrichment of H3K27ac and EP300 in response to OSS, and this enrichment was abolished by Hdac3 knockdown (Figure 2.17, A and B, and Figure 2.16B).

Figure 2.17

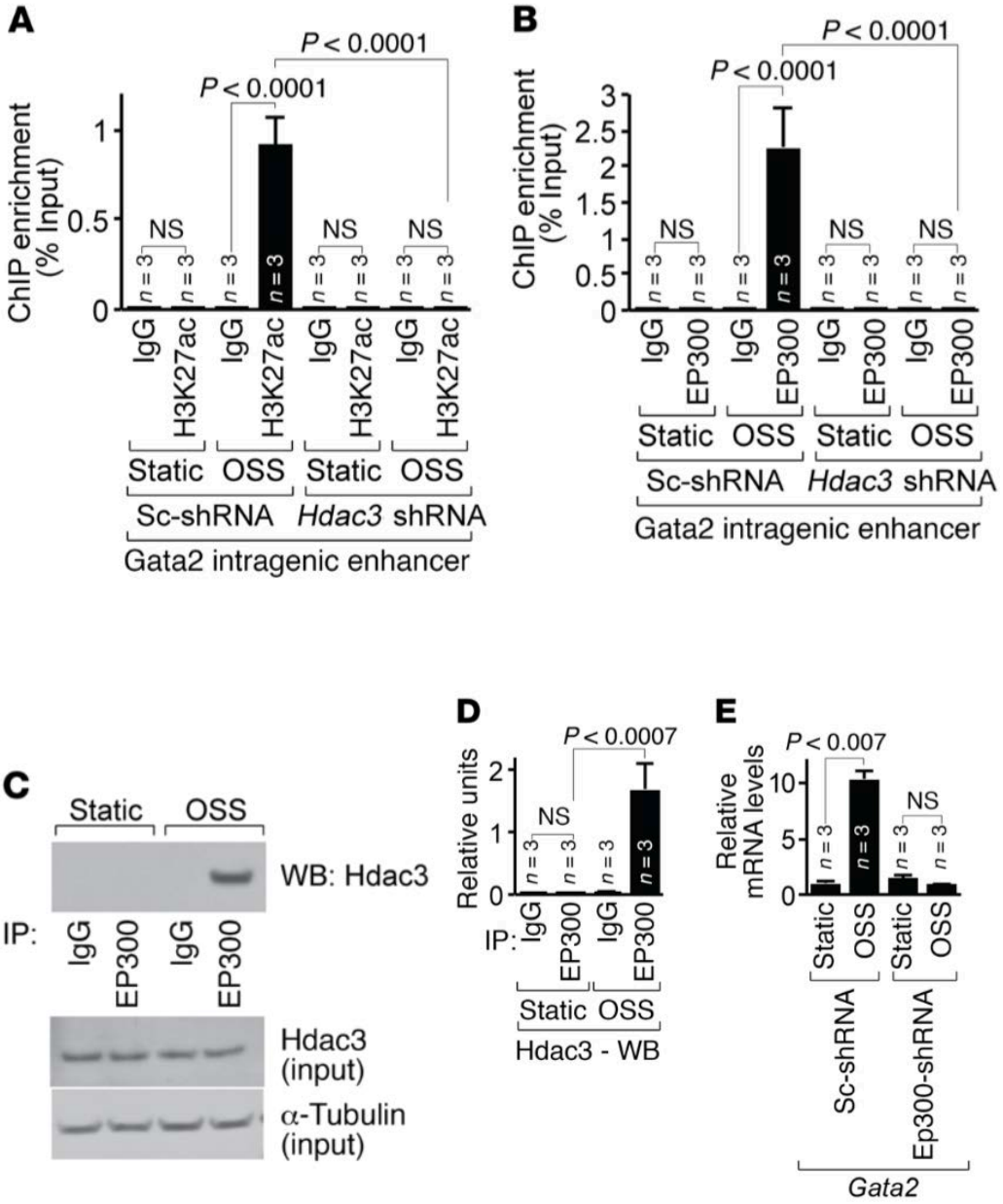
A
ChIP enrichment (% Input)
P < 0.0001
P < 0.0001
NS
IgG
H3K27ac
Static
OSS
Sc-shRNA
Hdac3 shRNA
Gata2 intragenic enhancer
B
ChIP enrichment (% Input)
P < 0.0001
P < 0.0001
NS
IgG
EP300
Static
OSS
Sc-shRNA
Hdac3 shRNA
Gata2 intragenic enhancer
C
Static
OSS
WB: Hdac3
IP:
IgG
EP300
Hdac3 (input)
α-Tubulin (input)
D
Relative units
P < 0.0007
NS
IP:
Static
OSS
Hdac3 - WB
E
Relative mRNA levels
P < 0.007
NS
Static
OSS
Sc-shRNA
Ep300-shRNA
Gata2

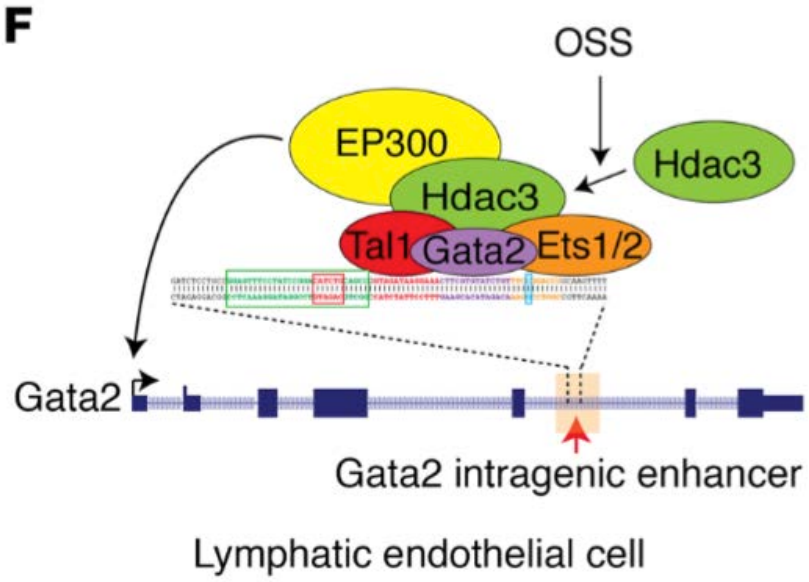

Figure 2.17 Hdac3 recruits EP300 to the Gata2 intragenic enhancer in response to lymphatic shear stress. (A and B) ChIP–qPCR analysis of H3K27 acetylation (A) and EP300 recruitment (B) to the Gata2 intragenic enhancer in scrambled shRNA– or Hdac3 shRNA–infected LECs subjected to static or OSS conditions. (C and D) Total lysates from pooled LECs subjected to static or OSS conditions were immunoprecipitated by IgG or EP300 antibody, and Western blot analysis was performed using Hdac3 antibody (C). Total Hdac3 and α-tubulin levels are shown as input controls. Hdac3 expression was quantified and normalized to total input using ImageJ software (n = 3) (D). (E) Transcripts for Gata2 were detected by ChIP-qPCR in scrambled shRNA– or EP300-shRNA–infected LECs subjected to static or OSS conditions. (F) In response to OSS, the transcription factors Tal1, Gata2, and Ets1/2 recruit Hdac3 to the Gata2 intragenic enhancer,which in turn recruits EP300 to promote Gata2 expression. In LECs lacking Hdac3, OSS failed to promote EP300 recruitment to the Gata2 intragenic enhancer, histone H3 Lys-27 acetylation, and, thereby, Gata2 expression. Data represent the mean ± SEM and are representative of 3 independent experiments. P values were determined by Student's t test (E) or by 1-way ANOVA with Sidak's multiple comparisons test (A, B, and D). See also Figure 2.16.

We observed that Ep300 transcript expression levels remained unchanged in LECs in response to OSS (Figure 2.16A). To test the physical interaction of Hdac3 and EP300, we performed immunoprecipitation of endogenous EP300 protein from LECs cultured under static or OSS conditions, followed by immunoblotting for Hdac3. OSS induced physical interaction between Hdac3 and EP300 in LECs (Figure 2.17, C and D). Taken together, these results suggest that Hdac3 recruits EP300 to the Gata2 intragenic enhancer in response to OSS. By contrast, EP300-deficient LECs failed to demonstrate transcriptional activation of Gata2 in response to OSS (Figure 2.17E and Figure 2.16B). LECs expressing Tal1, Gata2, or Ets1/2 shRNAs showed similar expression levels of Ep300 transcripts (Figure 2.16C). These data suggest that EP300 recruitment to the Gata2 intragenic enhancer is important for lymphatic flow–dependent Gata2 expression (Figure 2.17F).

Discussion

This study reveals a unique, unexpected, and nonredundant role of Hdac3 as a key regulator of blood-lymph separation during development. Our results demonstrate that endothelial inactivation of ubiquitously expressed Hdac3, but not Hdac1 or Hdac2, in mice causes embryonic lethality, failure of blood-lymph separation, lymphedema, and defects in both lymphatic and lymphovenous valves. Despite the sequence homology among class I Hdacs, these results suggest a unique function of Hdac3 to mediate blood-lymph separation during development.

To our knowledge, this is the first report of a histone-modifying enzyme regulating separation of the blood and lymphatic vascular systems. Recent studies revealed that platelets and podoplanin (an LEC receptor) cooperate to prevent blood from entering the lymphatic system at the lymphovenous valve (Bianchi et al., 2017; Fu et al., 2008; Geng et al., 2016; Hess et al., 2013; Schacht, 2003; Uhrin et al., 2010). However, we found that ablation of Hdac3 in platelets caused no defects in blood-lymph separation (Figure 2.5, A–S), suggesting that Hdac3 functions specifically within LECs. Here, we show that Hdac3 ablation in LECs prior to lymphovenous valve formation (*Hdac3*^{TekKO}) resulted in a failure of blood-lymph separation at E12.5 and lethality as early as E13.5 (Figure 2.7 and Tables 2.1 and 2.2). Similarly, complete loss of Hdac3 in LECs after lymphovenous valve formation (*Hdac3*^{Cdh5KO} or *Hdac3*^{Lyve1KO}) led to a failure of blood-lymph separation soon after birth (Figure 2.2, B, C, and E–I), followed by complete neonatal lethality (Tables 2.3 and 2.4).

These alternative genetic approaches reveal that the timing of lethality in mice lacking LEC Hdac3 coincides with lymphovenous valve dysfunction and failure of blood-lymph separation. However, Hdac3-deficient lymphovenous valves and lymphatic vessels showed similar podoplanin expression levels compared with levels detected in controls (Figure 2.6F and Figure 2.11, A and D).

These results raise an interesting question: How does ubiquitously expressed Hdac3 function in a LEC-specific manner during development? Lacking intrinsic DNA-binding capacity, Hdac3 must be recruited to the chromatin via

its interaction with multiple protein nuclear complexes, transcription factors, and cofactors (Yang and Seto, 2008). Emerging data from genome-wide mapping reveal that approximately 60% of Hdac3 occupies intragenic and intergenic regions including those marked by H3K27ac (Feng et al., 2011; Wang et al., 2009; You et al., 2013; Zhang et al., 2016; Mullican et al., 2008). This distribution suggests enhancer-specific functions for Hdac3. Enhancers recruit a multitude of protein complexes to orchestrate gene expression in a temporal, spatial, or cell type–specific manner (Calo and Wysocka, 2013). The GATA2 intragenic enhancer is both sufficient and necessary to drive GATA2 expression in LECs (Khandekar et al., 2007; Lim et al., 2012). Our findings support a model in which Hdac3 functions in concert with EP300 to activate, rather than repress, the Gata2 intragenic enhancer and thereby establish a specific transcriptional program for LECs. This model challenges long-held assumptions that HDACs replace HATs to promote both histone deacetylation and repression of transcription. Taken together, our findings warrant further investigation of the extent, if any, to which the intragenic and intergenic occupancy of HDACs contributes to the regulation of enhancer functions that modulate gene expression.

Our finding that HDAC3 contributes to the function of the GATA2 intragenic enhancer dovetails with recent GWAS revealing that the majority of genetic variants or mutations associated with human diseases map to the noncoding elements in the genome (Tak and Farnham, 2015). A substantial fraction of such mutations are thought to disrupt enhancer elements to alter gene expression and cause disease; however, only a few examples have been

identified (Cheryl A Scacheri, 2015). Consistent with this notion, patients with c.1017+512del28 deletion or a c.1017+572C>T point mutation within the evolutionarily conserved GATA2 intragenic enhancer (divergence ~350 million years ago) have lymphedema and significantly reduced GATA2 expression (Douzery et al., 2004; Ganapathi et al., 2015; Hsu et al., 2013; Spinner et al., 2014). The present study takes this scenario one step further by revealing that Hdac3 functions as an important epigenetic switch to promote complex formation at a deeply conserved Gata2 intragenic enhancer element in response to OSS. Disruption of the E-box or ETS motif nullifies Hdac3-mediated induction of Gata2 expression, suggesting that perturbation of these regions disrupts the assembly of the Tal1-Gata2-Ets1/2-Hdac3-Ep300 complex in developing lymphatic endothelium. These results suggest a mechanism by which c.107+512del28 or c.107+572C>T mutations cause lymphedema. This model supports the hypothesis that protein complexes at enhancers function as a transcription activation switch for developmentally important transcription factors in response to intrinsic or extrinsic signaling cues (Boffelli et al., 2004; Spitz and Furlong, 2012). While we do not yet fully understand the nature of the enhancer elements in the developing lymphatic system, these studies broaden the role of protein complexes at deeply conserved enhancer elements in lymphatic valve development.

Here, we highlight the integrated nature of extracellular forces and epigenetic signatures at the enhancer elements. Our data show that OSS promotes assembly of a protein complex containing the transcription factors Gata2, Tal1, Ets1/2 and the histone-modifying enzymes Hdac3 and EP300 at the

Gata2 intragenic enhancer–specific E-box–GATA–ETS composite element. Concentrated clusters of transcription factor recognition motifs within the composite element facilitate direct cooperative binding of multiple transcription factors prior to enhancer activation (Spitz and Furlong, 2012). Such “priming” of enhancer elements allows additional recruitment of both cofactors and effectors of signal transduction pathways to integrate intrinsic and extrinsic signaling cues during key stages of development (Long et al., 2016). We propose that cooperative interactions among Gata2, Tal1, and Ets1/2 at the E-box–GATA–ETS composite element lead to priming of the Gata2 intragenic enhancer. OSS-mediated mechanotransduction promotes recruitment of Hdac3 and thereby EP300 at the primed Gata2 intragenic enhancer to modify the epigenetic signature, which in turn rapidly activates Gata2 transcription (Figure 7F). In line with this concept, developing LECs subjected to OSS exhibit robust upregulation of Gata2, which is important for lymphatic valve development (Kazenwadel et al., 2015; Sweet et al., 2015). In addition, murine embryos lacking endothelial Tal1 display edema, blood-filled superficial vessels, and complete lethality at E14.5 (Schlaeger, 2005). Global loss of both Ets1 and Ets2 in murine embryos also causes edema, blood-filled dilated superficial vessels, pooling of blood in the jugular region, and complete lethality at E15.5 (Wei et al., 2009). These phenotypes appear very similar to those in murine embryos lacking endothelial Hdac3. Hence, our data warrant a reexamination of Tal1-knockout and Ets1/2-knockout phenotypes to determine whether Tal1 and Ets1/2 regulate blood-lymph separation and lymphatic valve development.

While the transcriptional regulators of Gata2 are defined, the epigenetic modifiers remain unknown. Our data identify Hdac3 as a positive transcriptional regulator of Gata2. Consistent with this notion, embryos lacking endothelial Hdac3 (our observations) or Gata2 (Geng et al., 2016; Kazenwadel et al., 2015) show highly similar phenotypes. For instance, endothelial ablation of Hdac3 causes shortened lymphovenous valve leaflets with defective perpendicular alignment to the flow direction, similar to those seen in murine embryos lacking endothelial Gata2 (Geng et al., 2016). Loss of endothelial Hdac3 or Gata2 also causes reduced expression of Foxc2 and Prox1 within developing murine lymphovenous valves (Geng et al., 2016; Kazenwadel et al., 2015). In addition, embryos lacking lymphatic Hdac3 or Gata2 have dysplastic mesenteric lymphatic vessels with fewer and disorganized valve-forming territories (Kazenwadel et al., 2015). Furthermore, Hdac3 or Gata2 ablation in blood endothelial cells causes failure of blood-lymph separation in murine embryos between E12.5 and E13.5 (Geng et al., 2016; Kazenwadel et al., 2015). Interestingly, Prox1-CreERT2–mediated inducible Gata2 ablation in lymphatic vasculature at E10.5, prior to lymphovenous valve formation, recapitulates this phenotype at E13.5 (Kazenwadel et al., 2015). In contrast, Lyve1-Cre–mediated Hdac3 deletion in lymphatic vasculature causes blood-lymph separation failure between E17.5 and P0 (Figure 2.2, C and I, and Figure 2.1G). Pan-endothelial Cre-expressing mice (*Tek-Cre* mice) show recombinase activity in LEC precursors at E10.5, prior to lymphovenous valve formation (Srinivasan et al., 2007). However, Lyve1-Cre–expressing embryos reveal fully penetrant recombinase

activity within lymphovenous valves at E14.5, after lymphovenous valve formation (Crosswhite et al., 2016). These alternative genetic approaches reveal that failure of blood-lymph separation due to lymphovenous valve defects corresponds with the timing of endothelial Hdac3 ablation in both *Lyve1-Cre* and *Tek-Cre* mice.

Overall, our study suggests that enhancer-specific epigenetic signatures are functional components of mechano-induced transcriptional responses during lymphatic valve development. Future studies will define the precise mechanotransduction and mechanosensory pathways that integrate extracellular signaling at enhancers during lymphatic vascular development.

Materials and Methods

Mice. *Tek-Cre* (Kisanuki et al., 2001), *Cdh5-Cre* (Alva et al., 2006), *Lyve1-Cre* (Pham et al., 2010), *Pf4-iCre* (codon-improved Cre recombinase) (Tiedt et al., 2007), and *Gt(ROSA)26Sor* (Soriano, 1999) reporter mice were obtained from The Jackson Laboratory. *Hdac1*$^{fl/fl}$ (Milstone et al., 2017), *Hdac2*$^{fl/fl}$ (Anokye-Danso et al., 2011), and *Hdac3*$^{fl/fl}$ (Mullican et al., 2008) mice have been previously described.

Antibodies and reagents. Detailed antibody information is provided in Table 2.6. Biotinylated secondary antibodies, VECTASHIELD mounting medium, the VECTASTAIN Elite ABC Kit, and the DAB Peroxidase Substrate Kit were purchased from Vector Laboratories. Harris modified hematoxylin, eosin Y, ethanol, methanol, chloroform, glacial acetic acid, xylenes, paraformaldehyde, paraffin, potassium ferricyanide, potassium ferrocyanide, and deoxycholic acid were purchased from Thermo Fisher Scientific. X-Gal was purchased from Five Prime Therapeutics. Linear polyethylenamine (PEI) was purchased from Polysciences. The RNeasy Mini Kit and GST bead slurry were purchased from QIAGEN. Power SYBR Green PCR Master Mix, a Superscript First Strand Synthesis Kit, a TOPO-TA Cloning Kit, DMEM high-glucose with NA pyruvate, penicillin-streptomycin, horse serum, a CellsDirect One-Step qRT-PCR Kit, insulin-transferrin-selenium (ITS), epoxy M-450 dynabeads, and TRIzol were purchased from Life Technologies (Thermo Fisher Scientific). iScript Reverse Transcription Supermix was purchased from Bio-Rad. Passive lysis buffer and a dual-luciferase reporter assay kit were purchased from

Promega. BALB/c murine primary LECs, basal medium, and complete mouse endothelial cell medium were purchased from Cell Biologics. FBS, donkey serum, gelatin, rabbit serum, Evans blue dye, protease inhibitor mixture, and magnetic anti-Flag beads were purchased from MilliporeSigma. Agarose IgG and IgA bead slurry were purchased from Santa Cruz Biotechnology and Life Technologies (Thermo Fisher Scientific). µ-Slide VI 0.4 Luer was purchased from Ibidi. The EZ-ChIP Assay Kit was purchased from MilliporeSigma. The RecoverAll Total Nucleic Acid Isolation Kit was purchased from Thermo Fisher Scientific. The CellAmp Whole Transcriptome Amplification Kit and the Takara DNA Ligation Kit were purchased from Takara. Membrane slides and isolation caps were purchased from Molecular Machines & Industries.

Plasmids. WT, c.1017+512del28, and c.1017+572C>T Gata2 intragenic enhancer fragments with flanking restriction enzyme sites were purchased as MiniGenes cloned into a pIDTSMART-AMP vector from Integrated DNA Technologies. The enhancer fragments were digested with MluI and XhoI, gel purified, and cloned into the pGL3-Promoter Luciferase Vector (Promega). All plasmids were verified by restriction analyses and sequencing (Eurofins MWG Operon). Lentiviral plasmids expressing Hdac3 shRNA, EP300 shRNA, Tal1 shRNA, Ets1/2 shRNA, Gata2 shRNA, and scrambled shRNA controls were obtained from the University of Massachusetts shRNA Core Facility. Plasmids expressing human *GFP*, *HDAC3*, *HDAC3*^{HEBI}, and *HDAC3*$^{H134A,\ H135A}$ have been previously described (Lewandowski et al., 2015; Sun et al., 2013).

Table 2.6

Antibody	Company	Catalogue Number	Species	Clonality	Final Conc.
Hdac1	Abcam	ab19845	Rabbit	Polyclonal	0.91-1μg/ml
Prox1	Abcam	ab101851	Rabbit	Polyclonal	10μg/ml
Prox1	Abcam	ab37128	Rabbit	Polyclonal	1:100
Foxc2	Abcam	ab5060	Goat	Polyclonal	5μg/ml
H3K27ac	Abcam	Ab4729	Rabbit	Polyclonal	10μg/ml
alpha-SMA	Abcam	ab5694	Rabbit	Polyclonal	2μg/ml
Tal1	Santa Cruz Biotechnologies	sc-12984	Goat	Polyclonal	200ng/ml
Ets1/2	Santa Cruz Biotechnologies	sc-374509	Mouse	Monoclonal	200ng/ml
Ep300	Santa Cruz Biotechnologies	sc-585	Rabbit	Polyclonal	200ng/ml
Gata2	Santa Cruz Biotechnologies	sc-9008	Rabbit	Polyclonal	2μg/ml
Emcn	Santa Cruz Biotechnologies	sc-53941	Rat	Monoclonal	4μg/ml
Hdac3	Santa Cruz Biotechnologies	sc-11417	Rabbit	Polyclonal	2μg/ml
Vegfr3	R&D Systems	AF743	Goat	Polyclonal	1μg/ml
Lyve1	R&D Systems	AF2125	Goat	Polyclonal	2μg/ml
Nrp1	R&D Systems	AF566	Goat	Polyclonal	4μg/ml
Pdpn	R&D Systems	AF3244	Goat	Polyclonal	4μg/ml
Alexa Fluor 488	Life Technologies	A-21208	Donkey	Polyclonal	4μg/ml
Alexa Fluor 488	Life Technologies	A-11055	Donkey	Polyclonal	4μg/ml
Alexa Fluor 568	Life Technologies	A10042	Donkey	Polyclonal	4μg/ml
Donkey anti-Goat TRITC	Santa Cruz Biotechnologies	Sc-3855	Donkey	N/A	0.8μg/ml
Hdac2	Life Technologies	51-5100	Rabbit	Polyclonal	2.5μg/ml
Flag	Sigma	F-3165	Mouse	Monoclonal	200ng/ml
CD31	BD Pharmingen	550274	Rat	Monoclonal	78.125ng/ul
Pdpn	Hybridoma Bank	8.1.1-c	Hamster	Polyclonal	1.4μg/ml
Itga9	R&D Systems	AF3827	Goat	Polyclonal	0.2μg/ml
Lyve1	Abcam	Ab14917	Rabbit	Polyclonal	10μg/ml
Anti-syrian hamster Immunopure FITC	Life Technologies	31587	Rabbit	Polyclonal	4μg/ml
Anti- Goat Alexa Fluor 568	Life Technologies	A-11079	Rabbit	Polyclonal	4μg/ml

Imaging. Images of dissected embryos, mice, and tissue sample were captured using a Leica MZ10 F fluorescence stereomicroscope equipped with a ×0.7 C-mount, Achromat 1.0 × 90 mm objective, a SOLA light engine, a DS-Fi1 color camera (Nikon), and NIS-Elements Basic Research software (Nikon). Stained section images were captured using a Nikon Eclipse 80i microscope equipped with CFI Plan Fluor ×4/×10/×20/×40 objective lenses, a SOLA light engine (Lumencor), a DS-Fi1 color camera, and NIS-Elements Basic Research software. Whole-mount immunostained images were captured using a Zeiss LSM710 confocal scanning microscope equipped with a W Plan-Apochromat ×20/1.0 DIC D = 0.17 M27 70-mm objective lens as previously described (Shin et al., 2016). Whole-mount immunostained mesenteric vessels were flat mounted onto histobond glass slides using VECTASHIELD mounting medium for immunofluorescence and imaged using a Nikon Eclipse 80i microscope or a Leica TCS SP5 II Laser Scanning Confocal microscope. Alexa Fluor 488 and 568 were simultaneously excited at 488 nm and 561 nm with confocal lasers, respectively. Emissions were split by an MBS 488/561/633 beam splitter and captured with 2 detection ranges (ch1: 493–536 nm, ch2: 576–685 nm). For nuclear staining, Hoechst was excited using a Chameleon Ti:Sapphire pulse laser (755 nm) (Coherent Inc.) and was emission detected at 387 to 486 nm. Image stacks of vertical projections were assembled using ImageJ software (NIH).

Histology. Embryos and tissues samples were fixed in 2% paraformaldehyde at 4°C overnight, ethanol dehydrated, embedded in paraffin, and sectioned at 6- to 8-µm thickness using a Leica fully motorized rotary microtome.

H&E staining. Formalin-fixed, paraffin-embedded tissue sections were deparaffinized in xylene and rehydrated through an ethanol gradient, followed by 2-minute Harris modified hematoxylin and 30-second eosin-Y staining. Slides were dehydrated with ethanol, cleared with xylene, and mounted with VECTASHIELD mounting medium.

In vitro OSS experiments. Transiently transfected or infected murine primary LECs were seeded at confluence on µ-Slide VI 0.4 Luer, cultured for 24 hours, and subjected to OSS (4 dynes/cm2, 4 Hz) in a parallel-plate flow chamber system (Ibidi Pump System; Ibidi) or under static conditions for 48 hours.

β-Gal staining. Embryos were dissected and placed in ice-cold 1× PBS and then fixed in 4% paraformaldehyde for 1 hour at 4°C. Embryos were washed in 1× PBS for 30 minutes at room temperature and then incubated in β-gal staining solution (5 mM potassium ferricyanide, 5 mM potassium ferrocyanide, 2 mM MgCl2, 0.04% NP-40, 0.01% deoxycholate, and 0.1% X-gal substrate in 1× PBS) for 48 to 72 hours at 37°C in the dark. Embryos were then washed 3 times for 20 minutes each in 1× PBS at room temperature and fixed overnight in 4% paraformaldehyde.

IHC. IHC was performed as we previously described (Lewandowski et al., 2015). Briefly, slides with sections were deparaffinized and immersed in sodium citrate buffer (10 mM sodium citrate, 0.05% Tween-20, pH 6) or R-buffer A (pH 6; Electron Microscopy Sciences) and placed in a 2100 Antigen Retriever (Aptum Biologics) for heat-induced antigen retrieval. IHC was conducted using a VECTASTAIN Elite ABC Kit and a DAB Peroxidase Substrate Kit (both from Vector Laboratories) according to the manufacturer's guidelines. Sections were incubated with primary antibodies overnight at 4°C (Table 2.6). Biotinylated universal pan-specific antibody (1:62.5) (horse anti-mouse/rabbit/goat IgG); biotinylated universal antibody (horse anti-mouse/rabbit IgG); or biotinylated rabbit anti-rat IgG antibody (1:62.5) (all from Vector Laboratories) were used as secondary antibodies for 1 hour at 25°C according to the manufacturer's instructions. For counterstaining, slides were rinsed and then incubated with 30% hematoxylin for 30 seconds after DAB development. All slides were ethanol dehydrated, cleared with xylenes, and mounted with VECTASHIELD mounting medium. For immunofluorescence staining, after antigen retrieval, sections were blocked in 10% donkey serum and 0.3% Triton X-100 in PBS for 1 hour at room temperature. Sections were then washed in PBS and coincubated with primary antibodies in 10% donkey serum and PBS overnight at 4°C (Table 2.6). Finally, slides were washed in PBS, incubated in Alexa Fluor 488– or 546/568–conjugated secondary antibodies (1:500) with Hoechst (1:1,000) for 1 hour at room temperature, rinsed in PBS, and mounted with VECTASHIELD mounting medium.

Cell culture, transient transfection, lentiviral infection, and luciferase assay. Murine primary LECs were maintained in complete mouse endothelial cell medium in a 37°C incubator with 5% CO2 according to the manufacturer's protocol (Cell Biologics). All experiments were conducted using passage 3–6 LECs. HEK293T cells were maintained in DMEM with 10% FBS, 100 mg/ml penicillin, and 100 mM/ml streptomycin in a 37°C incubator with 5% CO2. Subconfluent HEK293T cells were transfected in 100-mm plates with 5 µg lentiviral plasmid expressing the relevant cDNA or shRNA, 5 µg pCMV-dR8.2, 2.5 µg pCMV-VSVG, and 5 µl PEI, in 10 ml of 2% FBS media. Media were changed to fresh FBS media (10 ml of 1%) 24 hours after transfection. Supernatant media were collected 24 hours later and filtered through a 40-µm cell strainer. Murine primary LECs were infected with fresh-filtered viral media supplemented with 10 µg/ml polybrene reagent. Murine primary LECs were transiently transfected using a PEI-based transfection protocol (Boussif et al., 1995; Lewandowski et al., 2014; 2015; Longo et al., 2013). Each well of a 6-well plate containing subconfluent (~60% confluent) LECs was transfected with a total of 1 µg plasmid DNA, including 0.5 µg WT or c.1017+512del28, or the c.1017+572C>T Gata2 intragenic enhancer pGL3-promoter luciferase vector, with or without 0.5 µg Hdac3 shRNA–expressing vector and 2 µl PEI (1 mg/ml in double-distilled H2O, pH 7.0), in 2 ml complete mouse endothelial cell medium. The PEI-DNA complex was incubated at room temperature for 20 minute before adding it to LECs in a drop-wise manner. The DNA amount was maintained constant using pcDNA3.1(-) DNA. LECs were trypsinized and reseeded to a µ-Slide VI 0.4 Luer (~100% confluence) 24 hours after

transfection. Transiently transfected LECs were subjected to static or OSS conditions for 48 hours and lysed with passive lysis buffer. Lysates were analyzed using a dual luciferase reporter assay kit according to the manufacturer's protocol (Promega). Luciferase activity was measured using a Berthold microplate reader according to the manufacturer's guidelines.

LCMD. LCMD was performed according to the manufacturer's protocol (Molecular Machines & Industries). Briefly, embryos were dissected at E13.5 in cold DEPC–treated 1× PBS, fixed in methacam (60% methanol, 30% chloroform, 10% glacial acetic acid) overnight at 4°C, ethanol dehydrated, embedded in paraffin, sectioned at 8-μm thickness, and mounted onto membrane slides. Tissue sections were deparaffinized in xylene and rehydrated through an ethanol gradient, followed by a 10-second hematoxylin staining. LCMD was performed on an MMI CellCut System equipped with a fixed UV laser with a higher pulse rate using MMI CellTools software, phase-contrast objectives, and an MMI CellCamera (all from Molecular Machines & Industries). Microdissected tissue was collected directly into an adhesive MMI isolation cap.

ChIP. ChIP experiments were performed as previously described (Lewandowski et al., 2014). Briefly, primary LECs subjected to OSS or static conditions were pooled (total ~1 × 106 cells), cross-linked for 15 minutes in cross-linking solution (1% formaldehyde, 1.5 mM ethylene glycol-bis succinimidyl succinate, 20 mM sodium butyrate, 10% FBS), and then

quenched with 125 mM glycine solution for 5 minutes, followed by 2 washes with 1× PBS. Chromatin fragmentation was performed by sonication in ChIP SDS lysis buffer (50 mM Tris-HCl, pH 8.0, 10 mM EDTA, 1% SDS, 1× protease inhibitors) using the Branson Sonifier 250 (40% power amplitude, 120-second). Proteins were immunoprecipitated in ChIP dilution buffer (0.01% SDS, 1.1% Triton X-100, 1.2 mM EDTA, 16.7 mM Tris-HCl, pH 8.0, 167 mM NaCl, 20 mM sodium butyrate, 1× protease inhibitor) using IgG, Hdac3, Ep300, Tal1, Ets1/2, Gata2, or H3K27ac primary antibody. Specificity of the primary antibody at the relevant locus was determined using an IgG control antibody. Immunoprecipitated antibody-chromatin complexes were washed twice with low-salt wash buffer (20 mM Tris-HCl, pH 8.0, 150 mM NaCl, 2 mM EDTA, 0.1% SDS, and 1% Triton X-100), followed by 2 washes with lithium chloride wash buffer (10 mM Tris-HCl, pH 8.0, 250 mM LiCl, 1 mM EDTA, 1% deoxycholate, 1% Nonidet P-40) and TE buffer (10 mM Tris-HCl, pH 8.0, 1 mM EDTA). After removing the wash buffer, cross-linking was reversed at 65°C overnight in proteinase K buffer (20 mM Tris-HCl, pH 7.5, 5 mM EDTA, 50 mM NaCl, 1% SDS, 20 mM sodium butyrate, 50 µg/ml proteinase K). The following day, DNA was purified with phenol/chloroform/isoamyl alcohol. Using purified precipitated DNA, enrichment of the target sequences was measured by ChIP-qPCR using primers designed against the murine Gata2 intragenic enhancer.

RNA isolation and ChIP-qPCR. Chyle-filled mesenteric lymphatic vessels originating from mesenteric lymph nodes were identified and dissected from

P5 mice. Total RNA from cultured murine primary LECs or isolated mesenteric lymphatic vessels, and formalin-fixed, methacam-fixed, paraffin-embedded (MFPE) tissue was isolated using the CellAmp Whole Transcriptome Amplification Kit and the RecoverAll Total Nucleic Acid Isolation Kit, respectively. Total RNA was reverse transcribed using iScript Reverse Transcription Supermix (Bio-Rad) or the CellAmp Whole Transcriptome Amplification Kit (Takara) according to the manufacturers' protocols. Expression of relevant transcripts was measured by ChIP-qPCR using SYBR Green PCR Master Mix as previously described (Lewandowski et al., 2015). Signals were normalized to corresponding GAPDH controls and are represented as relative expression ratios of the experimental samples relative to controls.

Whole-mount IHC. Mesentery tissues from P5 mice were dissected, fixed in 4% paraformaldehyde overnight at 4°C, washed in 1× PBS twice at 4°C for 30 minutes, and dehydrated through a methanol gradient. The samples were then incubated with antibodies against Vegfr3 (1:200) and Hdac3 (1:50) or Prox1 (1:100) overnight at 4°C. Finally, tissue samples were washed in PBS, incubated overnight at 4°C in Alexa Fluor 488– or 546/568–conjugated secondary antibodies (1:200), with or without Hoechst (1:1,000), rinsed in PBS, and then imaged using confocal microscopy.

Evans Blue dye lymphangiography. Evans blue dye (50 µl of 1%, 10 mg/ml), prepared in 1× PBS (pH 7.4), was injected into the left hind footpad of anesthetized mice, with the needle pointed in the dorsal direction. Fifteen

minutes after injection, the mice were euthanized and dissected to examine lymphatic vessels, the thoracic duct, and lymph nodes of interest.

Platelet count. Approximately 100 µl of blood was drawn from each anesthetized P5 pup via intracardiac puncture and collected in 200 µl citrate-phosphate-dextrose (CPD) buffer (16 mM citric acid [anhydrous], 102 mM trisodium citrate, 18.5 mM NaH2PO4, 142 mM D-glucose, pH 7.4) as described previously (76). Platelet counts were obtained and calculated using an automated cell counter (Beckman Coulter; Ac.T 8).

Immunoprecipitation and Western blot analysis. Samples were homogenized in immunoprecipitation buffer (50 mM Tris-HCl pH 8.0, 150 mM NaCl, 0.5% Nonidet P-40, 1 mM EDTA, and 1 mM DTT) containing 1 mM PMSF and a protease inhibitor mixture. The homogenized samples were sonicated using a Branson 250 Digital Sonifier with 1-second-on and 1-second-off pulses at 40% power amplitude for 15 seconds. Precleared lysates were incubated with the relevant primary antibody–conjugated magnetic beads for 16 hours at 4°C. Immune complexes were collected, washed 4 times with immunoprecipitation buffer, and applied to 4%–12% SDS-polyacrylamide gels for Western blot analysis before transferring to PVDF membranes. Primary antibodies against HDAC3 (1:1,000), Tal1 (1:1,000), Gata2 (1:1,000), and Ets1/2 (1:1,000) were used and visualized by chemiluminescence using HRP-conjugated secondary antibodies. Blots were probed with α-tubulin (1:1,000) for the loading control.

Statistics. Statistical significance was determined using a 2-tailed Student's t test, a χ2 test, or a 1-way ANOVA with Sidak's multiple comparisons test (GraphPad Prism 7.0; GraphPad Software). A P value of less than 0.05 was considered significant.

Study approval. The University of Massachusetts Medical School is accredited by the Association for Assessment and Accreditation of Laboratory Animal Care (AAALAC) International and follows the Public Health Service Policy for the Care and Use of Laboratory Animals. Animal care was provided in accordance with the procedures outlined in the Guide for the Care and Use of Laboratory Animals (National Academies Press, 2011). The IACUC of the University of Massachusetts Medical School approved all animal use protocols.

Acknowledgements. We gratefully acknowledge Mitchell Lazar (University of Pennsylvania, Philadelphia, Pennsylvania, USA) for providing *Hdac3*$^{fl/fl}$ mice and the *HDAC3*^{HEBI} plasmid. We also gratefully acknowledge Jane Freedman and Milka Koupenova (University of Massachusetts Medical School, Worcester, Massachusetts, USA) for providing assistance with platelet counts. This work was supported by National Heart, Lung, and Blood Institute grants R01 HL118100 (to CMT) and HL092122 (to JFK).

Chapter III: Discussion & Future Directions

The elucidation of in vivo developmental and tissue-specific functions of histone modifying enzymes is an active area of investigation. Histone deacetylases (Hdacs) play critical roles during embryonic organogenesis including development of the cardiovascular, nervous and musculoskeletal systems (Haberland et al., 2009b). Here we identified a novel and unexpected endothelial specific function of Hdac3, during lymphovenous and lymphatic valve formation. Mice lacking endothelial Hdac3, but not Hdac1 or Hdac2, exhibit defective blood-lymphatic separation, lymphatic dysfunction and lethality. This is important, as no other histone-modifying enzyme, including HDACs, has been shown to affect lymphatic system. Surprisingly, endothelial ablation of Hdac3 did not cause any overt defects in arterial or venous development. In contrast, mice lacking Hdac7 exhibit severe vascular defects, suggesting a specific role for Class II HDACs during vascular development (Chang et al., 2006). Similarly, Hdac6, a class II HDAC, regulate blood vessel formation in zebrafish by deacetylation of an actin- remodeling protein cortactin (Kaluza et al., 2011). However, mice lacking Hdac6 apparently do not show any vascular defects (Kaluza et al., 2011).

Separation of blood and lymphatic vascular systems is necessary for survival and occurs early during lymphatic vascular development. Two key mechanisms, established embryonically, are required to attain the separation of the blood and lymphatic vascular systems. First, the development of lymphovenous valves at the junction between the cardinal vein and lymph sac

around embryonic day 12 (E12), which prevents the backflow of venous blood into the lymphatic system. Indeed, mice with defective lymphovenous valves exhibit blood-filled lymphatic vasculature at various stages of embryonic development (Turner et al., 2014; Geng et al., 2016; Kazenwadel et al., 2015; Srinivasan et al., 2011). Second, platelet mediated inter-vascular hemostasis at the junction of the cardinal vein and budding lymph sacs around E11.5 is essential for blood-lymph separation. Defective lymphovenous hemostasis in mouse models causes blood filled lymphatic vessels as early as E11.5 (Abtahian et al., 2003). However, these mice show normal lymphovenous valve development, suggesting that lymphovenous hemostasis is not required for lymphovenous valve development (Hess et al., 2013). Endothelial Hdac3 deficient mice show anomalous lymphovenous valve development and blood filled lymphatic vessels as early as E12.5. Interestingly, lymphatic endothelial cell specific Hdac3 ablation causes failure of blood-lymph separation during late embryonic gestation. The variability in the timing of appearance of blood filled lymphatics in the different Cre models is likely due to timing of activation of Cre-recombinase and Hdac3 deletion with earlier activity and deletion seen in Tie2-Cre model versus that in Lyve1-Cre models. Most endothelial specific Cre-recombinase mice have variable amounts of expression in hematopoietic cells such as platelets and macrophages, hence, it is pertinent to establish the specific cell type in which Hdac3 functions to regulate blood-lymph separation (Joseph et al., 2013). Mice lacking Hdac3 in lymphatic endothelial cells exhibit anomalous lymphovenous valve morphogenesis and failure of blood lymph separation, suggesting that Hdac3 functions in a lymphatic endothelial cell

autonomous manner during lymphovenous valve development. Consistent with this, platelet or macrophage specific Hdac3 knockout mice show normal blood-lymph separation.

Platelet mediated lymphovenous hemostasis is critical for maintenance of blood lymph separation throughout postnatal life (Hess et al., 2013). Whether lymphovenous valves and Hdac3 are required for such maintenance is not known and requires further study. Experiments involving transfer of hematopoietic cells deficient in Hdac3; into wild type mice depleted of hematopoietic cells, is an additional way of testing whether Hdac3 functions in hematopoietic cells to effect blood lymph separation. Although no difference in expression of podoplanin was noted in the lymphovenous junction region, it is possible that lymphovenous hemostasis maybe impacted by altering the expression of other endothelial ligands of Clec2 as has been proposed (Suzuki-Inoue et al., 2010). Taken together, our results provide the first evidence for histone-modifying enzymes in regulation of lymphovenous valve development and blood lymph separation.

In addition to defective lymphovenous valves, we observed significant reduction in valve number in murine mesenteric lymphatic vessels lacking Hdac3. Several reports have highlighted common genes that regulate development of both lymphovenous valves and lymphatic valves (Geng et al., 2016; Kazenwadel et al., 2015; Martin-Almedina et al., 2016; Zhang et al., 2015). For instance, conditional ablation of Gata2 or Foxc2 in endothelial cells perturbs both lymphovenous and lymphatic valve formation (Cha et al., 2016; Geng et al., 2016). In addition, physiological factors such as fluid pressure

and shear stress also regulate development, maturation, and function of the lymphatic system (Schwartz and Simons, 2012). Embryonic lymphatic vessels coordinate their growth in respond to changes in interstitial fluid pressure (Planas-Paz et al., 2011). Lymphatic flow, which starts prior to lymphatic valve initiation, is an important physiological stimulus that initiates lymphatic valve development in collecting lymphatic vessels (Sabine et al., 2012). A recent study showed that presence of blood in developing lymphatic vessels could impair lymph flow and hence perturb lymphatic vessel valve formation (Sweet et al., 2015). Endothelial Hdac3 deficient mice display blood filled lymphatic vessels and impaired lymphatic valve formation raising the possibility that defective lymphatic valve formation could be secondary to blood impeding forward lymph flow. However, several points argue against this possibility and suggest that Hdac3 is a primary regulator of lymphatic valve development. First, blood filled lymphatic vessels in endothelial Hdac3 deficient mice appear after the initiation of mesenteric lymphatic valve formation. Second, mesenteric vessel remodeling appears unaffected in endothelial Hdac3 deficient mice in contrast to Clec2 deficient mice. Finally, our studies using murine lymphatic endothelial cells subjected to oscillatory shear stress suggest that Hdac3 regulates the transcription of Gata2, a critical gene required for lymphatic valve formation.

Lymphatic valves are often formed in vessel regions subject to oscillatory shear stress (OSS). Consistent with this, cultured LECs subjected to OSS alter their cellular morphology and upregulate expression of genes critical for lymphatic valve formation (Sabine et al., 2012). Hdac3-deficient

LECs fail to upregulate these critical genes in response to OSS, suggesting requirement of Hdac3 function during OSS-dependent transcriptional activation.

In response to OSS, our data show that Hdac3 interacts with transcription factors Gata2, Tal1 and Ets1/2. The exact mechanism by which Gata2 or Tal1 or Ets1/2 interacts with and recruits Hdac3 to chromatin in a flow responsive manner remains to be determined. Reversible, post-translational modifications of proteins are a common mechanism to regulate protein-protein interactions in response to signaling pathways, including external stimuli (Duan and Walther, 2015). Notch, BMP and retinoic acid signaling pathways have been shown to affect Gata2 transcription and/or activity in different contexts (Oren, 2005; Robert-Moreno, 2005; Tsuzuki et al., 2004). Notch1 directly promotes Gata2 transcription in embryonic hemogenic endothelium (Robert-Moreno, 2005). Gata2 via its association with Retinoic acid receptor alpha (RARα) becomes responsive to RA signaling (Tsuzuki et al., 2004). Interestingly, Notch and BMP9 signaling pathways regulate lymphatic valve development, however, whether they affect Gata2 transcription in lymphatic endothelial cells is not known (Levet et al., 2013; Murtomaki et al., 2014). Gata2 is acetylated by p300 and GCN5 acetyl transferases with consequent increases in its DNA binding ability (Hayakawa et al., 2003). Although our studies suggest that Hdac3 functions in a deacetylase-independent manner in regulating transcription of Gata2, it remains to be determined whether Hdac3 interaction with Gata2 is affected by its acetylation.

Genome-wide associations studies (GWAS) implicate variations in non-coding DNA elements as potential drivers of disease (Maurano et al., 2012). In addition, non-coding elements account for a large fraction of evolutionarily constrained sequences suggesting that they may serve important biological functions. Mutations or deletions encompassing enhancers and other cis-regulatory elements have been implicated in disease causation (Smith and Shilatifard, 2014). For example, a single nucleotide change in ZRS enhancer results in altered sonic hedgehog (SHH) expression resulting in pre-axial polydactyly, a developmental defect (Lettice, 2003). Genome-wide ChIP-Seq analysis of p300 binding together with other histone modifications such as H3K4me1 (mono-methylated H3 Lysine 4) and H3K27ac have been used to identify active enhancers in a tissue specific manner (Visel et al., 2009; Heintzman et al., 2007). Studies that have determined genome-wide binding profiles of Hdac3, across different cell types, have shown that Hdac3 is bound mostly to intergenic regions and enhancer elements (Zhang et al., 2016; Mullican et al., 2008). Our data show that Hdac3 binds to and regulates the activity of an evolutionarily conserved enhancer element critical for Gata2 transcription. Additional studies, probing genome wide chromatin binding of Hdac3 together with chromatin binding profiles of p300, H3K4me1 and H3K27ac within lymphatic endothelial cells will help identify other potential enhancers critical for lymphatic vascular development and function.

References

Abtahian F., Guerriero A., Sebzda E., Lu MM., Zhou R., Mocsai A., Myers EE., Huang B., Jackson DG., Ferrari VA., Tybulewicz V., Lowell CA., Lepore JJ., Koretzky GA., Kahn ML. (2003). Regulation of Blood and Lymphatic Vascular Separation by Signaling Proteins SLP-76 and Syk. Science *299*, 247–251.

Adrain, C., and Freeman, M. (2012). New lives for old: evolution of pseudoenzyme function illustrated by iRhoms. Nature Reviews Molecular Cell Biology *13*, 489.

Alders, M., Al-Gazali, L., Cordeiro, I., Dallapiccola, B., Garavelli, L., Tuysuz, B., Salehi, F., Haagmans, M.A., Mook, O.R., Majoie, C.B., et al. (2014). Hennekam syndrome can be caused by FAT4 mutations and be allelic to Van Maldergem syndrome. Hum Genet *133*, 1161–1167.

Alders, M., Hogan, B.M., Gjini, E., Salehi, F., Al-Gazali, L., Hennekam, E.A., Holmberg, E.E., Mannens, M.M.A.M., Mulder, M.F., Offerhaus, G.J.A., et al. (2009). Mutations in CCBE1 cause generalized lymph vessel dysplasia in humans. Nat Genet *41*, 1272–1274.

Alitalo, K. (2011). The lymphatic vasculature in disease. Nature Medicine *17*, 1371–1651.

Alitalo, K., Tammela, T., and Petrova, T.V. (2005). Lymphangiogenesis in development and human disease. Nature *438*, 946–953.

Alva, J.A., Zovein, A.C., Monvoisin, A., Murphy, T., Salazar, A., Harvey, N.L., Carmeliet, P., and Iruela-Arispe, M.L. (2006). VE-Cadherin-Cre-recombinase transgenic mouse: a tool for lineage analysis and gene deletion in endothelial cells. Dev. Dyn. *235*, 759–767.

Anokye-Danso, F., Trivedi, C.M., Juhr, D., Gupta, M., Cui, Z., Tian, Y., Zhang, Y., Yang, W., Gruber, P.J., Epstein, J.A., et al. (2011). Highly Efficient miRNA-Mediated Reprogramming of Mouse and Human Somatic Cells to Pluripotency. Cell Stem Cell *8*, 376–388.

Baeyens, N., Mulligan-Kehoe, M.J., Corti, F., Simon, D.D., Ross, T.D., Rhodes, J.M., Wang, T.Z., Mejean, C.O., Simons, M., Humphrey, J., et al. (2014). Syndecan 4 is required for endothelial alignment in flow and atheroprotective signaling. Proceedings of the National Academy of Sciences *111*, 17308–17313.

Bannister, A.J., and Kouzarides, T. (2011). Regulation of chromatin by histone modifications. Cell Research *21*, 381–395.

Bazigou, E., Xie, S., Chen, C., Weston, A., Miura, N., Sorokin, L., Adams, R., Muro, A.F., Sheppard, D., Makinen, T. (2009). Integrin-α9 is required for

fibronectin matrix assembly during lymphatic valve morphogenesis. Dev. Cell *17*, 175–186.

Bellini, C., Donarini, G., Paladini, D., Calevo, M.G., Bellini, T., Ramenghi, L.A., and Hennekam, R.C. (2015). Etiology of non-immune hydrops fetalis: An update. Am. J. Med. Genet. *167*, 1082–1088.

Bertozzi, C.C., Schmaier, A.A., Mericko, P., Hess, P.R., Zou, Z., Chen, M., Chen, C.-Y., Bin Xu, Lu, M.M., Zhou, D., et al. (2010). Platelets regulate lymphatic vascular development through CLEC-2–SLP-76 signaling. Blood *116*, 661–670.

Bhaskara, S., Chyla, B.J., Amann, J.M., Knutson, S.K., Cortez, D., Sun, Z.-W., and Hiebert, S.W. (2008). Deletion of histone deacetylase 3 reveals critical roles in S phase progression and DNA damage control. Mol. Cell *30*, 61–72.

Bianchi, R., Russo, E., Bachmann, S.B., Proulx, S.T., Sesartic, M., Smaadahl, N., Watson, S.P., Buckley, C.D., Halin, C., and Detmar, M. (2017) Postnatal Deletion of Podoplanin in Lymphatic Endothelium Results in Blood Filling of the Lymphatic System and Impairs Dendritic Cell Migration to Lymph Nodes. Arteriosclerosis, Thrombosis, and Vascular Biology. *37(1)*, 108-117

Blum, K.S., and Pabst, R. (2006). Keystones in lymph node development. Journal of Anatomy *209*, 585–595.

Boffelli, D., Nobrega, M.A., and Rubin, E.M. (2004). Comparative genomics at the vertebrate extremes. Nat Rev Genet *5*, 456.

Boussif, O., Lezoualc'h, F., Zanta, M.A., Mergny, M.D., Scherman, D., Demeneix, B., and Behr, J.P. (1995). A versatile vector for gene and oligonucleotide transfer into cells in culture and in vivo: polyethylenimine. Proceedings of the National Academy of Sciences *92*, 7297–7301.

Bouvrée, K., Brunet, I., del Toro, R., Gordon, E., Prahst, C., Cristofaro, B., Mathivet, T., Xu, Y., Soueid, J., Fortuna, V., et al. (2012) Semaphorin3A, Neuropilin-1, and PlexinA1 Are Required for Lymphatic Valve Formation. Circulation Research. *111(4)*, 437-45

Bowles, J., Secker, G., Nguyen, C., Kazenwadel, J., Truong, V., Frampton, E., Curtis, C., Skoczylas, R., Davidson, T.-L., Miura, N., et al. (2014). Control of retinoid levels by CYP26B1 is important for lymphatic vascular development in the mouse embryo. Developmental Biology *386*, 25–33.

Boyer, L.A., Latek, R.R., and Peterson, C.L. (2004). The SANT domain: a unique histone-tail-binding module? Nature Reviews Molecular Cell Biology *5*, 158–163.

Bresnick, E.H., Lee, H.-Y., Fujiwara, T., Johnson, K.D., and Keles, S. (2010).

GATA Switches as Developmental Drivers. Journal of Biological Chemistry *285*, 31087–31093.

Brouillard, P., Boon, L., and Vikkula, M. (2014) Genetics of lymphatic anomalies. J. Clin. Invest. *124*, 898–904.

Calnan, J.S., Pflug, J.J., Reis, N.D., and Taylor, L.M. (1970). Lymphatic pressures and the flow of lymph. Br J Plast Surg *23*, 305–317.

Calo, E., and Wysocka, J. (2013). Modification of enhancer chromatin: what, how, and why? Mol. Cell *49*, 825–837.

Carla Danussi., Spessotto P., Petrucco A., Wassermann B., Sabatelli P., Montesi M., Doliana R., Bressan GM., Colombatti A. (2008). Emilin1 Deficiency Causes Structural and Functional Defects of Lymphatic Vasculature. Molecular and Cellular Biology *28*, 4026–4039.

Cavalli, G., and Paro, R. (1998). Chromo-domain proteins: linking chromatin structure to epigenetic regulation. Curr. Opin. Cell Biol. *10*, 354–360.

Cha, B., Geng, X., Mahamud, M.R., Fu, J., Mukherjee, A., Kim, Y., Jho, E.-H., Kim, T.H., Kahn, M.L., Xia, L., et al. (2016). Mechanotransduction activates canonical Wnt/β-catenin signaling to promote lymphatic vascular patterning and the development of lymphatic and lymphovenous valves. Genes & Development *30*, 1454–1469.

Chang, S., Young, B.D., Li, S., Qi, X., Richardson, J.A., and Olson, E.N. (2006). Histone deacetylase 7 maintains vascular integrity by repressing matrix metalloproteinase 10. Cell *126*, 321–334.

Cheryl A Scacheri, P.C.S. (2015). Mutations in the non-coding genome. Current Opinion in Pediatrics *27*, 659–664.

Coon, B.G., Baeyens, N., Han, J., Budatha, M., Ross, T.D., Fang, J.S., Yun, S., Thomas, J.-L., and Schwartz, M.A. (2015). Intramembrane binding of VE-cadherin to VEGFR2 and VEGFR3 assembles the endothelial mechanosensory complex. The Journal of Cell Biology *208*, 975–986.

Creyghton, M.P., Cheng, A.W., Welstead, G.G., Kooistra, T., Carey, B.W., Steine, E.J., Hanna, J., Lodato, M.A., Frampton, G.M., Sharp, P.A., et al. (2010). Histone H3K27ac separates active from poised enhancers and predicts developmental state. Proceedings of the National Academy of Sciences *107*, 21931–21936.

Crosswhite, P.L., Podsiadlowska, J.J., Curtis, C.D., Gao, S., Xia, L., Srinivasan, R.S., and Griffin, C.T. (2016). CHD4-regulated plasmin activation impacts lymphovenous hemostasis and hepatic vascular integrity. J. Clin. Invest. *126*, 2254–2266.

Davis, H.K. (1915). A statistical study of the thoracic duct in man. Developmental Dynamics *17*, 211–244.

Douzery, E.J.P., Snell, E.A., Bapteste, E., Delsuc, F., and Philippe, H. (2004). The timing of eukaryotic evolution: Does a relaxed molecular clock reconcile proteins and fossils? Proceedings of the National Academy of Sciences *101*, 15386–15391.

Duan, G., and Walther, D. (2015). The Roles of Post-translational Modifications in the Context of Protein Interaction Networks. PLOS Computational Biology *11*, e1004049.

El Zawahry MD, Sayed NM, El-Awady HM, Abdel-Latif A, El-Gindy M. (1983) A study of the gross, microscopic and functional anatomy of the thoracic duct and the lympho-venous junction. *Int Surg*. 1983;68(2):135–138.

Emiliani, S., Fischle, W., Van Lint, C., Al-Abed, Y., and Verdin, E. (1998). Characterization of a human RPD3 ortholog, HDAC3. Proceedings of the National Academy of Sciences *95*, 2795–2800.

Escobedo, N., Contreras, O., Muñoz, R., Farías, M., Carrasco, H., Hill, C., Tran, U., Pryor, S.E., Wessely, O., Copp, A.J., et al. (2013). Syndecan 4 interacts genetically with Vangl2 to regulate neural tube closure and planar cell polarity. Development *140*, 3008–3017.

Fang, J., Dagenais, S.L., Erickson, R.P., Arlt, M.F., Glynn, M.W., Gorski, J.L., Seaver, L.H., Glover, T.W. (2000). Mutations in FOXC2 (MFH-1), a Forkhead Family Transcription Factor, Are Responsible for the Hereditary Lymphedema-Distichiasis Syndrome. American Journal of Human Genetics *67*, 1382.

Feng, D., Liu, T., Sun, Z., Bugge, A., Mullican, S.E., Alenghat, T., Liu, X.S., and Lazar, M.A. (2011). A Circadian Rhythm Orchestrated by Histone Deacetylase 3 Controls Hepatic Lipid Metabolism. Science *331*, 1315–1319.

Finney, B.A., Schweighoffer, E., Navarro-Nunez, L., Benezech, C., Barone, F., Hughes, C.E., Langan, S.A., Lowe, K.L., Pollitt, A.Y., Mourao-Sa, D., et al. (2012). CLEC-2 and Syk in the megakaryocytic/platelet lineage are essential for development. Blood *119*, 1747–1756.

Finsen, A.V., Lunde, I.G., Sjaastad, I., Østli, E.K., Lyngra, M., Jarstadmarken, H.O., Hasic, A., Nygård, S., Wilcox-Adelman, S.A., Goetinck, P.F., et al. (2011). Syndecan-4 Is Essential for Development of Concentric Myocardial Hypertrophy via Stretch-Induced Activation of the Calcineurin-NFAT Pathway. Plos One *6*, e28302.

Fischle, W., Dequiedt, F., Hendzel, M.J., Guenther, M.G., Lazar, M.A., Voelter, W., and Verdin, E. (2002). Enzymatic activity associated with class II HDACs is dependent on a multiprotein complex containing HDAC3 and

SMRT/N-CoR. Mol. Cell *9*, 45–57.

Fotiou, E., Martin-Almedina, S., Simpson, M.A., Lin, S., Gordon, K., Brice, G., Atton, G., Jeffery, I., Rees, D.C., Mignot, C., et al. (2015). Novel mutations in *PIEZO1* cause an autosomal recessive generalized lymphatic dysplasia with non-immune hydrops fetalis. Nat Comms *6*, 8085.

Fu, J., Gerhardt, H., McDaniel, J.M., Xia, B., Liu, X., Ivanciu, L., Ny, A., Hermans, K., Silasi-Mansat, R., McGee, S., et al. (2008) Endothelial cell O-glycan deficiency causes blood/lymphatic misconnections and consequent fatty liver disease in mice. J. Clin. Invest. *118*, 3725–3737.

Fujisawa, T., and Filippakopoulos, P. (2017). Functions of bromodomain-containing proteins and their roles in homeostasis and cancer. Nature Reviews Molecular Cell Biology *18*, 246–262.

Ganapathi, K.A., Townsley, D.M., Hsu, A.P., Arthur, D.C., Zerbe, C.S., Cuellar-Rodriguez, J., Hickstein, D.D., Rosenzweig, S.D., Braylan, R.C., Young, N.S., et al. (2015). GATA2 deficiency-associated bone marrow disorder differs from idiopathic aplastic anemia. Blood *125*, 56–70.

Gao, L., Cueto, M.A., Asselbergs, F., and Atadja, P. (2002). Cloning and Functional Characterization of HDAC11, a Novel Member of the Human Histone Deacetylase Family. Journal of Biological Chemistry *277*, 25748–25755.

Geng, X., Cha, B., Mahamud, M.R., Lim, K.-C., Silasi-Mansat, R., Uddin, M.K.M., Miura, N., Xia, L., Simon, A.M., Engel, J.D., et al. (2016). Multiple mouse models of primary lymphedema exhibit distinct defects in lymphovenous valve development. Developmental Biology *409*, 218–233.

Goldfarb, Y., Kadouri, N., Levi, B., Sela, A., Herzig, Y., Cohen, R.N., Hollenberg, A.N., and Abramson, J. (2016). HDAC3 Is a Master Regulator of mTEC Development. Cell Reports *15*, 651–665.

Gonzalez-Garay, M.L., Aldrich, M.B., Rasmussen, J.C., Guilliod, R., Lapinski, P.E., King, P.D., Sevick-Muraca, E.M. (2016). A novel mutation in CELSR1 is associated with hereditary lymphedema. Vascular Cell *8*.

Haberland, M., Mokalled, M.H., Montgomery, R.L., and Olson, E.N. (2009a). Epigenetic control of skull morphogenesis by histone deacetylase 8. Genes & Development *23*, 1625–1630.

Haberland, M., Montgomery, R.L., and Olson, E.N. (2009b). The many roles of histone deacetylases in development and physiology: implications for disease and therapy. Nat Rev Genet *10*, 32.

Hayakawa, F., Towatari, M., Ozawa, Y., Tomita, A., Privalsky, M.L., and Saito, H. (2003). Functional regulation of GATA-2 by acetylation. Journal of

Leukocyte Biology *75*, 529–540.

Heintzman, N.D., Stuart, R.K., Hon, G., Fu, Y., Ching, C.W., Hawkins, R.D., Barrera, L.O., Van Calcar, S., Qu, C., Ching, K.A., et al. (2007). Distinct and predictive chromatin signatures of transcriptional promoters and enhancers in the human genome. Nat Genet *39*, 311–318.

Hess, P.R., Rawnsley, D.R., Jakus, Z., Yang, Y., Sweet, D.T., Fu, J., Herzog, B., Lu, M., Nieswandt, B., Oliver, G., et al. (2013). Platelets mediate lymphovenous hemostasis to maintain blood-lymphatic separation throughout life. J. Clin. Invest. *124*, 273–284.

Hsu, A.P., Johnson, K.D., Falcone, E.L., Sanalkumar, R., Sanchez, L., Hickstein, D.D., Cuellar-Rodriguez, J., Lemieux, J.E., Zerbe, C.S., Bresnick, E.H., et al. (2013). GATA2 haploinsufficiency caused by mutations in a conserved intronic element leads to MonoMAC syndrome. Blood *121*, 3830–3837.

Huntington, G.S., and McClure, C.F.W. (1910). The anatomy and development of the jugular lymph sacs in the domestic cat (Felis domestica). Developmental Dynamics *10*, 177–312.

Jepsen, K., and Rosenfeld, M.G. (2002). Biological roles and mechanistic actions of co-repressor complexes. Journal of Cell Science *115*, 689–698.

Johnson, K.D., Hsu, A.P., Ryu, M.-J., Wang, J., Gao, X., Boyer, M.E., Liu, Y., Lee, Y., Calvo, K.R., Keles, S., et al. (2012). *Cis*-element mutated in *GATA2*-dependent immunodeficiency governs hematopoiesis and vascular integrity. J. Clin. Invest. *122*, 3692–3704.

Joseph, C., Quach, J.M., Walkley, C.R., Lane, S.W., Celso, Lo, C., and Purton, L.E. (2013). Deciphering hematopoietic stem cells in their niches: a critical appraisal of genetic models, lineage tracing, and imaging strategies. Cell Stem Cell *13*, 520–533.

Jurisic, G., and Detmar, M. (2009) Lymphatic endothelium in health and disease. Cell Tissue Res. *335*, 97–108.

Jurisic, G., Hajjami, H.M.-E., Karaman, S., Ochsenbein, A.M., Alitalo, A., Siddiqui, S.S., Pereira, C.O., Petrova, T.V., and Detmar, M. (2012) An Unexpected Role of Semaphorin3A–Neuropilin-1 Signaling in Lymphatic Vessel Maturation and Valve Formation. Circulation Research. *111*, 426-36

Kaluza, D., Kroll, J., Gesierich, S., Yao, T.-P., Boon, R.A., Hergenreider, E., Tjwa, M., Rössig, L., Seto, E., Augustin, H.G., et al. (2011). Class IIb HDAC6 regulates endothelial cell migration and angiogenesis by deacetylation of cortactin. The EMBO Journal *30*, 4142–4156.

Kammerer, F.J., Schlude, B., Kuefner, M.A., Schlechtweg, P., Hammon, M.,

Uder, M., and Schwab, S.A. (2016). Morphology of the distal thoracic duct and the right lymphatic duct in different head and neck pathologies: an imaging based study. Head Face Med *12*, 1615.

Kanady, J.D., Dellinger, M.T., Munger, S.J., Witte, M.H., and Simon, A.M. (2011). Connexin37 and Connexin43 deficiencies in mice disrupt lymphatic valve development and result in lymphatic disorders including lymphedema and chylothorax. Developmental Biology *354*, 253–266.

Kanady, J.D., Munger, S.J., Witte, M.H., and Simon, A.M. (2015). Combining Foxc2 and Connexin37 deletions in mice leads to severe defects in lymphatic vascular growth and remodeling. Developmental Biology *405*, 33–46.

Kazenwadel, J., Secker, G.A., Liu, Y.J., Rosenfeld, J.A., Wildin, R.S., Cuellar-Rodriguez, J., Hsu, A.P., Dyack, S., Fernandez, C.V., Chong, C.E., et al. (2012). Loss-of-function germline GATA2 mutations in patients with MDS/AML or MonoMAC syndrome and primary lymphedema reveal a key role for GATA2 in the lymphatic vasculature. Blood *119*, 1283–1291.

Kazenwadel, J., Betterman, K.L., Chong, C.-E., Stokes, P.H., Lee, Y.K., Secker, G.A., Agalarov, Y., Demir, C.S., Lawrence, D.M., Sutton, D.L., et al. (2015). GATA2 is required for lymphatic vessel valve development and maintenance. J. Clin. Invest. *125*, 2979–2994.

Khandekar, M., Brandt, W., Zhou, Y., Dagenais, S., Glover, T.W., Suzuki, N., Shimizu, R., Yamamoto, M., Lim, K.C., and Engel, J.D. (2007). A Gata2 intronic enhancer confers its pan-endothelia-specific regulation. Development *134*, 1703–1712.

Kinnaert, P. (1973). Anatomical variations of the cervical portion of the thoracic duct in man. Journal of Anatomy *115*, 45-52.

Kisanuki, Y.Y., Hammer, R.E., Miyazaki, J., Williams, S.C., Richardson, J.A., and Yanagisawa, M. (2001). Tie2-Cre transgenic mice: a new model for endothelial cell-lineage analysis in vivo. Developmental Biology *230*, 230–242.

Klotz, L., Norman, S., Vieira, J.M., Masters, M., Rohling, M., Dubé, K.N., Bollini, S., Matsuzaki, F., Carr, C.A., and Riley, P.R. (2015). Cardiac lymphatics are heterogeneous in origin and respond to injury. Nature. *522(7554)*, 62-7.

Kochilas, L.K., Shepard, C.W., Berry, J.M., and Chin, A.J. (2014). Ultrasonographic Imaging of the Cervical Thoracic Duct in Children with Congenital or Acquired Heart Disease. Echocardiography *31*, E282–E286.

Lagger, G. (2002). Essential function of histone deacetylase 1 in proliferation control and CDK inhibitor repression. The EMBO Journal *21*, 2672–2681.

Langford, R.J., Daudia, A.T., and Malins, T.J. (1999). A morphological study of the thoracic duct at the jugulo-subclavian junction. J Craniomaxillofac Surg *27*, 100–104.

Lee, K.K., and Workman, J.L. (2007). Histone acetyltransferase complexes: one size doesn't fit all. Nature Reviews Molecular Cell Biology *8*, 284–295.

Lee LK., Ghorbanian Y., Wang W., Wang Y., Kim YJ., Weissman IL., Inlay AM ., Mikkola HKA. (2016) LYVE1 Marks the Divergence of Yolk Sac Definitive Hemogenic Endothelium from the Primitive Erythroid Lineage. Cell Reports *17*, 2286–2298

Lettice, L.A. (2003). A long-range Shh enhancer regulates expression in the developing limb and fin and is associated with preaxial polydactyly. Human Molecular Genetics *12*, 1725–1735.

Levet, S., Ciais, D., Merdzhanova, G., Mallet, C., Zimmers, T.A., Lee, S.J., Navarro, F.P., Texier, I., Feige, J.J., Bailly, S., et al. (2013). Bone morphogenetic protein 9 (BMP9) controls lymphatic vessel maturation and valve formation. Blood *122*, 598–607.

Lewandowski, S.L., Janardhan, H.P., Smee, K.M., Bachman, M., Sun, Z., Lazar, M.A., and Trivedi, C.M. (2014). Histone deacetylase 3 modulates Tbx5 activity to regulate early cardiogenesis. Human Molecular Genetics.

Lewandowski, S.L., Janardhan, H.P., and Trivedi, C.M. (2015). Histone Deacetylase 3 Coordinates Deacetylase-independent Epigenetic Silencing of Transforming Growth Factor-β1 (TGF-β1) to Orchestrate Second Heart Field Development. Journal of Biological Chemistry *290*, 27067–27089.

Lewandowski, S.L., Janardhan, H.P., Smee, K.M., Bachman, M., Sun, Z., Lazar, M.A., and Trivedi, C.M. Histone deacetylase 3 modulates Tbx5 activity to regulate early cardiogenesis. Hmg.Oxfordjournals.org.

Lim, K.-C., Hosoya, T., Brandt, W., Ku, C.-J., Hosoya-Ohmura, S., Camper, S.A., Yamamoto, M., and Engel, J.D. (2012) Conditional *Gata2* inactivation results in HSC loss and lymphatic mispatterning. J. Clin. Invest. *122*, 3705–3717.

Liu, M.-E., Barton F Branstetter, I.V., Whetstone, J., and Escott, E.J. (2006) Normal CT Appearance of the Distal Thoracic Duct. American Journal of Roentgenology. *187*, 1615-1620

Long, H.K., Prescott, S.L., and Wysocka, J. (2016). Ever-Changing Landscapes: Transcriptional Enhancers in Development and Evolution. Cell *167*, 1170–1187.

Longo, P.A., Kavran, J.M., Kim, M.-S., and Leahy, D.J. (2013). Transient

mammalian cell transfection with polyethylenimine (PEI). Meth. Enzymol. *529*, 227–240.

Loukas, M., Bellary, S.S., Kuklinski, M., Ferrauiola, J., Yadav, A., Shoja, M.M., Shaffer, K., and Tubbs, R.S. (2011). The lymphatic system: A historical perspective. Clin. Anat. *24*, 807–816.

Luger, K., Mäder, A.W., Richmond, R.K., Sargent, D.F., and Richmond, T.J. (1997). Crystal structure of the nucleosome core particle at 2.8 Å resolution. Nature *389*, 251–260.

Ma, G.-C., Liu, C.-S., Chang, S.-P., Yeh, K.-T., Ke, Y.-Y., Chen, T.-H., Wang, B.B.-T., Kuo, S.-J., Shih, J.-C., and Chen, M. (2008). A recurrent ITGA9missense mutation in human fetuses with severe chylothorax: possible correlation with poor response to fetal therapy. Prenat. Diagn. *28*, 1057–1063.

Mäkinen, T., Adams, R.H., Bailey, J., Lu, Q., Ziemiecki, A., Alitalo, K., Klein, R., Wilkinson, G.A. (2005). PDZ interaction site in ephrinB2 is required for the remodeling of lymphatic vasculature. Genes & Development *19*, 397.

Mansour, S., Connell, F., Steward, C., Ostergaard, P., Brice, G., Smithson, S., Lunt, P., Jeffery, S., Dokal, I., Vulliamy, T., et al. (2010). Emberger syndrome-Primary lymphedema with myelodysplasia: Report of seven new cases. Am. J. Med. Genet. *152A*, 2287–2296.

Margariti, A., Zampetaki, A., Xiao, Q., Zhou, B., Karamariti, E., Martin, D., Yin, X., Mayr, M., Li, H., Zhang, Z., et al. (2010) Histone Deacetylase 7 Controls Endothelial Cell Growth Through Modulation of β-Catenin. Circulation Research. *106(7)*, 1202-11

Martin-Almedina, S., Martinez-Corral, I., Holdhus, R., Vicente, A., Fotiou, E., Lin, S., Petersen, K., Simpson, M.A., Hoischen, A., Gilissen, C., et al. (2016) EPHB4 kinase–inactivating mutations cause autosomal dominant lymphatic-related hydrops fetalis. J. Clin. Invest. *126*, 3080–3088.

Martinez-Corral, I., Ulvmar, M.H., Stanczuk, L., Tatin, F., Kizhatil, K., John, S.W.M., Alitalo, K., Ortega, S., and Makinen, T. (2015) Nonvenous Origin of Dermal Lymphatic Vasculature. Circulation Research. *116(10)*, 1649-54

Marushige, K. (1976). Activation of chromatin by acetylation of histone side chains. Proc. Natl. Acad. Sci. U.S.a. *73*, 3937–3941.

Maurano, M.T., Humbert, R., Rynes, E., Thurman, R.E., Haugen, E., Wang, H., Reynolds, A.P., Sandstrom, R., Qu, H., Brody, J., et al. (2012). Systematic Localization of Common Disease-Associated Variation in Regulatory DNA. Science *337*, 1190–1195.

Michelini, S., Paolacci, S., Manara, E., Eretta, C., Mattassi, R., Lee, B.-B., and Bertelli, M. (2018). Genetic tests in lymphatic vascular malformations and

lymphedema. Journal of Medical Genetics jmedgenet–2017–105064.

Milstone, Z.J., Lawson, G., and Trivedi, C.M. (2017). Histone deacetylase 1 and 2 are essential for murine neural crest proliferation, pharyngeal arch development, and craniofacial morphogenesis. Dev. Dyn. *246*, 1015–1026.

Montgomery, R.L., Potthoff, M.J., Haberland, M., Qi, X., Matsuzaki, S., Humphries, K.M., Richardson, J.A., Bassel-Duby, R., and Olson, E.N. (2008). Maintenance of cardiac energy metabolism by histone deacetylase 3 in mice. J. Clin. Invest. *118*, 3588–3597.

Mortimer, P.S., and Rockson, S.G. (2014). New developments in clinical aspects of lymphatic disease. J. Clin. Invest. *124*, 915–921.

Mullican SE, et al. (2011) Histone deacetylase 3 is an epigenomic brake in macrophage alternative activation. *Genes Dev*. *25(23)*, 2480–2488.

Murtomaki, A., Uh, M.K., Kitajewski, C., Zhao, J., Nagasaki, T., Shawber, C.J., and Kitajewski, J. (2014). Notch signaling functions in lymphatic valve formation. Development *141*, 2446–2451.

Norrmén, C., Ivanov, K.I., Cheng, J., Zangger, N., Delorenzi, M., Jaquet, M., Miura, N., Puolakkainen, P., Horsley, V., Hu, J., et al. (2009). FOXC2 controls formation and maturation of lymphatic collecting vessels through cooperation with NFATc1. The Journal of Cell Biology *185*, 439–457.

Ong, C.-T., and Corces, V.G. (2011). Enhancer function: new insights into the regulation of tissue-specific gene expression. Nat Rev Genet *12*, 283–293.

Oren, T. (2005). An Oct-1 binding site mediates activation of the gata2 promoter by BMP signaling. Nucleic Acids Research *33*, 4357–4367.

Ostergaard, P., Simpson, M.A., Connell, F.C., Steward, C.G., Brice, G., Woollard, W.J., Dafou, D., Kilo, T., Smithson, S., Lunt, P., et al. (2011). Mutations in GATA2 cause primary lymphedema associated with a predisposition to acute myeloid leukemia (Emberger syndrome). Nat Genet *43*, 929–931.

Pelug, J., and Calnan, J. (1968). The valves of the thoracic duct at the angulus venosus. Br. J. Surg. *55*, 911–916.

Perino, M., and Veenstra, G.J.C. (2016). Chromatin Control of Developmental Dynamics and Plasticity. Dev. Cell *38*, 610–620.

Petrova, T.V., Karpanen, T., Norrmén, C., Mellor, R., Tamakoshi, T., Finegold, D., Ferrell, R., Kerjaschki, D., Mortimer, P., Ylä-Herttuala, S., et al. (2004). Defective valves and abnormal mural cell recruitment underlie lymphatic vascular failure in lymphedema distichiasis. Nature Medicine *10*, 974–981.

Pham, T.H.M., Baluk, P., Xu, Y., Grigorova, I., Bankovich, A.J., Pappu, R., Coughlin, S.R., McDonald, D.M., Schwab, S.R., and Cyster, J.G. (2010). Lymphatic endothelial cell sphingosine kinase activity is required for lymphocyte egress and lymphatic patterning. Journal of Experimental Medicine *207*, 17–27.

Planas-Paz, L., Strilić, B., Goedecke, A., Breier, G., Fässler, R., and Lammert, E. (2011). Mechanoinduction of lymph vessel expansion. The EMBO Journal *31*, 788–804.

Potente, M., Gerhardt, H., and Carmeliet, P. (2011). Basic and Therapeutic Aspects of Angiogenesis. Cell *146*, 873–887.

Pujol, F., Hodgson, T., Martinez-Corral, I., Prats, A.-C., Devenport, D., Takeichi, M., Genot, E., Makinen, T., Francis-West, P., Garmy-Susini, B., et al. (2017). Dachsous1-Fat4 Signaling Controls Endothelial Cell Polarization During Lymphatic Valve Morphogenesis-Brief Report. Arteriosclerosis, Thrombosis, and Vascular Biology *37*, 1732–1735.

Qu, X., Zhou, B., and Scott Baldwin, H. (2015). Tie1 is required for lymphatic valve and collecting vessel development. Developmental Biology *399*, 117–128.

Rada-Iglesias, A., Bajpai, R., Swigut, T., Brugmann, S.A., Flynn, R.A., and Wysocka, J. (2010). A unique chromatin signature uncovers early developmental enhancers in humans. Nature *470*, 279–283.

Ratnayake, C.B.B., Escott, A.B.J., Phillips, A.R.J., and Windsor, J.A. (2018). The anatomy and physiology of the terminal thoracic duct and ostial valve in health and disease: potential implications for intervention. Journal of Anatomy *233*, 1–14.

Risau, W. (1997). Mechanisms of angiogenesis. Nature *386*, 671EP—674.

Risau, W., and Flamme, I. (1995). Vasculogenesis. Annu. Rev. Cell Dev. Biol. *11*, 73–91.

Robert-Moreno, A. (2005). RBPj -dependent Notch function regulates Gata2 and is essential for the formation of intra-embryonic hematopoietic cells. Development *132*, 1117–1126.

Roth, S.Y., Denu, J.M., and Allis, C.D. (2001) Histone Acetyltransferases. Annual Reviews of Biochemistry *70*, 81-120.

Sabin, F.R. (1909). The lymphatic system in human embryos, with a consideration of the morphology of the system as a whole. Developmental Dynamics *9*, 43–91.

Sabine, A., Agalarov, Y., Maby-El Hajjami, H., Jaquet, M., Hägerling, R.,

Pollmann, C., Bebber, D., Pfenniger, A., Miura, N., Dormond, O., et al. (2012). Mechanotransduction, PROX1, and FOXC2 cooperate to control connexin37 and calcineurin during lymphatic-valve formation. Dev. Cell *22*, 430–445.

Sabine, A., Bovay, E., Demir, C.S., Kimura, W., Jaquet, M., Agalarov, Y., Zangger, N., Scallan, J.P., Graber, W., Gulpinar, E., et al. (2015) FOXC2 and fluid shear stress stabilize postnatal lymphatic vasculature. J. Clin. Invest. *125*, 3861–3877.

Schacht, V. (2003). T1 /podoplanin deficiency disrupts normal lymphatic vasculature formation and causes lymphedema. The EMBO Journal *22*, 3546–3556.

Schlaeger, T.M. (2005). Tie2Cre-mediated gene ablation defines the stem-cell leukemia gene (SCL/tal1)-dependent window during hematopoietic stem-cell development. Blood *105*, 3871–3874.

Schwartz, M.A., and Simons, M. (2012). Lymphatics thrive on stress: mechanical force in lymphatic development. The EMBO Journal *31*, 781–782.

Seeger, M., Bewig, B., Günther, R., Schafmayer, C., Vollnberg, B., Rubin, D., Hoell, C., Schreiber, S., Fölsch, U.R., and Hampe, J. (2009). Terminal part of thoracic duct: high-resolution US imaging. Radiology *252*, 897–904.

Shah, S., Conlin, L.K., Gomez, L., Aagenaes, Ø., Eiklid, K., Knisely, A.S., Mennuti, M.T., Matthews, R.P., Spinner, N.B., and Bull, L.N. (2013). CCBE1 Mutation in Two Siblings, One Manifesting Lymphedema-Cholestasis Syndrome, and the Other, Fetal Hydrops. Plos One *8*, e75770.

Shahbazian, M.D., and Grunstein, M. (2007). Functions of Site-Specific Histone Acetylation and Deacetylation. Annu. Rev. Biochem. *76*, 75–100.

Shimada, K., and Sato, I. (1997). Morphological and histological analysis of the thoracic duct at the jugulo-subclavian junction in Japanese cadavers. Clin. Anat. *10*, 163–172.

Shin, M., Male, I., Beane, T.J., Villefranc, J.A., Kok, F.O., Zhu, L.J., and Lawson, N.D. (2016). Vegfc acts through ERK to induce sprouting and differentiation of trunk lymphatic progenitors. Development *143*, 3785–3795.

Smith, E., and Shilatifard, A. (2014). Enhancer biology and enhanceropathies. Nat Struct Mol Biol *21*, 210–219.

Smith, M.E., Riffat, F., and Jani, P. (2013) The surgical anatomy and clinical relevance of the neglected right lymphatic duct: review. The Journal of Laryngology & Otology *127*, 128–133.

Soriano, P. (1999). Generalized lacZ expression with the ROSA26 Cre reporter strain. Nat Genet *21*, 70–71.

Spinner, M.A., Sanchez, L.A., Hsu, A.P., Shaw, P.A., Zerbe, C.S., Calvo, K.R., Arthur, D.C., Gu, W., Gould, C.M., Brewer, C.C., et al. (2014). GATA2 deficiency: a protean disorder of hematopoiesis, lymphatics, and immunity. Blood *123*, 809–821.

Spitz, F., and Furlong, E.E.M. (2012). Transcription factors: from enhancer binding to developmental control. Nat Rev Genet *13*, 613.

Srinivasan, R.S., Oliver, G. (2011). Prox1 dosage controls the number of lymphatic endothelial cell progenitors and the formation of the lymphovenous valves. Genes & Development *25*, 2187–2197.

Srinivasan, R.S., Dillard, M.E., Lagutin, O.V., Lin, F.J., Tsai, S., Tsai, M.J., Samokhvalov, I.M., Oliver, G. (2007). Lineage tracing demonstrates the venous origin of the mammalian lymphatic vasculature. Genes & Development *21*, 2422.

Stanczuk, L., Martinez-Corral, I., Ulvmar, M.H., Zhang, Y., Laviña, B., Fruttiger, M., Adams, R.H., Saur, D., Betsholtz, C., Ortega, S., et al. (2015). cKit Lineage Hemogenic Endothelium-Derived Cells Contribute to Mesenteric Lymphatic Vessels. Cell Reports.

Suka, N., Suka, Y., Carmen, A.A., Wu, J., and Grunstein, M. (2001). Highly specific antibodies determine histone acetylation site usage in yeast heterochromatin and euchromatin. pp. 473–479.

Sun, B., Hong, J., Zhang, P., Dong, X., Shen, X., Lin, D., and Ding, J. (2008). Molecular Basis of the Interaction of Saccharomyces cerevisiaeEaf3 Chromo Domain with Methylated H3K36. Journal of Biological Chemistry *283*, 36504–36512.

Sun, Z., Feng, D., Fang, B., Mullican, S.E., You, S.-H., Lim, H.-W., Everett, L.J., Nabel, C.S., Li, Y., Selvakumaran, V., et al. (2013). Deacetylase-Independent Function of HDAC3 in Transcription and Metabolism Requires Nuclear Receptor Corepressor. Mol. Cell *52*, 769–782.

Suzuki-Inoue, K. (2006). A novel Syk-dependent mechanism of platelet activation by the C-type lectin receptor CLEC-2. Blood *107*, 542–549.

Suzuki-Inoue, K., Inoue, O., Ding, G., Nishimura, S., Hokamura, K., Eto, K., Kashiwagi, H., Tomiyama, Y., Yatomi, Y., Umemura, K., et al. (2010) Essential in Vivo Roles of the C-type Lectin Receptor CLEC-2. Journal of Biological Chemistry *285*, 24494-507

Suzuki-Inoue, K., Kato, Y., Inoue, O., Kaneko, M.K., Mishima, K., Yatomi, Y., Yamazaki, Y., Narimatsu, H., and Ozaki, Y. (2007). Involvement of the Snake Toxin Receptor CLEC-2, in Podoplanin-mediated Platelet Activation, by Cancer Cells. Journal of Biological Chemistry *282*, 25993–26001.

Swartz, M.A. (2001). The physiology of the lymphatic system. Adv. Drug Deliv. Rev. *50*, 3–20.

Sweet, D.T., Jiménez, J.M., Chang, J., Hess, P.R., Mericko-Ishizuka, P., Fu, J., Xia, L., Davies, P.F., and Kahn, M.L. (2015) Lymph flow regulates collecting lymphatic vessel maturation in vivo. J. Clin. Invest. *125*, 2995–3007.

Tak, Y.G., and Farnham, P.J. (2015). Making sense of GWAS: using epigenomics and genome engineering to understand the functional relevance of SNPs in non-coding regions of the human genome. Epigenetics & Chromatin *8*, D1001.

Tammela, T., and Alitalo, K. (2010). Lymphangiogenesis: Molecular mechanisms and future promise. Cell *140*, 460–476.

Tang Y., Harrington A., Yang X., Friesel RE., Liaw L. (2010) The contribution of the Tie2+ lineage to primitive and definitive hematopoietic cells. Genesis. *48*, 563-7

Tatin, F., Taddei, A., Weston, A., Fuchs, E., Devenport, D., Tissir, F., and Makinen, T. (2013). Planar Cell Polarity Protein Celsr1 Regulates Endothelial Adherens Junctions and Directed Cell Rearrangements during Valve Morphogenesis. Dev. Cell *26*, 31–44.

Tiedt, R., Schomber, T., Hao-Shen, H., and Skoda, R.C. (2007). Pf4-Cre transgenic mice allow the generation of lineage-restricted gene knockouts for studying megakaryocyte and platelet function in vivo. Blood *109*, 1503–1506.

Trivedi, C.M., Lu, M.M., Wang, Q., and Epstein, J.A. (2008). Transgenic Overexpression of Hdac3 in the Heart Produces Increased Postnatal Cardiac Myocyte Proliferation but Does Not Induce Hypertrophy. Journal of Biological Chemistry *283*, 26484–26489.

Trivedi, C.M., Luo, Y., Yin, Z., Zhang, M., Zhu, W., Wang, T., Floss, T., Goettlicher, M., Noppinger, P.R., Wurst, W., et al. (2007). Hdac2 regulates the cardiac hypertrophic response by modulating Gsk3β activity. Nature Medicine *13*, 324–331.

Trivedi, C.M., Zhu, W., Wang, Q., Jia, C., Kee, H.J., Li, L., Hannenhalli, S., and Epstein, J.A. (2010). Hopx and Hdac2 interact to modulate Gata4 acetylation and embryonic cardiac myocyte proliferation. Dev. Cell *19*, 450–459.

Tsai, F.-Y., Keller, G., Kuo, F.C., Weiss, M., Chen, J., Rosenblatt, M., Alt, F.W., and Orkin, S.H. (1994). An early haematopoietic defect in mice lacking the transcription factor GATA-2. Nature *371*, 221–226.

Tsuzuki, S., Kitajima, K., Nakano, T., Glasow, A., Zelent, A., and Enver, T. (2004). Cross Talk between Retinoic Acid Signaling and Transcription Factor GATA-2. Molecular and Cellular Biology *24*, 6824–6836.

Turner, C.J., Badu-Nkansah, K., Crowley, D., van der Flier, A., Hynes, R.O. (2014) Integrin-α5β1 is not required for mural cell functions during development of blood vessels but is required for lymphatic-blood vessel separation and lymphovenous valve formation. Developmental Biology *392*, 381.

Tzima, E., Irani-Tehrani, M., Kiosses, W.B., Dejana, E., Schultz, D.A., Engelhardt, B., Cao, G., DeLisser, H., and Schwartz, M.A. (2005). A mechanosensory complex that mediates the endothelial cell response to fluid shear stress. Nature *437*, 426–431.

Uebelhoer, M., Boon, L.M., and Vikkula, M. (2012) Vascular Anomalies: From Genetics toward Models for Therapeutic Trials. Cold Spring Harb Perspect Med *2*, a009688

Uhrin, P., Zaujec, J., Breuss, J.M., Olcaydu, D., Chrenek, P., Stockinger, H., Fuertbauer, E., Moser, M., Haiko, P., Fassler, R., et al. (2010). Novel function for blood platelets and podoplanin in developmental separation of blood and lymphatic circulation. Blood *115*, 3997–4005.

Ulvmar, M.H., and Makinen, T. (2016). Heterogeneity in the lymphatic vascular system and its origin. Cardiovascular Research *111*, 310–321.

Urbich, C., Rossig, L., Kaluza, D., Potente, M., Boeckel, J.N., Knau, A., Diehl, F., Geng, J.G., Hofmann, W.K., Zeiher, A.M., et al. (2009). HDAC5 is a repressor of angiogenesis and determines the angiogenic gene expression pattern of endothelial cells. Blood *113*, 5669–5679.

Visel, A., Blow, M.J., Li, Z., Zhang, T., Akiyama, J.A., Holt, A., Plajzer-Frick, I., Shoukry, M., Wright, C., Chen, F., Afzal, V., Ren, B., Rubin, E.M., Pennacchio, L.A. (2009). ChIP-seq accurately predicts tissue-specific activity of enhancers. Nature *457*, 854.

Wang, A. (2002). Requirement of Hos2 Histone Deacetylase for Gene Activity in Yeast. Science *298*, 1412–1414.

Wang, Y., Baeyens, N., Corti, F., Tanaka, K., Fang, J.S., Zhang, J., Jin, Y., Coon, B., Hirschi, K.K., Schwartz, M.A., et al. (2016). Syndecan 4 controls lymphatic vasculature remodeling during mouse embryonic development. Development *143*, 4441–4451.

Wang, Z., Zang, C., Cui, K., Schones, D.E., Barski, A., Peng, W., and Zhao, K. (2009). Genome-wide Mapping of HATs and HDACs Reveals Distinct Functions in Active and Inactive Genes. Cell *138*, 1019–1031.

Wassef, M., Blei, F., Adams, D., Alomari, A., Baselga, E., Berenstein, A., Burrows, P., Frieden, I.J., Garzon, M.C., Lopez-Gutierrez, J.-C., et al. (2015). Vascular Anomalies Classification: Recommendations From the International Society for the Study of Vascular Anomalies. Pediatrics peds.2014–peds.3673.

Wei, G., Srinivasan, R., Cantemir-Stone, C.Z., Sharma, S.M., Santhanam, R., Weinstein, M., Muthusamy, N., Man, A.K., Oshima, R.G., Leone, G., et al. (2009). Ets1 and Ets2 are required for endothelial cell survival during embryonic angiogenesis. Blood *114*, 1123–1130.

Welsh, J.D., Kahn, M.L., and Sweet, D.T. (2016). Lymphovenous hemostasis and the role of platelets in regulating lymphatic flow and lymphatic vessel maturation. Blood *128*, 1169–1173.

Williams, R.J. (2005). Trichostatin A, an inhibitor of histone deacetylase, inhibits hypoxia-induced angiogenesis. Expert Opinion on Investigational Drugs *10*, 1571–1573.

Witte, M.H., Dumont, A.E., Clauss, R.H., Rader, B., Levine, N., and Breed, E.S. (1969) Lymph Circulation in Congestive Heart Failure. Circulation. *39*, 723–733

Woo, K.V., Qu, X., Babaev, V.R., Linton, M.F., Guzman, R.J., Fazio, S., and Baldwin, H.S. (2011) Tie1 attenuation reduces murine atherosclerosis in a dose-dependent and shear stress–specific manner. J. Clin. Invest. *121*, 1624–1635.

Xu, F., Zhang, K., and Grunstein, M. (2005). Acetylation in histone H3 globular domain regulates gene expression in yeast. Cell *121*, 375–385.

Yalakurthi, S., Vishnumukkala, T.R., Siri, C.C., Raj, S.S.J.D., puttagunta, B., and M, K. (2013) Anatomical Variations of The Termination of The Thoracic Duct In Humans. International Journal of Medical and Health Sciences *2*, 230–234.

Yamagoe, S., Kanno, T., Kanno, Y., Sasaki, S., Siegel, R.M., Lenardo, M.J., Humphrey, G., Wang, Y., Nakatani, Y., Howard, B.H., et al. (2003). Interaction of Histone Acetylases and Deacetylases In Vivo. Molecular and Cellular Biology *23*, 1025–1033.

Yang, S.H., Vickers, E., Brehm, A., Kouzarides, T., and Sharrocks, A.D. (2001). Temporal Recruitment of the mSin3A-Histone Deacetylase Corepressor Complex to the ETS Domain Transcription Factor Elk-1. Molecular and Cellular Biology *21*, 2802–2814.

Yang, W.-M., Yao, Y.-L., Sun, J.-M., Davie, J.R., and Seto, E. (1997). Isolation and Characterization of cDNAs Corresponding to an Additional Member of the Human Histone Deacetylase Gene Family. Journal of

Biological Chemistry *272*, 28001–28007.

Yang, X.-J., and Seto, E. (2008). The Rpd3/Hda1 family of lysine deacetylases: from bacteria and yeast to mice and men. Nature Reviews Molecular Cell Biology *9*, 206–218.

Yang, Y., and Oliver, G. (2014). Development of the mammalian lymphatic vasculature. J. Clin. Invest. *124*, 888–897.

You, S.-H., Lim, H.-W., Sun, Z., Broache, M., Won, K.-J., and Lazar, M.A. (2013). Nuclear receptor co-repressors are required for the histone-deacetylase activity of HDAC3 in vivo. Nat Struct Mol Biol *20*, 182–187.

Yu, J. (2003). A SANT motif in the SMRT corepressor interprets the histone code and promotes histone deacetylation. The EMBO Journal *22*, 3403–3410.

Zampetaki, A., Zeng, L., Margariti, A., Xiao, Q., Li, H., Zhang, Z., Pepe, A.E., Wang, G., Habi, O., deFalco, E., et al. (2010) Histone Deacetylase 3 Is Critical in Endothelial Survival and Atherosclerosis Development in Response to Disturbed Flow. Circulation *121,* 132-42

Zhang, B., Day, D.S., Ho, J.W., Song, L., Cao, J., Christodoulou, D., Seidman, J.G., Crawford, G.E., Park, P.J., and Pu, W.T. (2013). A dynamic H3K27ac signature identifies VEGFA-stimulated endothelial enhancers and requires EP300 activity. Genome Research *23*, 917–927.

Zhang, G., Brady, J., Liang, W.-C., Wu, Y., Henkemeyer, M., and Yan, M. (2015). EphB4 forward signalling regulates lymphatic valve development. Nat Comms *6*, 638.

Zhang, L., He, X., Liu, L., Jiang, M., Zhao, C., Wang, H., He, D., Zheng, T., Zhou, X., Hassan, A., et al. (2016). Hdac3 Interaction with p300 Histone Acetyltransferase Regulates the Oligodendrocyte and Astrocyte Lineage Fate Switch. Dev. Cell *36*, 316–330.

Zhou, B., Margariti, A., Zeng, L., and Xu, Q. (2011). Role of histone deacetylases in vascular cell homeostasis and arteriosclerosis. Cardiovascular Research *90*, 413–420.